Université de Montréal

Molecular mode of action of Cry6Aa1, a new insecticidal *Bacillus thuringiensis* toxin

par
Eva Fortea Verdejo

Département de physiologie moléculaire et intégrative
Faculté de médecine

Mémoire présenté en vue de l'obtention du grade de Maîtrise
en physiologie moléculaire, cellulaire et intégrative option physiologie et biophysique moléculaires

Membres du jurée Lucie Parent, Réjean Couture et Jean-Louis Schwartz

Août 2016

ABSTRACT

Cry6Aa1 is a new toxin produced by *Bacillus thuringiensis* (*Bt*), which displays insecticidal activity against the Western corn rootworm (WCRW). The present work demonstrates that Cry6Aa1 is a pore-forming toxin (PFT) in planar lipid bilayers (PLBs). Contrary to other *Bt* toxins tested so far, pore formation by Cry6Aa1 does not require protease pretreatment and takes place at doses that are two to three orders of magnitude lower than those required for other *Bt* toxins under similar conditions.

Pore formation by Cry6Aa1 is pH-dependent; the conductances of the pores range between 31 and 689 pS under symmetrical 150 mM KCl conditions; they are cationic and display a complex kinetic behaviour. The treatment of the toxin with midgut juice (Cry6Aa1 WCR1) does not change the biophysical properties of the pores. However, the treatment with trypsin (Cry6Aa1 TT) affects their conductance and selectivity at pH 5.5 (the WCRW gut physiological pH). The incorporation in PLBs of native membrane material from WCRW midgut affects the behaviour of the Cry6Aa1 pores. The molecular determinants of the mode of action of this new PFT appear therefore to differ from those reported before for other *Bt* toxins.

The three-dimensional (3-D) atomic structure of Cry6Aa1 has just been elucidated. It shows that the toxin assumes an α-helix-rich configuration, which is quite similar to that of the ClyA PFT produced by *E. coli*. Based on the data available for ClyA, we have studied how different changes in the N- and C-terminal regions of Cry6Aa1 affect its pore formation ability in PLBs.

Key words: Planar lipid bilayer, bacterial toxin, *Bacillus thuringiensis*, pore-forming toxin, Western corn rootworm, Cry6Aa1, δ-endotoxin.

RÉSUMÉ

Cry6Aa1, une nouvelle toxine produite par *Bacillus thuringiensis* (*Bt*), agit comme insecticide sur la chrysomèle du maïs (WCRW). Dans cette étude, on démontre que Cry6Aa1 est une toxine formeuse de pores (TFP) en bicouches lipidiques planes (BLP). Contrairement aux autres toxines de *Bt* étudiées jusqu'à présent, la formation de pores par Cry6Aa1 ne requiert pas de prétraitement par protéases et se produit à des doses de toxine deux à trois ordres de grandeur plus faibles que celles nécessaires pour les autres toxines de *Bt* dans les mêmes conditions.

La formation de pores par la forme non traitée de Cry6Aa1 dépend du pH; les pores obtenus ont des conductances comprises entre 31 et 689 pS en conditions symétriques de 150 mM de KCl; ils sont cationiques avec un comportement cinétique complexe. Les propriétés biophysiques des pores ne changent pas lorsque la toxine est traitée avec le suc du mésenthéron de l'insecte (Cry6Aa1 WCR1). Par contre, un traitement à la trypsine (Cry6Aa1 TT) modifie la conductance et la sélectivité des pores à pH 5,5 (le pH physiologique de l'intestin de WCRW). La reconstitution en BLP de fraction de membrane native du mésenthéron de WCRW affecte les propriétés des pores formés par Cy6Aa1. Les déterminants moléculaires du mode d'action de cette nouvelle toxine formeuse de pores semblent donc différer de ceux décrits précédemment pour d'autres toxines de *Bt*.

La structure atomique tridimensionnelle de Cry6Aa1 vient tout juste d'être élucidée. Elle montre que la toxine adopte une conformation riche en hélices α qui ressemble fortement à celle de la TFP ClyA produite par *E. coli*. En se fondant sur les données disponibles pour ClyA, on a étudié l'effet de divers changements dans les régions N et C terminales de Cry6Aa1 sur sa capacité de former des pores en BLP.

Mots-clés: Bicouche lipidique plane, toxine bactérienne, *Bacillus thuringiensis*, toxine formeuse de pore, Western corn rootworm, Cry6Aa1, δ-endotoxine

CONTENTS

LIST OF FIGURES

LIST OF TABLES

ABBREVIATION TABLE

3-D	Three-dimensional
ABC	ATP-binding cassette
ALP	Alkaline phosphatase
APN	Aminopeptidase N
BBM	Brush border membrane
BBMF	Brush border membrane fragment
BBMV	Brush border membrane vesicle
Bt	*Bacillus thuringiensis*
Bt-R_1	*Bt* cadherin receptor
CAPS	3-(Cyclohexylamino)-1-propanesulfonic acid
CHES	3-[(3-Cholamidopropyl) dimethylammonio]-1-propanesulfonate.
ClyA	Hemolysin E
Cry	Crystal protein
Cyt	Cytolytic protein
DPhPC	Diphytanoylphosphatidylcholine
EGTA	Ethylene glycol-bis(β-aminoethyl ether)-N,N,N',N'-tetraacetic acid
HEPES	4-(2-hydroxyethyl)-piperazine-1-ethanesulfonic acid
HBL	Hemolysin BL
JNK	c-Jun N-terminal kinase
kDa	kilodalton
MAPK	Mitogen-activated protein kinase
MES	2-(N-morpholino)ethanesulfonic acid
MET	β- mercaptoethanol
Mtx3	Mosquitocidal toxin
NCRW	Northern corn rootworm
PC	L-alpha-phosphatidylcholine
PFT	Pore-forming toxin

POPC	1-palmitoyl-2-oleoyl-*sn*-glycero-3-phosphocholine
POPE	1-palmitoyl-2-oleoyl-sn-glycero-3-phosphoethanolamine
PLB	Planar lipid bilayer
Sip	Secreted insecticidal protein
TEP	
TPCK	N-tosyl-L-phenylalanine chloromethyl ketone
Tris	Tris(hydroxymethyl)aminomethane
Vip	Vegetative insecticidal protein
WCRW	Western corn rootworm

ACKNOWLEDGEMENTS

I would like to thank everyone that has contributed to this thesis and to my Master's degree during the past two years.

First of all, I would like to thank *Dr. Jean-Louis Schwartz* for giving me the opportunity to work in this incredible project. For guiding me during the whole project and introducing me to the field of biophysics.

I would also like to thank *James-Christopher Bernard* and *Maxime Schmidt* for being so supportive inside and outside the laboratory. For the great afternoons having a beer and for being such amazing friends. I would also like to thank *Lena Potvin* for her tough love and for teaching me how to properly do bilayers. Thank you *Vincent Lemieux* for starting this project and introducing me into the lipid bilayer technique. I would also like to thank *Dr. Vincent Vachon* for his patience and for his help during the writing process. I would also like to thank all the internship students, who have always been great supporters and have always made me feel at home in Montreal and in the laboratory. *Daline Tho*, *Maxime Schmidt Jr*., *Emilie Huynh* and especially to *Thomas Cauchi*, whose help with the abstract in French has been very much appreciated.

Moreover, I would like to thank Dr. *Lucie Parent* and *Dr. Rikard Blunck* for accepting to be in my Master's committee and giving me advice during our meeting. Also, I would like to thank Dr. *Réjean Couture* for accepting to judge my thesis. Thank you also to all the other members of the GEPROM and the Département de physiologie moléculaire et integrative for supporting me and always helping me in every way they could. Especially, thanks to *Michel Brunette* for all the technical support that has made it possible to complete my experiments. Also, thank you to all the members of Dow AgroDciences for being so open to our ideas and for providing us with all of the toxins. It has been a very enriching and interesting process to have the opportunity to collaborate.

I would also like to thank NSERC for funding the project and Université de Montréal and Département de physiologie moléculaire et integrative for the financial support through the recruitment scholarship, the scholarship of exemption of international tuition fees and the end of master's scholarship.

CHAPTER 1. INTRODUCTION

1.1. *Bacillus thuringiensis (Bt)*

Bacillus thuringiensis (Bt) is a rod-shaped, Gram-positive bacterium that forms spores when facing difficult conditions. This bacterium is a ubiquitous soil microorganism. It can be found in Asia, Europe, Africa, America and Australia (1). Strains have been isolated from insects, stored product dust, water and leaves (2).

The most noticeable characteristic of this microorganism, is that it is pathogenic to invertebrates, mostly insects, by the production of proteins that are toxic to specific species of several orders (3,4). These toxins are produced either as parasporal crystals during sporulation (Fig. 1) or during the vegetative growth of the bacterium (5).

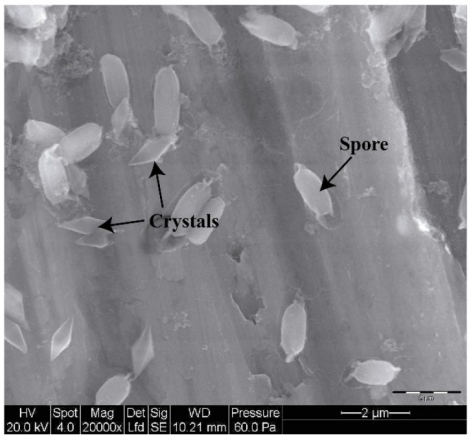

Fig. 1. Spores and parasporal crystals of *Bacillus thuringiensis* from strain H29.3 (5)**.**

Until now more than 700 crystal toxins that are produced by different strains of *Bt* have been discovered (Crickmore, N. et al. "*Bacillus thuringiensis* toxin nomenclature" http://www.btnomenclature.info, June 2016). The genes that code for these proteins are usually located on large plasmids and, for most of them, between transposable elements (6).

1.1.1. Nomenclature

Since the identification and cloning of the first gene that codes for an insecticidal crystal protein, Cry1 (2), the number of novel insecticidal proteins has increased every year, which has produced a need for a coherent nomenclature system. In the first classification system that was

created, the names of Cry toxins and their genes included a primary rank distinction with a Roman numeral, which depended on the insecticidal activity of each protein: CryI for Lepidoptera, CryII for Lepidoptera and Diptera, CryIII for Coleoptera and CryIV for Diptera (7). However, this system presented important drawbacks for the fast classification of these toxins once discovered, the main problem being the fact that, to classify the protein, it had to be bioassayed against different insects to find its target, which was not always possible. This why a new nomenclature system was proposed where, instead of concentrating on the toxicity of the proteins, the classification is based on amino acid sequence (8).

In this system, all of the toxins are given a four-rank name depending on their degree of pairwise amino acid identity with previously discovered and classified toxins. As a result, the toxin denomination and classification is independent of the three-dimensional (3-D) protein structure, host range and even mode of action. Arabic numbers are used for the first and fourth ranks and uppercase and lowercase letters are assigned for second and third ranks, respectively. Proteins that share less than 45% amino acid identity are assigned a different primary rank, proteins sharing less than 78% amino acid identity are assigned a different secondary rank, proteins sharing less than 95% amino acid identity are assigned a different tertiary rank and a quaternary rank is assigned for already established toxins that differ only in a few amino acids because of mutational changes or an imprecision in sequencing (8). For a protein to be included in this nomenclature, it has to be a *Bt* parasporal inclusion that shows toxicity against an organism or share more than 95% amino acid identity with an already established *Bt* toxin (Crickmore, N. et al. "*Bacillus thuringiensis* toxin nomenclature" http://www.btnomenclature.info, June 2016).

1.1.2. Organisms affected by *Bt* toxins

Many Cry proteins have properties that are useful for the control of pests in agriculture to limit the use of hazardous chemical insecticides. However, this is not the only target for *Bt* toxins. *Bt* proteins target a wide range of organisms that are mainly insects, which extend their use in health protection (medical entomology, disease vector control), although some of them are active against other invertebrates and even mammalian cancer cells. More specifically, these toxins have well documented toxicity against Lepidoptera, Coleoptera, Diptera, Hemiptera,

nematodes, snails and human cancer cells of various origins (2,5). Some Cry toxins might possess novel toxin properties that have not been discovered yet, since there are some proteins whose toxicity has not been reported (5).

Some proteins such as Cry11A and Cry1Ab have shown toxicity against several anaerobic bacteria and archaea, such as *Clostridium butyricum*, *Clostridium acetobutylicum* and *Methanosarcina barkeri*. Furthermore, some protein fragments, like a 49-kDa fragment of Cry3Aa, have been shown to have a lytic effect on some bacteria (9). An interesting fact about the mode of action of these Cry toxins on prokaryotes is that they are far less specific than when they target insects.

1.2. Mode of action of *Bt* toxins

From a biological point of view, it has always been thought that the main purpose of *Bt* toxin action was to destroy the epithelial barrier of insects so that the spores would germinate and colonize the hemolymph of the insect, a perfect environment in which the bacteria would live (10). The mode of action by which this would happen has been studied in different organisms but is still far from being fully elucidated.

During the last 30-40 years, most of the research has concentrated on studying the "classical mode of action" (Fig. 2), which states that the toxin is ingested, solubilised, activated, crosses the peritrophic membrane, binds to one or more membrane proteins and forms a pore that leads to osmotic lysis of the cell. In recent years, two more models of *Bt* mode of action have been proposed, which are poorly supported by experimental data so far (11).

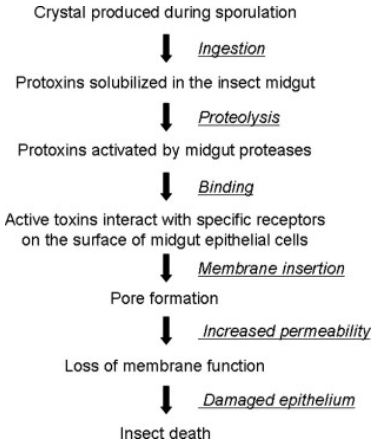

Fig. 2. Schematic representation of the « classical » mode of action (11)**.**

1.2.1. Ingestion of *Bt* toxins

The first step of the mode of action is for the crystal to enter the digestive system of the target insect. This step could explain why some sucking insects and other invertebrates such as spiders and mites are not sensitive to Cry proteins.

1.2.2. Solubilization of *Bt* toxins

After ingestion, the crystal is solubilised inside the midgut of the insect larvae. The difference in the solubility of the inclusion bodies of different *Bt* toxins is mostly determined by the cysteine composition of their protoxins. Although some crystals lack disulphide bridges (12), most of the cysteine residues present in the crystal protein form interchain disulphide bonds. These cysteine residues are highly conserved among the different *Bt* toxins, and are found in the C-terminal half of the toxin. The specific orientation of the thiol groups also plays a role in crystal formation and ultimately in insecticidal activity (13,14). Moreover, solubility of the crystals is also affected by temperature. Crystals that have been frozen (-80 °C) or subjected to very high temperatures were found to be less soluble (15).

Generally, the toxins that target Lepidoptera are solubilised at alkaline pH (9.5 – 11), which is coherent since the midgut of lepidopteran larvae is a highly alkaline environment. The solubilisation step is more difficult to understand for toxins that target coleopteran insects: they are also optimally solubilised at alkaline pH, whereas the midgut of coleopteran larvae has an acidic environment. For example, Cry3Aa remains mostly in its crystal form (95%) between pH 5 and pH 9.5, while the midgut pH of coleopteran larvae is around 6 (16,17) . Therefore, although low solubility does not seem to prevent toxicity in Coleoptera, its role is still not fully understood.

1.2.3. Activation of *Bt* toxins

After solubilisation, the crystal proteins undergo the next step in the mode of action, activation. During this step the proteins are cleaved by insect midgut proteases in various ways, which are determined by the insect species. Depending on how this activation happens, the toxins will show specificity to different species of insects. For example, Cry2 activated by *Pieris brassicae* midgut juice was only toxic to lepidopteran cells, while the same toxin was activated by *Aedes aegypti* midgut juice did only affect dipteran cells (18).

The activation step has been mostly studied in the years of *Bt* research that dealt with Cry1, Cry2 and Cry3. Cry1 protoxins are cleaved at the N-terminal and C-terminal, losing 70-kDa. Cry2 protoxins are only cleaved at the C-terminal, losing around 5-kDa. Cry3 is cleaved at the N-terminal, losing between 6 and 18-kDa, depending on the activation process (19,20).

Activation has been demonstrated to be an important step for toxicity. Moreover, it has been shown that in vitro activation of some Cry toxins could render them toxic towards orders of insects against which they are not naturally active (21).

An alteration of protein activation by midgut proteases has been found to be involved in insect resistance to *Bt* toxins (22). *Bt* resistant insects have been shown to have either proteases with a higher proteolytic activity or a higher concentration of proteases in the gut that resulted in the complete hydrolysis of the toxin core, which therefore resulted in resistance to the toxin. This was also supported by some experiments in planar lipid bilayers (PLBs) where, depending on the enzyme used to activate the protein, the pore formation ability changed, suggesting that proteases directly influence pore formation (23).

1.2.4. Crossing the peritrophic membrane

Once the toxin has been solubilised and activated, and before it reaches to the brush border membrane (BBM) of the insect midgut, where it will interact with different membrane proteins that act as a receptors, it has to go through the peritrophic membrane.

The peritrophic membrane is a layer that surrounds the food bolus in the midgut of various organisms, such as insects. It is mainly composed of chitin, which forms interconnected chains arranged in different layers. There are also around 35-40% of associated proteins, some of them proteases that could cleave the toxins under specific conditions. This composition varies depending on the insect. The main function of this membrane is to protect the midgut epithelium from food particles and microorganisms (24,25).

Some cry toxins are thought to bind to the peritrophic through sugar groups (25). For example, the truncated Cry1Ie, that shows strong insecticidal activity against the Asian corn borer, binds to the peritrophic membrane in a specific way and its domain III is involved in this process (26).

1.2.5. Molecular recognition of *Bt* toxins

The binding of Cry toxins to insect midgut epithelial membrane molecules, which constitutes the next step in their mode of action after crossing the peritrophic membrane, is one of the most important factors in specificity. Direct correlation between species toxicity and specific binding in brush border membrane vesicles (BBMVs) has been demonstrated in some cases. For example, in *Manduca sexta* and *P. brassicae* BBMVs, where Cry1b would only bind to *M. sexta* BBMV while Cry1Ab and Cry1Ba bound specifically to *P. brassicae* BBMVs (27). Binding of Cry toxins to their molecular recognisers has been proposed to be a two-step kinetic model, one step where binding can be reversible and the toxin can dissociate from the receptor irreversible and another step where the toxin binding to the receptor is irreversible. It has been shown that the rate constant for irreversible binding, which is thought to reflect the insertion step of the toxin into the membrane, is better correlated with toxicity than the overall binding. This was proved by showing a direct relationship of Cry1A toxins binding to *Lymantria dispar* BBMVs (28).

Many Cry toxin receptors have been reported so far, although not all of them have been studied in the same depth. The best characterized receptors are aminopeptidase N (APN), cadherin-like molecules, glycolipids and alkaline phosphatases (ALPs). APN, cadherins and ALPs have been studied mainly in Lepidoptera, while glycolipids have been studied as receptors of toxins that target nematodes (29).

1.2.5.1. Aminopeptidase N (APN) receptors

The APN protein family is a class of enzymes whose function is to cleave neutral amino acids from the N-terminus of polypeptides. In 1994 a 120-kDa glycoprotein that showed high similarity with members of the APN family was purified from the midgut membrane of *M. sexta* larvae (30). That same year it was also demonstrated that the mixture of APN from *M. sexta* enhanced Cry1Ac pore formation in lipid vesicles. Actually, these proteins were shown to increase the toxin binding by 35% (31). This interaction was further demonstrated by using PLBs to which the *M. sexta* receptor complexes had been fused. This caused Cry1Aa, Cry1Ac and Cry1Ca to form pores at concentrations that were much lower than when the receptor was not present in the bilayers (32).

So far, several different Cry toxins have been shown to bind APN molecules. Their different patterns of binding complicates further understanding of the whole mechanism (29). It has also been attempted to express APN in cell lines to study how the binding of Cry toxins affects cell toxicity. However, most of the efforts have been unsuccessful (29). On the other hand, expressing *M. sexta* APN in *Drosophila*, was successful and demonstrated that Cry1Ac was 100% toxic to transformed flies at a concentration of 50 ug/ml, in comparison to the control larvae which were unaffected by toxin concentrations up to 1 mg/ml (33).

1.2.5.2. Cadherin receptors

The cadherin superfamily of proteins serves diverse functions such as cell adhesion, migration, cytoskeletal organization and morphogenesis. The most important characteristic of this family of proteins is the presence of repeating calcium-binding domains. These proteins are also glycosylated and anchored to the membrane by a single transmembrane domain, although there are also some GPI-anchored variants. Normally, cadherins are primarily located within adherent junctions and are involved in cell-to-cell adhesion. However, the cadherins that have been identified to be involved in Cry recognition are found in the apical membrane of midgut columnar cells and their physiological role is unknown. In this case glycosylation does not seem to be essential for toxin binding (29). The first identified and purified cadherin that serves as a *Bt* toxin receptor is a 210-kDa protein found in BBMVs of *M. sexta*. It specifically recognizes and binds Cry1Ab with high affinity (34).

Contrary to APN receptors, cadherins have been successfully expressed in cell lines, such as Sf21 cells. Cells that express the Bt-R_1 (a *Bt* cadherin receptor) have acquired sensitivity to Cry1Aa, Cry1Ab and Cry1Ac. This toxicity is similar to the sensitivity of *M. sexta* to these three toxins (35). Cadherin-like receptors have also been expressed in COS7 and HEK293 cell lines. The cells bound and became susceptible to Cry1Aa, Cry1Ab and Cry1Ac (36). Cadherins have also been demonstrated to bind dipteran targeting toxins such as Cry4Ba (37).

1.2.5.3. Alkaline phosphatase (ALP) receptors

Alkaline phosphatases (ALP) have also been identified as Cry toxin receptors, but the knowledge about ALP-Cry toxin interaction is considerably smaller than for other receptors. ALP is a molecule that removes phosphate groups from proteins and nucleotides. In 1994, it

was suggested that ALP might act as a Cry1Ac receptor in *M. sexta.* It was also noted that the ALP expression levels were reduced in some *Bt* resistant strains of *Heliothis virescens,* suggesting that it played a role in the toxin's mode of action (31). However, the role of ALP in mediating Cry1Ac susceptibility has yet to be established. ALP has been shown to be an important receptor for Cry11Aa in *A. aegypti* (38). It has been demonstrated that *A. aegypti* larvae can increase their resistance to Cry11Aa 124-fold by modifying the expression of receptor proteins such as ALPs and APNs (39).

1.2.5.4. Glycolipid receptors

The interaction between glycosphingolipids and Cry toxins was first proposed in 1986 (40). It was also shown that Cry1A bind to different parts of glycolipids depending on activation (41). It was not until 2005 that the presence of an invertebrate-type glycolipid receptor for Cry toxins was found in *Caenorhabditis elegans* (42). This was discovered when mutants that failed to produce ceramide-based glycolipids that bind Cry5Ba were found, which made them resistant to the toxin. Some preliminary results also suggested that glycolipids were not only responsible for binding Cry5Ba toxins in *C. elegans*, but that they were also found in other order of insects such as Lepidoptera. Glycolipids extracted from the midgut of *M. sexta* were shown to bind Cry1Aa, Cry1Ab and Cry1Ac (42). Yet, the importance of this interaction and its role in toxin susceptibility remains to be explored.

1.2.5.5. ATP-binding cassette (ABC) transporter receptors

ATP-binding cassette (ABC) transporters are membrane proteins that are widespread in prokaryotes and eukaryotes. They are responsible for transporting molecules through cell membranes. Linkage mapping analysis showed that resistance to Cry1Ab in some strains of *H. virescens* was linked to several mutations in an ATP-binding cassette transporter gene, which had never before been considered to play a role in the mode of action of Cry toxins (43).
This was later confirmed by a study showing that the same mutation in ABCC2 from Cry1Ab-resistant insects resulted in a much reduced susceptibility to Cry1Ac and Cry1Ab in Sf9 cells that were expressing the truncated ABCC2 (44).

1.2.6. Pore formation

After the molecular recognition step, the toxins are thought to insert into the membrane and form pores, which eventually leads to osmotic lysis of the cell. This step of the mode of action has been extensively studied using different biophysical techniques such as light scattering assays, fluorescence assays, PLBs and cellular electrophysiology.

Pore formation has been shown in receptor-free PLBs (Fig. 3A), the first time using toxins Cry1Ac and Cry3A, which target lepidopteran and coleopteran insects respectively. These early experiments showed that the toxins were able to form pores at very alkaline pH with a strong cationic selectivity. It was also shown that the pores had several conductance levels. In the case of Cry1Ac main conductances of the pores are 450 pS and Cry3A forms pores of around 500 pS, both in alkaline conditions (45-48). Selectivity experiments performed later have proven that the general cationic selectivity of *Bt* toxins is not as strong as it was thought in the first place (49,50).

Pore formation by the binary toxin Cry34Ab1/Cry35Ab1 has also been investigated (51). This toxin was not a very efficient pore former under alkaline conditions, which may be expected since the midgut conditions of the coleopteran target insect are acidic (17). While the two components were able to form pores separately in PLBs, optimal pore formation was attained when they were used together (51).

Pore formation in the presence of receptors has also been studied (Fig. 3B). Initially, this was done by doing light scattering assays with BBMVs isolated for *M. sexta* (52). It was demonstrated that activated Cry1Ac produced a change in the solute permeability of the BBMVs, which could be explained by pore formation. Pore formation by Cry1Ac occurred at physiologically relevant toxin concentrations and it was shown that these pores are also not very selective.

The effect of the receptor on pore formation was also demonstrated by fusing BBMVs or purified receptors into PLBs (32,53). It was shown that the integration of purified APN molecules, which are receptors for Cry1Ac, into PLBs increased the conductance of the Cry1Ac pore, decreased the concentration needed for pore formation by 250-fold and induced current rectification. Yet for Cry1Aa, the concentration of toxin in receptor rich bilayers was only reduced 100-fold, conductance was also enlarged and there was no rectification, which could mean that Cry1Ac and Cry1Aa did not interact in the same way with their receptor (54). Pore

formation by Cry1Ca and its receptor modulation also been studied in Sf9 cells by using patch clamp (55). The pore formation mechanism in Sf9 cells was proven to be very similar than that in PLBs. The only difference being in the selectivity, which afterwards was shown to be due to the difference in pH conditions (50) .

Finally, the size of the pores of Cry1Ac has been estimated by using two different techniques. Initially, this was done by using an osmotic swelling assay on *M. sexta* BBMVs using molecules of different sizes, such as polyethylene glycols (56). Later, it was estimated by using PLBs and polyethylene glycols (57). The pores made by Cry1C had a uniform radius around 1-1.3nm in both cases. The results in the latter study show that the multiple conductance levels observed experimentally may be due to clusters composed of different numbers of similar pores that are cooperatively gated.

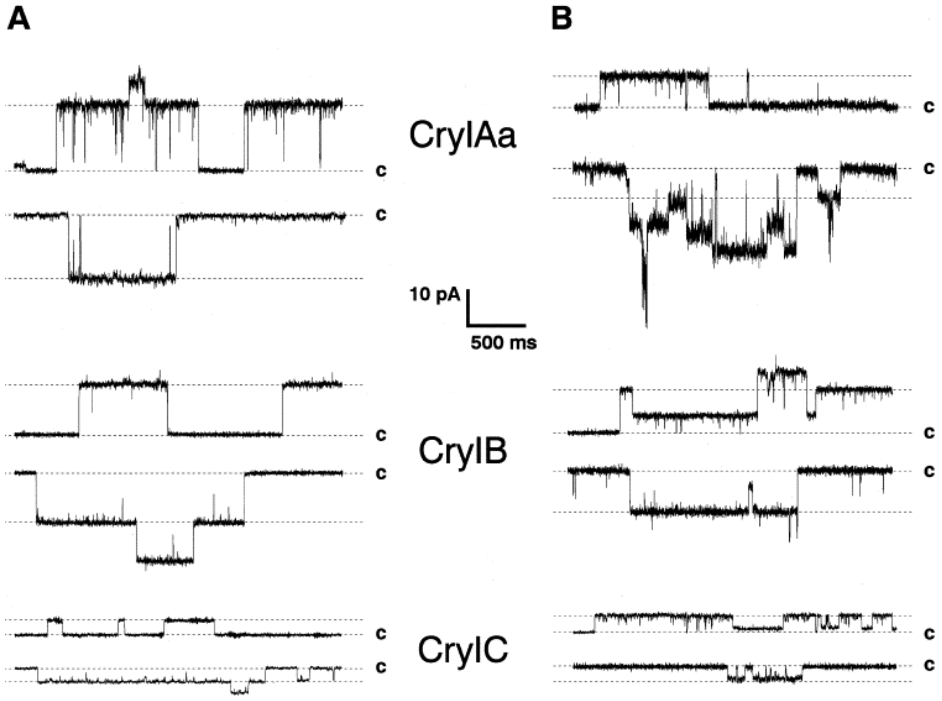

Fig. 3. Pore formation demonstration of Cry1Aa, Cry1B and Cry1C in PLBs. In the absence of receptors (A) and in the presence of M. sexta APN receptor (B). The currents correspond to +40mV (upper traces) and -40mV (lower traces) (32).

1.2.7. *Bt* toxin effect on the membrane potential of lepidopteran insect midgut cells

In lepidopteran midgut cells, the electrochemical K^+ gradient across the apical membrane, serves as the main driving force for the absorption of solutes, such as amino acids. A vacuolar-type proton ATPase, coupled with an electrogenic K^+/H^+ exchanger, generates this

gradient (58-60). When a *Bt* toxin forms pores in the apical membrane of these cells, this gradient is abolished and the cells lose their capacity to transport the solutes and allow the equilibration of pH between the highly alkaline content of the midgut lumen and the cells' cytoplasm. To study how *Bt* toxins directly affect the potential of the midgut cells, the glass microelectrode technique was used on freshly isolated midguts of lepidopteran larvae (61). The potential across the membrane midgut cells of *Lymantria dipar* and *Bombyx mori*, which was around -80 mV in the absence of toxin, decreased rapidly in the presence of different activated Cry toxins. Cry1Aa, Cry1Ab, Cry1Ac, Cry1C, Cry1E and Cry1F all caused a fast depolarization of the apical membrane of the cells from the midgut of *L. dispar*. However, toxins such as Cry1Aa and Cry1C had no effect on the potential of the basolateral membrane of these cells. Also, Cry1B and Cry3A did not have any effect on the potential of these cells, which is expected since they also show no toxicity in vivo against this insect. Yet, the proteins' toxicity in vivo and in vitro did not fully correlate in *L. dispar* since for example Cry1Ac was not very active in the bioassays but triggered the same depolarization as Cry1Aa, which had a very high toxicity bioassays. For *B. mori* Cry1Aa caused a fast depolarization of the apical membrane of the midguts but Cry1Ab and Cry1Ac were inactive, a result which correlates with in vivo toxicities.

1.2.8. Intracellular effects of *Bt* toxins

The effect of *Bt* toxins in Sf9 cells has been not only studied at the pore-formation level, but also at the level of intracellular events. When the cells were exposed to Cry1C, there was a very fast rise in the intracellular calcium followed by the activation of anion selective channels. This was the first demonstration that intracellular signals occurred in response to *Bt* toxin exposure (55).

Lately, researchers have started to be interested in putative defense mechanisms in cells under attack by pore-forming toxins (PFTs). Such mechanisms have been studied using Cry5B, a *Bt* toxin active against *C. elegans* and streptolysin O, which permeabilizes mammalian cells (62). One hundred and six genes have been identified though RNA interference screening, which play some kind of cellular protection role against a PFTs. Two previously identified mitogen-activated protein kinase (MAPK) pathways, the p38 pathway and the c-Jun N-terminal kinase (JNK) pathway, are crucial components of the defense system. It was demonstrated that the JNK MAPK pathway is the key central regulator of PFT induced transcriptional and functional

responses, while the p38 is not. The transcription factor activator protein 1 (AP-1) is the first cellular component involved in this defense mechanism. This research area on cell protection against PFTs may provide a solid starting point to further understand the intracellular effect of *Bt* toxins.

1.2.9. Proposed models of *Bt* mode of action

Since the early 2000s, two different models of *Bt* toxin mechanisms of action have been proposed. One is the sequential binding model that attempts to describe a number of intermediate steps leading to pore formation and osmotic-colloidal lysis of target cells (63,64). The other model is the signalling pathway model, which states that pore formation is not important. Cell death is triggered by the signalling pathways activated by *Bt* toxins in target cells (65,66).

1.2.9.1. The sequential binding model

The sequential binding model postulates that following activation of *Bt* toxin by midgut proteases, the toxin first binds to a cadherin molecule with low affinity but high capacity. This binding causes a conformational change of the toxin that eases the proteolytic cleavage of its first α-helix (63). Once this helix is removed, the toxin oligomerizes and forms different pre-pore structures, depending on the activation step (64), that bind to APN receptors with very high affinity. This allows the insertion of the pore into the membrane, which results in the osmotic unbalancing and death of the cell (63). Unfortunately, the data in which this model is based have not been independently obtained in other laboratories and may have been overinterpreted (11).

1.2.9.2. The signalling pathway model

The signalling pathway model states that pore formation, which has been demonstrated in a number of laboratories worldwide for decades, does not kill the cells. More specifically, in this model Cry1Ab binds to Bt-R_1, which activates Mg^{2+}- dependent pathways never reported elsewhere (65). The binding also stimulates the production of alpha G proteins (GαS) and cAMP, which activates a protein kinase A leading to necrotic cell death (66). This model suffers from severe experimental flaws that lead to rushed conclusions. It cannot reasonably be supported (11).

1.3. *Bt* toxins structures and function

Bt produces a wide range of toxins such as δ-endotoxins, enterotoxins, β-endotoxins, haemolysins, Vegetative insecticidal proteins (Vip) and Secreted insecticidal proteins (Sip). The *Bt* toxins that have been studied the most, are the δ-endotoxins, Cry (crystal) toxins and Cyt (Cytolytic) toxins.

1.3.1. Cry toxins

So far, the most studied Cry toxins display a 3-D structure of three domains. However, in the past decade, due to the fast rise in insect resistance to commercialized toxins, efforts have been made to discover toxins that may possess a different molecular structure and possibly a different mode of action (67).

1.3.1.1. Cry toxins with 3-domain structures

The first atomic structure of a *Bt* toxin was that of the activated coleopteran Cry3Aa (Fig. 4A) at a resolution of 2.5Å (68). A few years later, the 3-D structure at 2.25Å resolution of the activated lepidopteran-targeting Cry1Aa toxin (Fig. 4B) was described (48). Both structures showed a very similar arrangement of their three different domains (Fig. 4C).

Domain I of Cry3Aa starts at Thr61 up to Leu290 and is a 7-helix bundle, with a central helix surrounded by 6 helices (68). On the other hand, in Cry1Aa, domain I is composed by 8 α-helices, where α2 corresponds to α2a and α2b. In the 3-D structure, α5 is surrounded by the others (48). This α-helix bundle shows structural similarity to other PFTs such as colicin A. Due to this similarity, it was suggested and later demonstrated that Domain I was responsible for pore formation in the membrane (47,48,69).

Domain II is a β-prism that contains 3 antiparallel β-sheets packed around a hydrophobic core. It has a triangular cross-section and goes from Tyr291 to Phe500 in Cry3Aa (68). Cry1Aa is very similar. However, apart from the β-sheets there are two short α-helices in the structure (48).

Domain III, which is the C-terminal part of the protein, extends from Phe501 to Asn644 in Cry3Aa. It is very similar in Cry1Aa, with a jelly-roll topology with the strands forming a β-sandwich (48,68).

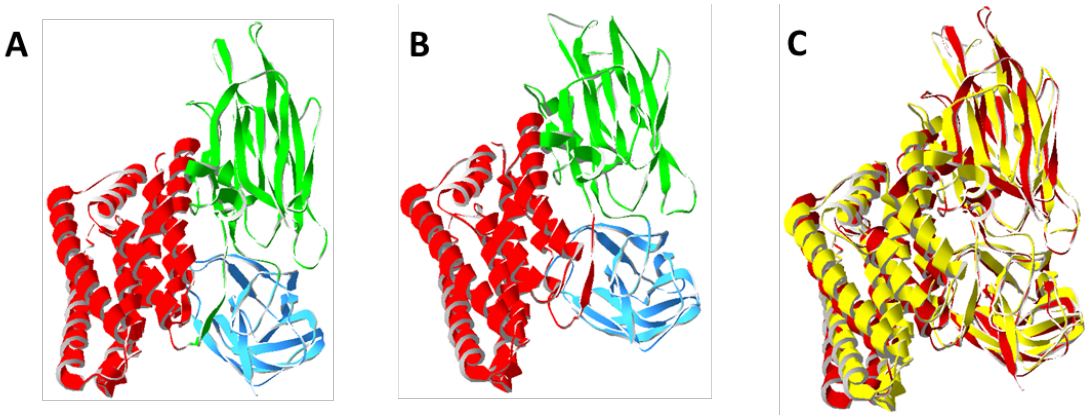

Fig. 4. 3-D ribbon representation of (A) Cry3A activated toxin (1DLC) and (B) Cry1Aa activated toxin (1CIY). Domain I is colored in red, Domain II is colored in green and Domain III is colored in Blue. (C) Superimposed Cry1Aa (yellow) and Cry3A (red).

The structures of other 3-domain Cry toxins have been determined later. One of them, at a 2.2Å resolution, is that of the Cry2Aa protoxin, the first available structure of a toxin that is specific to both Diptera and Lepidoptera. The overall topology of Cry2Aa is similar to that of Cry3Aa and Cry1Aa (70), despite little sequence identity between Cry2Aa and the two other toxins (20% or less) (71). In recent years more structures of 3-domain toxins have been elucidated (Table I).

Table I. Three-domain Cry toxins that have been crystalized so far (Modified from (72))**.**

Toxin	Target Insects	Activation	Resolution	PDB ID	References
Cry1Aa	Lepidoptera	Trypsin 65-kDa	2.25Å	1CIY	(48)
Cry1Ac	Lepidoptera	Trypsin 65-kDa	2.35Å	4ARX	(73)
Cry1Ac	Lepidoptera	Protoxin 130-kDa	3.2Å	4W8J	(74)
Cry2Aa	Diptera / Lepidoptera	Protoxin 62-kDa	2.2Å	1I5P	(70)
Cry3Aa	Coleoptera	Papain 67-kDa	2.5Å	1DLC	(68)
Cry3Bb	Coleoptera	Chymotrypsin 67.2-kDa	2.4Å	1JI6	(75)

Cry4Aa	Diptera	Trypsin 65-kDa	2.8Å	2C9K	(76)
Cry4Ba	Diptera	Chymotrypsin 68-kDa	1.75Å	1W99	(77)
Cry8Ea	Coleoptera	Chymotrypsin 66.2-kDa	2.2Å	3EB7	(78)
Cry5B	Nematodes	Elastase 66.14-kDa	2.3Å	4D8M	(79)

Until 2014, all of the available *Bt* toxin crystal structures, except for that of Cry2Aa, were those of the activated form of the toxins. However, the full length structure of Cry1Ac protoxin was recently solved (74). The structure of the full-length Cry1Ac protoxin was solved a 3.2-3.5Å resolution (Fig. 5). It is made of 7 domains, the already known three domains, and four more. Two of these are mainly α-helices and the other two display β-sheet arrangements. Interestingly, the part of the structure that corresponds to the activated Cry1Ac and of Cry1Ac protoxin are very similar (74).

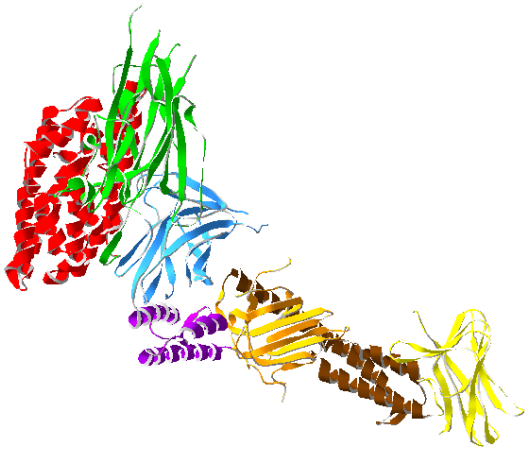

Fig. 5. 3-D ribbon representation of Cry1Ac protoxin (4W8J). Domain I is colored in red, Domain II is colored in green, Domain III is colored in blue, Domain IV is colored in purple, Domain V is colored in orange, Domain VI is colored in brown and Domain VII is colored in yellow.

1.3.1.1.1. Structure-function relationships of 3-domain toxins

Once the structure of the first 3-domain *Bt* toxin was elucidated, a considerable amount of effort was put into understanding its structure-function relationships.

Domain I was proposed to be the pore-forming domain (48,68). It was demonstrated that the first domain of these *Bt* toxins was sufficient for pore formation in PLBs and Rb^+ efflux in lipid vesicles (47,80-82). Interestingly, the first domain alone of the toxin did not have insecticidal activity towards *H. virescens* (80). Other studies on the mosquitocidal toxin Cry4B and its α1-α5 fragment demonstrated that they formed slightly cation selective pores in PLBs, supporting the initial experiments showing that the first domain of Cry3Aa formed a functional pore that had similar properties to those of the full toxin (47,83). It was also shown that the conductance and gating depended on the pH conditions used for the processing of the protoxin, which provided a link between pore formation and the earlier steps of solubilisation and activation. The umbrella model for toxin insertion was proposed based on the Cry3Aa structure and on its similarity to colicin A (84). In this model α4 and α5 of domain I would be the ones penetrating the membrane. This hypothesis was further studied by using different techniques such as the biotinylation of several cysteine residues in α4, α5 and surroundings that affected the toxin's pore formation (85) and disulphide bridge engineering(85,86). It was demonstrated that the mutation of amino acid residues of α4 of domain I had a large impact on the pore's biophysical characteristics, which not only supported the umbrella model but showed that α4 lines the lumen of the pore (87-89). Several studies done also concentrate on α3, using circular dichroism, protease sensitivity, electrophoretic mobility analysis and point mutations. It was shown that several mutations in α3 affected pore formation and oligomerization (85,90). Finally, Domain I interhelical loops appear to be important for conformational changes that lead to pore insertion, and unfolding of the protein around a hinge region between domain I and II is thought to play an important role (85,86,89,91).

Domain II was proposed to be the binding domain due to the identification of specificity-determining regions (92). For instance, the specificity of Cry2A for Lepidoptera and Diptera as opposed to the Lepidoptera specificity of Cry2B was due to residues 307-382, which are located in domain II (71). Further studies of Cry2Aa, and correlation with chimeric scanning data of Cry2Aa and Cry2Ab, indicated that the putative receptor binding epitope lied on the core of the β-sheets of the domain (70,71).

Domain III, which was thought to be mainly involved in structural stability of *Bt* toxins, also played a role in binding and pore formation. Several mutations in a conserved alternating arginine region had a direct effect in pore formation and pore conductance (93,94).

Finally, taking into account the structural and functional features of 3-domain toxins mentioned before, a model of Domain I disassembly was proposed (78). In this model, after the binding of the Cry toxin to its receptors, there is a conformational change in the β-sheets of domain II. This change mainly influences the interface between domain I and domain II, which makes α7, which has a kink, move towards the center of the helix bundle in domain I. This forces helices α2b and α3, which are acting as a lid in domain I, to swing away from the central helix α5, a displacement that is facilitated by proline 105 of α3 that is highly conserved among the 3-domain Cry toxins. Finally, after the lid is open, α4 and α5 are exposed and can penetrate the membrane.

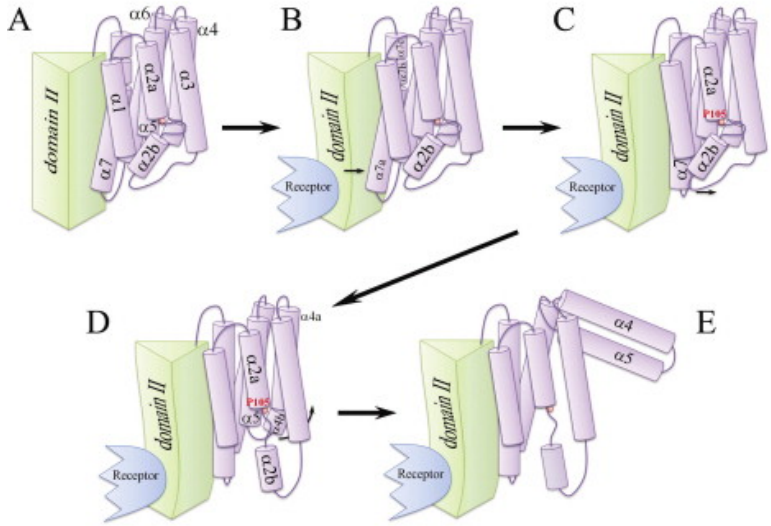

Fig. 6. Model for domain I disassembly (78)**.**

1.3.1.2. Cry toxins with non 3-domain structures

Other *Bt* atomic structures that do not display three domains such as binary toxins, like Cry34Ab1/Cry35Ab1, and aerolysin-like toxins, like parasporin 2, have also been elucidated.

1.3.1.2.1. Binary toxin: Cry34Ab1/Cry35Ab1

Cry34Ab1 and Cry35Ab1 is a binary toxin produced by *Bt*. The structures of Cry34Ab1 and Cry35Ab1 have been elucidated at resolutions of 2.15Å and 1.8Å respectively (95).

Cry34Ab1 (Fig. 7A) is a 14-kDa protein. Its structure is similar to that of actinoporins, PFTs produced by sea anemones, or hemolysins, which are membrane interacting proteins. The

protein folds in a β-sandwich conformation with two β-sheets packed against each other. The entire protein has a relatively flat layer-like conformation with only two slightly twisted β-sheets. Cry35Ab1 (Fig. 7B), on the other hand, is a 44-kDa protein that has structural features of the Toxin_10 family, which includes insecticidal proteins such as the binary toxin BinA and BinB (Fig. 7C) from *Lysinibacillus sphaericus*. It has an elongated rectangular shape and is composed of two domains. The N-terminal domain has a β-trefoil fold with a very hydrophobic core, while the C-terminal domain contains 6 helices and three antiparallel β-sheets. An interesting characteristic about this toxin is that it contains two cysteine residues that are too far apart to form a disulphide bridge, but the replacement of one of these cysteines reduces the toxin's activity.

Although both Cry34Ab1 and Cry35Ab1 were able to form pores in PLBs at pH 5.5 separately, maximum pore formation efficiency was achieved when both toxins were combined (51).

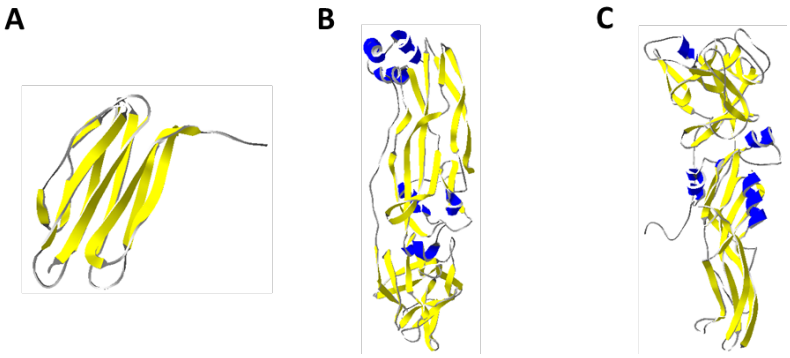

Fig. 7. 3-D ribbon structure of (A) Cry34Ab1 (4JOX), (B) Cry35Ab1 (4JP0) and (C) BinB (3WA1).

1.3.1.2.2. Aerolysin-like toxins: Parasporin-2 (PS2) and Cry51Aa1

In the last decade new *Bt* toxins have been discovered (96,97) that share structural properties with aerolysin (98), a protein produced by *Aeromonas hydrophila* that belongs to the family of β-PFTs, even though they share very little sequence similarity.

Parasporin-2 (PS2), also classified as Cry46 (97), is a *Bt* toxin active against cancer cells. Upon activation by proteases, the 37-kDa protoxin is transformed into a 30-kDa toxin. The structure of this toxin was elucidated at 2.38Å resolution (Fig. 8A) (99). It has an unusually elongated structure that is mostly dominated by β-strands, which twist and run along the long axis of the molecule. The structure is divided in 3-domains. Domain I comprises a small β-sheet

and short α-helices and is thought to be the part of the molecule that binds to the cancer cells. The other two domains are thought to be involved in protein oligomerization and pore formation. One of the most interesting features of the toxin, can be found in domain II, where there is a putative pore-forming β-hairpin that is characteristic of the aerolysin-type toxins. Furthermore, at the surface of domain II, there is a large number of exposed side chains of serine and threonine residues that might orient the molecule on the cell membrane when domain I binds to the target. This protein is a PFT as demonstrated in PLBs and by patch clamp experiments on HepG2 cells (*unpublished data, Schwartz' laboratory*).

The complete structure of the Cry51Aa1 protoxin has been elucidated by X-ray crystallography at 1.65Å resolution (Fig. 8B) (100). This is the first coleopteran active *Bt* toxin that has a high structural similarity to the aerolysin-type PFTs. This protein is structurally very similar to PS2. Almost a quarter of the residues are serines or threonines scattered throughout the protein. They may be involved in allowing the molecule to move freely and closely to the membrane when the N-terminal domain binds to the receptor, in guiding the amphipathic loop towards the membrane and in promoting oligomerization.

These proteins have very little sequence similarity with most of the Cry toxins with an already elucidated structure. It also has a very limited sequence similarity to the family of aerolysin-like PFTs too even if the structure (Fig. 8C) is similar.

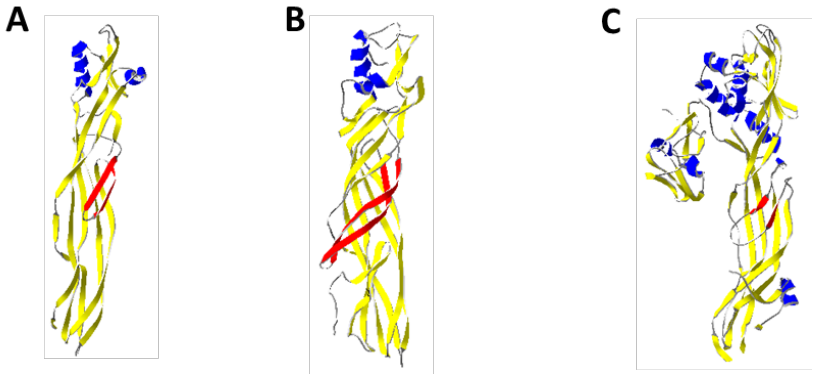

Fig. 8. 3-D ribbon structure of (A) Cry46 (Parasporin 2) (2ZTB) (B) Cry51Aa1 protoxin (4PKM) and (C) Proaerolysin (1PRE). The β-hairpin is colored in red.

1.3.2. Other toxins

In addition to Cry toxins, *Bt* produces Cyt, Vip and Sip toxins, which have been shown to have very different 3-D structures.

1.3.2.1. Cyt

Cyt toxins are produced as parasporal crystals, at the same time as Cry toxins by *Bt* subsp. *israelensis* (101) mainly, but have cytolytic activity and their molecular mode of action is poorly understood (102). These toxins have specific insecticidal activity towards dipteran insects, such as mosquitoes and black flies (103). They are also toxic against mammalian cell lines in vitro (104,105). Until now, three different Cyt toxins have been crystalized and their structure is very different from that of any other *Bt* toxin, which might be related to their different mode of action.

Cyt2Aa and Cyt2Ba (Fig. 9A) structures have been resolved at 2.6Å and 1.8Å resolution, respectively (106,107). They are composed of a single αβ-domain that comprises a β-sheet between two outer layers of α-helix hairpins. In the protoxin form, Cyt2Aa is a nonhemolytic dimer that is linked by the N-terminal β-strands. Activation cleaves the N-terminal and C-terminal domain segments, which leads to dimer dissociation (106).

The activated monomeric form of Cyt1Aa, which is the most toxic protein in the Cyt family, was crystalized and solved at 2.2Å resolution (Fig. 9B) (108). Cyt1Aa adopts a similar structure as Cyt2Aa. It has been hypothesized that Cyt toxins could undergo a conformational change that would be necessary for membrane insertion. The α-helical layers would swing away, exposing the hydrophobic β-sheets that would then insert into the membrane. This hypothesis has been supported by the identification of a lipid binding pocket between the β-sheet and the helical layer of Cyt1Aa, which explains the binding of this Cyt toxin to specific unsaturated membrane phospholipids. It should be noted that the Cyt structure resembles that of volvatoxin (Fig. 9C), a pore-forming cardiotoxic protein (109).

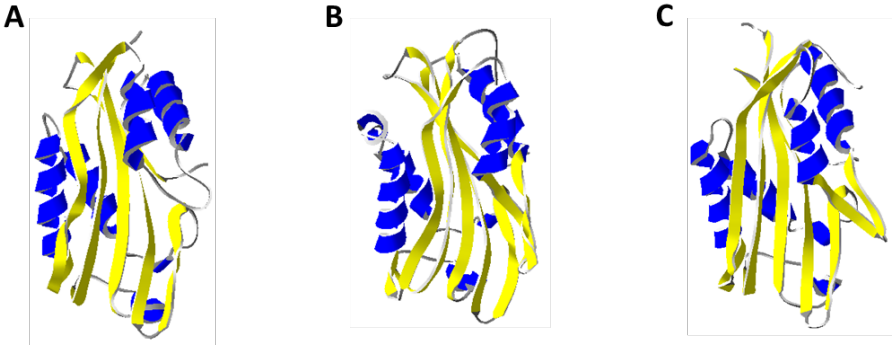

Fig. 9. 3-D ribbon representation of (A) Cyt2Ba (2RCI), (B) Cyt1Aa (3RON) and (C) Vovlatoxin (1PP0).

1.3.2.2. Vip

Vip toxins (vegetative insecticidal proteins) are produced by *Bt* and *Bacillus cereus* during their vegetative growth phase (For review see (110)). Vip1 and Vip2 is a binary toxin that targets coleopteran insects. At least one Vip toxin, Vip1, has been shown to be a PFT (111), while Vip2 is NAD-dependent enzyme that interferes with polymerization of actin (112).

Vip2Aa has been crystalized and its structure has been elucidated at 1.5Å resolution (Fig. 10) (113). It shows a high structural homology in the C-terminal and N-terminal αβ-domains with the family of ADP ribosylating toxins, which regulate post translational modification of proteins. He structure of Vip3 has not been elucidated yet, however it has been shown that it is a PFT (114).

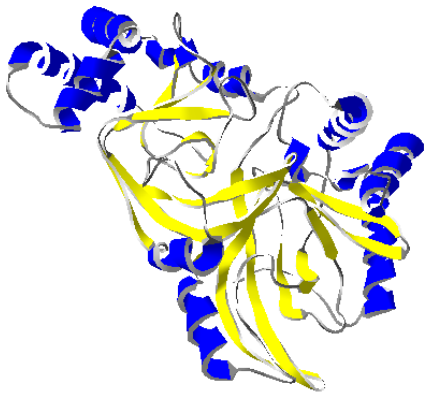

Fig. 10. 3-D ribbon representation of Vip2 (1QS1)

1.3.2.3. Sip

Sip toxins are insecticidal proteins secreted by *Bt* during growth. It is active against coleopteran larvae. So far, only one Sip toxin has been identified, Sip1Aa1, a 367 amino acid, 41-kDa protein (115). It shows a significant similarity to Mtx3, a mosquitocidal toxin from *L. sphaericus*. Its mode of action remains unknown, although based on its homology to Mtx3 it has been hypothesised that Sip1Aa might be a pore former. The structure of this toxin has not been elucidated yet.

1.4. *Diabrotica virgifera virgifera* (Western corn rootworm, WCRW)

Diabrotica virgifera virgifera LeConte (Western corn rootworm, WCRW) is one of the most important insect pests of maize around the world, being especially detrimental in the major

maize producing states of the north-central USA (116). In North America only, the cost of insect control and losses to WCRWs account for more than 1000 million dollars every year. In Europe, 472 million euros a year have been estimated only in crop losses due to this pest, since it was first introduced in the 1990s (117). A closely related species, the Northern corn rootworm (NCRW, *Diabrotica barberi*), is becoming a major pest in Northern United States and Canada (Centre for agriculture and biosciences international, http://www.cabi.org/, August 2016).

1.4.1. Geographic distribution

The WCRW originates from America, more specifically from Central America (118). It uses different means of dispersal: while larvae can only move relatively small distances, adults can fly to different maize fields and are able to migrate short and long distances. Adults may be carried by wind during cold fronts or thunderstorms (116). Several studies have determined that in-field dispersal of male WCRWs respond to pheromone release by reproductive females and by available food (119). WCRWs have been detected in all North America and Eastern Europe, while NCRWs have only been detected in North America.

1.4.2. Biological cycle and ecology

The biological cycle of WCRWs consists in four different stages (Fig. 11): egg, larvae, pupae and adult. Flattened oval eggs, around 500 µm long, are laid just before the winter and require a cold-induced diapause period before hatching. These are usually concentrated in the top 5 to 20 cm of soil. Three larval instars develop in corn roots. The larvae are slender and white to pale yellow. The third instar larvae can be up to 10 mm long. The pupae are white, turning brownish just before adult emergence. They are found in the soil near the roots of corn plants. Finally the adults emerge in the summer and prevail in the maize field until the autumn. These adults are elongated and of a greenish-yellowish colour (118). WCRW insects are univoltine, there is one generation per year (120).

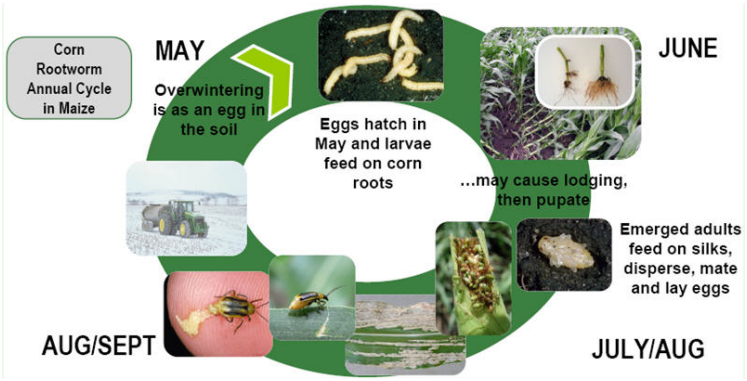

Fig. 11. Life cycle of *Diabrotica virgifera virgifera* (permission asked, www.pioneer.com, August 2016).

1.4.3. Physiology relevant to *Bt* studies

The physiology of WCRWs has not been as well investigated as that of lepidopteran or other coleopteran insects, one of the reasons being the very small size of the larvae that are difficult to study with available tools and methods.

1.4.3.1. Midgut pH and proteases

The general midgut pH has been measured in homogenized midgut juice of third instar WCRW larvae. It was found to be acidic around 5.75 units of pH by using a pH microelectrode (17). However, it cannot be excluded that pH is compartmentalized and the presence of more alkaline microenvironments in the larval gut.

A large number of proteases has been detected in third instar larvae of WCRWs. The main serine endopeptidases are trypsin, chymotrypsin, elastase, cathepsin G, plasmin and thrombin. Cysteine endopeptidases, which are often combined with aspartic endopeptidases, are thought to be the main proteases in the midgut of WCRWs due to its low pH. The main proteases of this category that have been identified are cathepsin L, papain, cathepsin B and cathepsin H. There is also an exopeptidase aminopeptidase, which is surprising considering that this protease activity is optimum at pH 9 (17).

1.4.3.2. Receptors

Finding *Bt* toxin receptors in WCRWs has proven to be a very difficult task. Using an expressed sequence tag, a coleopteran cadherin was identified as a putative *Bt* receptor. This

cadherin contains several regions of high identity to lepidopteran cadherin proteins (121), suggesting a common molecular basis for susceptibility to Cry toxins in lepidopteran and coleopteran species (122).

So far, no other receptor in coleopteran species has been identified. However, competitive binding studies in WCRW BBMs have demonstrated that Cry34Ab1/35Ab1 does not share binding sites with other coleopteran-active *Bt* proteins such as Cry3Aa, Cry6Aa and Cry8Ba (123).

1.4.4. *Bt* toxins currently used to control WCRWs

Bt toxins have been used for WCRW pest control for a number of years with different strategies and mitigated success. In European countries pheromone traps are used to detect WCRW infestation, followed by insecticide treatment (124). In the US, where this pest is a main problem, other methods are also used such as crop rotation (125), which consists in planting different kinds of plants that are not affected by WCRWs so that WCRWs will not be able to feed and will not complete its biological cycle. Biological control has also proven to be a somehow efficient method to fight WCRW pests by using a dipteran parasite like *Celatoria compressa* or entomophatogenic nematodes such as *Heterorhabditis bacteriophora* (126). Chemical control still represents the most economically feasible approach, using chlorinated hydrocarbons, carbamates or organophosphates (127).

Bt toxins have also proven to be a very efficient tool to control WCRWs. Commercial *Bt* plants contain Cry3Bb1, mCryA and Cry34Ab1/35Ab1 toxins. They are either being commercialized as traits with one or two *Bt* toxin genes registered in the US (120). However, insect resistance to *Bt* continues to increase. There is, therefore, a strong need to find new *Bt* toxins against WCRWs and to use different strategies such as setting refuges, host plants that do not produce *Bt* toxins, or developing transgenic plants that express more than one *Bt* toxin in order to delay resistance (120).

1.4.4.1. Cry3Bb1

Cry3Bb1 is currently used as a bioinsecticide against WCRWs. However, this protein is not very toxic to WCRWs. WCRWs became rapidly resistant to this toxin in the laboratory,

greenhouses and fields (120). Evidence of resistant populations of WCRW to Cry3Bb1 was reported in Iowa fields in 2009 (128). Experimental evidence has demonstrated that WCRW's rapid evolution of resistance to Cry3Bb1 happened when adequate refuges were not provided.

1.4.4.2. mCry3A

Cry3A is the first *Bt* toxin that showed activity against a coleopteran insect species, *Leptinotarsa decemlineata* (129), but it has no effect on WCRW pests. However, it was demonstrated that the addition of a chymotrypsin/cathepsin H protease recognition site in an exposed region of domain I, in the loop between α2 and α3 of Cry3A, results in toxicity of the modified protein (mCry3A) against neonate WCRW larvae. It is thought that the introduction of this site enhanced the activation and binding of the toxin to the BBM of midgut cells (130). Nevertheless, after four generations of greenhouse selection, the survival of the selected WCRW strain was similar on mCry3A *Bt* corn and non-*Bt* corn (120).

1.4.4.3. Cry34Ab1/Cry35Ab1

Cry 34Ab1/35Ab1 is one of the newest *Bt* toxins currently commercialized for WCRW pest management. However, after 8 generations of selection, the survival rate of WCRWs increased up to 58.5 fold (120). This suggests that there is a very high risk of resistance of WCRWs to *Bt* corn producing this binary toxin. This risk is thought to be similar to the one for Cry3Bb1 corn.

1.5. Cry6Aa1 toxin

There are two different proteins that belong to the Cry6 family, Cry6A and Cry6B. They are both active against coleopteran pests (131,132). Furthermore, Cry6A is also active against several nematode species (133). The two toxins share 50% identity. Cry6B lacks 88 amino acids found in the C-terminus of Cry6A (133).

1.5.1. Target organisms

Cry6Aa has been shown to be toxic to one coleopteran species, *Diabrotica virgifera virgifera*, and three different species of nematodes, *Panagrellus radivivus*, *C. elegans* and

Distolabrellus veechi (131,133). The interaction of Cry6A with *C. elegans* has been investigated. This toxin suppresses growth, decreases brood size, reduces feeding and alters the locomotion ability of this nematode (134). Besides, all *C. elegans bre* mutants, selected for resistance to Cry5B, remain susceptible to Cry6Aa (135). Until now, it has only been possible to identify one coleopteran species that is susceptible to Cry6B, *Hypera postica* (132).

1.5.2. Structure

The crystal structure of Cry6Aa, a 475 amino acid protein, has been elucidated at 2.70 Å resolution (136) for the native form and by two different research groups at 2.0 Å and 1.90Å resolution for the trypsin-treated form (136,137). Nematode bioassays showed that the minimal toxic fragment of Cry6Aa was located between Arg11 and Asn389, indicating a molecular weight of 43 kDa, whereas the fragment starting at His12 was much less active than the ones that started at Arg11 (133).

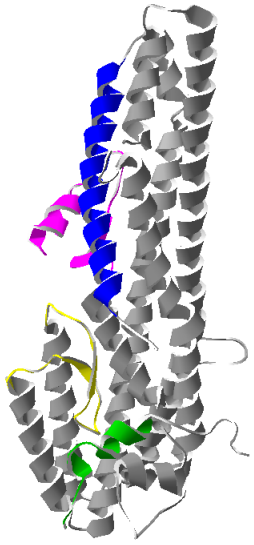

Fig. 12. 3-D ribbon representation of Cry6Aa1 trypsin-treated (5J65). α1 is colored in magenta, the β-tongue is colored in yellow, α9 is colored in blue and α10 is colored in green.

1.5.2.1. Structure of the trypsin-treated Cry6Aa

The trypsin-treated Cry6Aa1 is composed of two polypeptide chains, one that goes from His12 to Ser390 and the other that starts at Ser445 and ends at Trp472. These two polypeptides are linked by a disulphide bridge between residues Cys88 and Cys451. The trypsin-treated

Cry6Aa1 (Fig. 12A) is a helix bundle made out of 10 helices and two β-sheets, where the last helix is attached to the rest of the protein by a disulphide bridge. The head subdomain is folded across the helices at one end and is formed by the residues closer to the C-terminal of the protein. One of the most interesting characteristics of the head domain is that it contains a very hydrophobic β-tongue that confers on this protein a structural similarity to other proteins such as hemolysin E. The tail subdomain is made of residues close to the N-terminal of the toxin (136). The main difference between both elucidated structures of Cry6Aa is that the one solved at 1.9Å resolution ends at α9 (137), while the other one shows α10 attached by a disulphide bridge (136).

1.5.2.2. Structure of the native Cry6Aa

The full length structure of the native Cry6Aa was also elucidated, and shown to be very similar to that of the trypsin-treated Cry6Aa (Fig. 12B) (136). Because there were some segments of the protein that were too flexible to be identified by X-ray analysis, Cry6Aa1 treated with trypsin was used to model these missing parts. The native Cry6Aa, a 55-kDa protein, extends from Met1 to Asn475. The structure contains 70% α-helices and 1.7% β-sheets, consistent with circular dichroism data.

The native Cry6Aa1 has a total of five cysteine residues at positions 88, 162, 402, 404 and 451. Cys88 and Cys451 are forming a disulphide bridge, which after treatment with trypsin keeps the two fragments of the toxin together. The disulphide bridge between Cys402 and Cys404 is lost during trypsin treatment and Cys162, which is buried in the core of the protein, is not forming any disulphide bond in either form of the toxin. The pairing of the cysteines and the buried one also indicate that intermolecular disulphide bonds do not stabilize Cry6Aa crystals.

1.5.3. Similarity of Cry6A to other toxins

The Cry6Aa1 structures are strikingly similar to those of previously described bacterial toxins, such as HblB of *Bacillus cereus*, NheA of *B. cereus* and hemolysin E of *E. coli*. The hemolysin E structure-function relationships have been studied in depth.

1.5.3.1. Hemolysin E

Hemolysin E (ClyA) is a PFT produced by *E. coli*, *Salmonella typhimurium* and *Shigella flexneri* that, despite a very high structural similarity to Cry6Aa1, shows very small amino acid sequence similarity (10%). ClyA displays cytotoxicity towards cultured mammalian cells (138), such as HeLa cells and erythrocytes. It induces apoptosis in murine-derived macrophages and promotes tissue pervasion (139). It was also shown that the transcriptional regulator *slyA* induces ClyA production in *E. coli.* SlyA has been shown to confer the hemolytic phenotype to different microbial strains that produce ClyA, but is incapable to form pores by itself (140).

1.5.3.1.1. Sequence and structure

Four different sequences of ClyA have been identified from different organisms that produce the toxin (141), with only 68% identity. Furthermore, only two cysteines are conserved (Cys87 and Cys285), and they do not form disulfide bonds, although they are closely positioned. The monomer ClyA structure (Fig.13 a,c) has been solved at 2Å resolution in its soluble form (141). The main part of the molecule is formed by a bundle of 4 α-helices: αA (1-34) that has a kink at residues 35-36, αB (56-101), αC (106-159) and αF (207-258). At one end of the structure there is a "tail" subdomain, αG, which is packed between αA and αB, and assumes a topology rarely found in toxins. At the other end, there is a "head" subdomain called the "β-tongue", which is a short hairpin flanked by two short helices (αD and αE).

The 3.3Å resolution crystal structure of a dodecameric transmembrane ClyA pore has also been elucidated (139). From the structural information it was hypothesized that the monomer (Fig. 13 A,C) in contact with lipids undergoes a conformational change, which involves more than half of its amino acids, becoming a protomer (Fig. 13 B, D). Finally, the protomer oligomerizes and forms a pore in the membrane. In the protomer, the residues of the β-tongue are transformed into an α-helical extension of αC and αE. Once the conformational change has occurred, the protomers are arranged in a three-helix bundle (αB, αC and αF) instead of four-helix bundle. At the top of the bundle αA is arranged to form the constriction of the pore inside the membrane. On the other side, αG flanks the three-helix bundle on the outside of the pore.

In the assembled pore, all helices contribute to protomer-protomer interaction except αG. There is a network of 25 hydrogen bonds and 13 salt bridges that play a role in this interaction. These interfaces do not exist in the monomer form of ClyA, therefore it is thought that the monomer to protomer conversion must happen before oligomerization. As far as transmembrane domains are concerned, the β-tongue, αE, αD and αA play a role in membrane interaction. The β-tongue contains a large amount of hydrophobic residues and αA is an amphipathic helix whose polar residues line the inside of the pore's constriction.

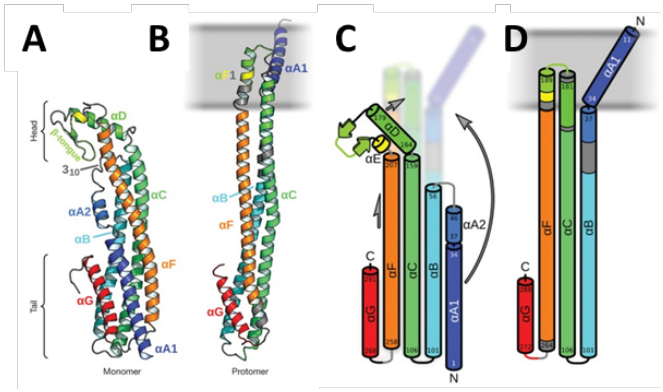

Fig. 13. Conformational change of ClyA monomer into a protomer. A,B) Ribon representation of ClyA monomer and protomer, C,D) Schematic representation of ClyA monomer and protomer (139)

1.5.3.1.2. Pore formation in PLBs

ClyA has been tested in diphytanoylphosphatidylcholine (DPhPC) PLBs by two research groups under different experimental conditions. In 1M KCl at pH 6 and at 10-50 ng/ml toxin concentration, a conductance of 10 nS was observed (142). With 10-100 pg/ml of toxin in 150 mM NaCl at pH 7.5 the conductance was 1.8 nS (143). The pores of ClyA were cation-selective (142).

1.5.3.1.3. Structure and function

With both the monomer and oligomer structures available, ClyA has been the target of numerous structure-function studies.

Head subdomain: β-tongue and αA

As mentioned before, the head subdomain is composed by a β-tongue flanked by two short helices (αD and αE) and by αA.

αA has been shown to be necessary for pore formation and for retaining the biophysical properties of the transmembrane pore, suggesting that αA is directly involved in pore structure (144). Mutations in this region strongly impair or fully abolish the hemolytic activity of ClyA without preventing binding. Deletions affecting up to the 10^{th} amino acid had only minor effects on the pore biophysical characteristics such as decreasing conductance of pores or shortening the pore lifespan in the membrane during PLB experiments. However, the deletion of more amino acids prevented pore insertion into the membrane. This is consistent with the prediction that was inferred from the crystal structure of the dodecameric ClyA complex, in which αA helices of the oligomerized toxin penetrate the lipid bilayer (139). Moreover, despite the fact that αA in the ClyA monomer starts at residue 1, it starts at residue 11 in the pore structure, suggesting that residues 1 to 10 are located on the *trans* side of the membrane.

Although the β-tongue has been shown to be crucial for ClyA hemolytic activity, mutants that are missing that part are still able to form pores in PLBs that resemble wild-type ClyA in terms of conductance, ion permeability and stability (144,145). However, they are less efficient pore-formers than the wild-type toxin. All in all, the results suggest that the β-tongue seems to be important for efficient pore formation but it is not an essential component of the transmembrane pore.

Tail subdomain: αG, disulphide bridge and cysteines

It has been hypothesized that αG plays different roles in the toxin's function (144,146). αG and the two hydrophobic regions found in the head and tail domains of the monomer promote membrane interaction without being necessary for pore formation in PLBs. It has been proposed that the dissociation of αG would expose a hydrophobic region of the four-helix bundle that plays a role in protomer-protomer interactions, stabilizing the pore in the membrane. This is further supported by the fact that αG mutations and deletions did not prevent ClyA from forming pores with the same biophysical characteristics than the wild-type ClyA in PLBs. Even when the entire αG region was deleted, the biophysical characteristics of the pores still remained very similar and only pore-formation efficiency was affected, suggesting that this region is multifunctional and plays a role in secretion, membrane targeting and pore formation.

Another component of the tail subdomain is the disulphide bridge between the two cysteines in αB and αG. This disulphide bridge would lock αG to the main body of the protein.

It has been proposed that locking αG would prevent premature oligomerization and allow activation of the toxin only in a reducing environment (141,145-147). During the last decade research groups have studied the function of the bridge (141,145-147), yet their results contradict one another, leaving unclear if the disulphide bridge plays a role in the toxin's function or not. It has been suggested that the disulfide bridge could play a crucial role during the export of ClyA from the bacterial cell and have no direct impact in the structure or ability of the toxin to form pores (147).

1.5.3.2. Other toxins

A few other toxins have been reported that share highly similar structures to Cry6Aa. One of them is hemolysin BL (HbL), which is a diarrheal enterotoxin secreted by *Bacillus cereus*. This toxin is composed of three distinct protein components: B, L1 and L2. The structure of HBL-B (Fig. 14A) has been solved at 2.03Å resolution. It is very similar to Cry6Aa, although the two protein primary sequences are only 12% similar (148). The structure of HBL-B is composed of 7 α-helices and a β-strand. There is also a head domain that includes a β-hairpin and two short α-helices, and a tail domain that consists of the five remaining α-helices.

Nhe proteins (NheA, NheB and NheC) produced by *Bacillus cereus* are also similar to Cry6Aa on a structural point of view (Fig. 14B and 14C). These proteins belong to the family of hemolysins responsible for osmotic lysis in epithelia. Whereas the structure of these proteins has not been solved yet and their amino acid similarity to Cry6Aa1 is only 12%, it has been shown by computer modeling that they display similar structures. They also have similar functional properties to those of ClyA (Fig.14D) in PLBs (149).

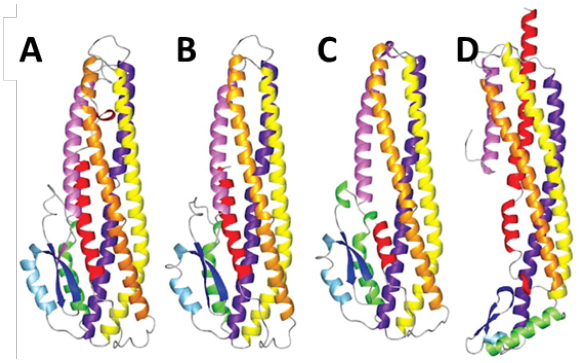

Fig. 14. Structural similarity between A) Hbl, B) the homology model of NheB, C) the homology model of NheC and D) ClyA (149)**.**

1.6. Contribution of co-authors and conferences

All the experiments that are shown in the manuscript, except the bioassay data have been done by me. The results were discussed with Jean-Louis Schwartz, the team at Dow AgroSciences and Vincent Vachon. The toxins that I used to do all of the experiments were produced, purified, solubilised and activated by the team at Dow AgroSciences. The manuscript's first draft was written by me and was corrected and enriched by Jean-Louis Schwartz. The team at Dow AgroSciences has contributed in writing the materials and methods for protein production, purification, solubilisation and bioassays.

Preliminary data of this project was shown in a poster named "*Unusual pore formation by a new* Bacillus thuringiensis *toxin"* at the 48th Society for Invertebrate Pathology meeting, Vancouver, August 2015. The data presented as additional results was shown in a poster named *"Structure-function relationships in a new* Bacillus thuringiensis *pore-forming toxin"* at the 60th Biophysical Society meeting, Los Angeles, February 2016. Finally, the data presented in the manuscript was shown in a poster named "*Propriétés inédites d'une nouvelle toxine insecticide de* Bacillus thuringiensis" at the 84th ACFAS meeting, Montreal, May 2016.

1.7. Objectives and hypotheses

Cry6Aa1's structure was recently elucidated by the company Dow AgroSciences (136). Because of the difference in structure in comparison with any other Cry toxins studied so far, this toxin may function with a very different mode of action, compared to that of the other Cry toxins. Furthermore, while this toxin does not show close amino acid sequence similarity to any *Bt* toxins, it shows a very close tertiary structure similarity to a few other bacterial PFTs such as ClyA, as mentioned in section 1.5 above.

Cry6Aa1 has never been tested before in an artificial environment and hardly any work has been done regarding its mode of action. Therefore, the studies described in this thesis are based on the following hypotheses and objectives:

1.7.1. Hypotheses

We hypothesised that like the other *Bt* Cry toxins, Cry6Aa1 is a PFT. Moreover, its mode of action differs from that of other Cry toxins due to the difference in structure and that the structure-function relationships of Cry6Aa1 compare to those of ClyA.

1.7.2. Objectives

The first objective was to demonstrate that Cry6Aa1 is a PFT and to characterise the membrane pores in PLBs. After, we wanted to get a better understanding on how different elements that play a role in the mode of action, such as solubilisation, pH, protease activation, target organism receptors and dose, modify the pore formation ability of Cry6Aa1. Finally, due to the extensive information on ClyA we wanted to understand the structure-function of Cry6Aa1 by using various mutants and protease treatments of the toxin and compare it to that of ClyA

CHAPTER 2. MATERIALS AND METHODS

2.1. Cry6Aa preparation

To use Cry6Aa1 in PLBs, the toxin was prepared by solubilising and activating it when necessary. This part of the project was done by our collaborators at Dow AgroSciences (Indianapolis, IN, USA). For experimental procedure see Chapter 3.

2.1.1. Toxins used

To better understand pore formation by Cry6Aa1, different forms of the toxin were used (Fig. 15). Native Cry6Aa1 is the full length form of the toxin that is not activated. Cry6Aa1 WCR1 and Cry6Aa1 WCR2 are the two different products of the toxin that are obtained after treating Cry6Aa1 with midgut juice of WCRWs. Cry6Aa1 TT is the form of the toxin that has been treated with trypsin. Cry6Aa1 TT MET is the form of the toxin that has been trypsinized and experiments are done in the presence of β-mercaptoethanol (MET). Finally, Cry6Aa1 mod is an engineered variant where the amino acids 391 to 442 of Cry6Aa1 have been replaced by a 7AA linker. In Chapter 3 Cry6Aa1 WCR1 will be referred as Cry6Aa1 WCR.

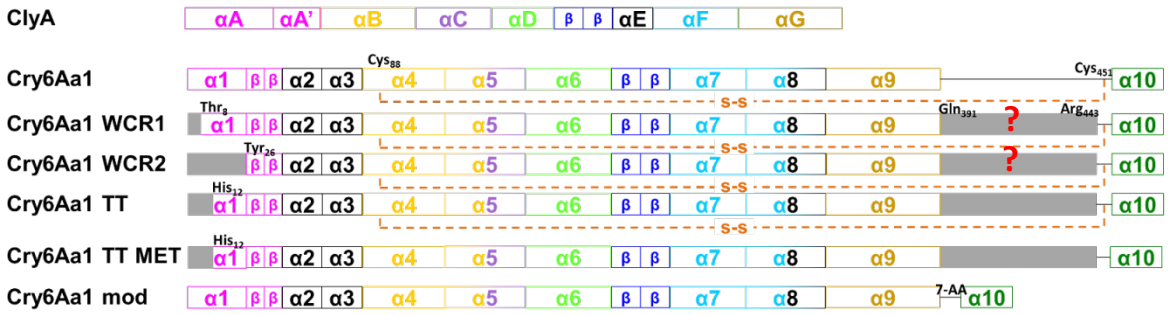

Fig. 15. Diagram of the secondary structures of ClyA and Cry6Aa1 TT, and the predicted secondary structures of the other forms of Cry6Aa1. The regions labeled with the same colors have highly similar primary sequences. The black labeled regions show no similarity. Grey regions are fragments cleaved off by proteases. The regions marked with dual color labels correspond to highly similar AA stretches in two different regions of ClyA. The questions marks correspond to regions in between Gln391 and Arg443 that may or may not be present in the toxin.

2.1.2. Solubilisation

Since the toxin is produced as a crystal, it must first be solubilized so that proteases can access the cleavage sites. For PLB experiments, the native Cry6Aa1 and Cry6Aa1 TT toxins were solubilised in a solution containing: 150 mM KCl and 50 mM Tris at pH = 10.

Cry6Aa1 WCR1 was directly solubilised with the midgut juice of the target insect and Cry6Aa1 mod was already produced as a soluble protein.

The following protocol was used to study the effect of different pH (3-10) on the solubilisation of Cry6Aa1:

1. 100 µl of Cry6Aa1 inclusion bodies were pipetted in an Eppendorf tube.
2. The inclusion bodies were centrifuged for 20 minutes at 20800x*g* at 4°C and the excess supernatant was removed from each sample.
3. 2 ml of solubilisation buffer was added. The composition of the solubilisation buffers varied depending on the desired pH and are listed in table II:

Table II. Composition of the buffer solution used to solubilise Cry6Aa1.

pH	Buffer composition
3	150 mM KCl and 50 mM sodium citrate
4	150 mM KCl and 50 mM sodium citrate
5	150 mM KCl and 50 mM sodium citrate
6	150 mM KCl and 50 mM MES
7	150 mM KCl and 50 mM HEPES
8	150 mM KCl and 50 mM Tris
9	150 mM KCl and 50 mM CHES
10	150 mM KCl and 50 mM CAPS

4. The inclusion bodies were initially vortexed in the solubilisation buffer and subsequently mixed in a rocker for 2 hours at room temperature.
5. The inclusion bodies were centrifuged at 55000 rpm to pellet the non-solubilised toxin.
6. Finally, a Bradford assay was made to measure the protein concentration.

2.1.3. Activation

Cry6Aa1 WCR1 and Cry6Aa1 WCR2 were incubated with midgut juice extracted from WCRW larvae.

The protocol for trypsin activation of Cry6Aa1 to produce CryAa1 TT was the following:

1. TPCK-treated trypsin (SIGMA, Oakville, Ontario, Canada) was added to solubilize the native Cry6Aa1 at an enzyme:protein ratio of 1:15 (w/w).
2. The protein was digested at room temperature overnight while shaking on a rocker.
3. The mixture was centrifuged at 14000 rpm at 4°C for 25 min and the pellet was disposed.
4. Size exclusion chromatography was used to purify the activated toxin.

2.2. Planar lipid bilayers (PLBs)

Electrophysiology is the discipline that studies the electrical properties of proteins, cells and tissues. The PLB technique consists in testing the electrical activity of proteins that are inserted into a lipid bilayer. The advantage of this technique is that the lipid composition of the membrane and its environment (pH and ionic concentration of the solutions) are fully controlled. It allows the study of membrane proteins at a single molecule level.

2.2.1. Experimental setup

The experimental setup used for PLB experiments is represented in Fig.16. First, there is a disposable bilayer chamber, which is composed of the compartments *cis* and *trans* and is placed in a Faraday cage. The Faraday cage is set on top of an anti-vibration table. This reduces the electrical and mechanical interferences from the environment during experiments. The voltage is applied to the *cis* side of the chamber and is produced by the amplifier (Axopatch - 1D, Axon Instruments, Molecular Devices, Sunnyvale, CA, USA). On the other hand, the *trans* compartment is maintained at virtual ground.

The current going through the bilayer is detected by the amplifier and filtered at 5kHz. This analog signal is digitized at 50kHz by a Digidata 1440A A/D converter (Axon Instruments). It is then recorded in a computer and displayed on the computer monitor.

Moreover, the analog signal is also displayed on an oscilloscope used to monitor the currents in real time and evaluate the membrane capacitance at the beginning of each experiment by means of a triangular voltage waveform produced by a Wavetek signal generator (Willtek, San Diego, CA, USA).

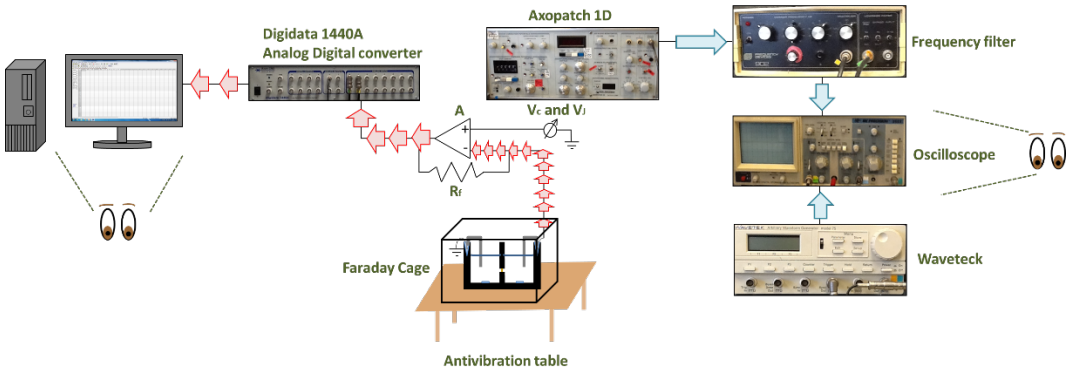

Fig. 16. Simplified schematic representation of the experimental setup for PLB experiments. A: amplifier, Vc: voltage applied to the experiment, Vj: voltage applied to balance the junction potentials, Rf: resistance.

2.2.1.1. Disposable holders

Disposable bilayer holders were designed to prevent contamination from experiment to experiment. The holder consists of two polystyrene cuvettes that are cut into 11.7 x 11.9 x 17 mm chambers, each with an 8.2-mm diameter hole (Fig. 17A). A 0.127 mm thick membrane, which is formed from Delrin (polyoxymethylene) and has a small 250-µm diameter aperture (Fig. 17B) on which the lipid bilayer is supported, is glued with a silicone sealant between the two chambers.

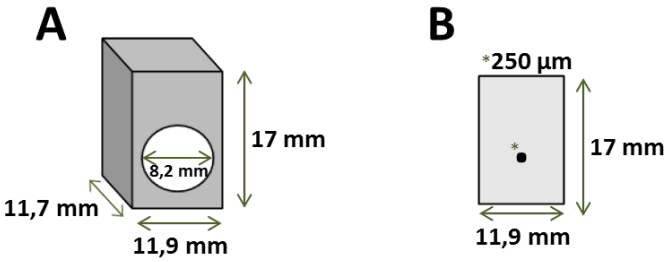

Fig. 17. Schematic drawing of the different parts of the disposable holder. (A) One of the two identical cuvettes and (B) the Delrin membrane.

2.2.1.2. Lipids and solutions

A 1:1 mixture of 1-palmitoyl-2-oleoyl-sn-glycero-3-phosphoethanolamine (POPE) and 1-palmitoyl-2-oleoyl-*sn*-glycero-3-phosphocholine (POPC) is used for the experiments. POPE and POPC are artificial phospholipids that have hydrophobic tails that will interact to avoid contact with water molecules to form a bilayer. Both lipids have a polar head formed by a negatively charged phosphate group and a positively charged amino group (Fig. 18). The overall charge of the bilayer obtained with this lipid mixture is neutral.

Lipids were purchased from Avanti Polar Lipids (Alabaster, AL, USA) in solution and stored in chloroform.

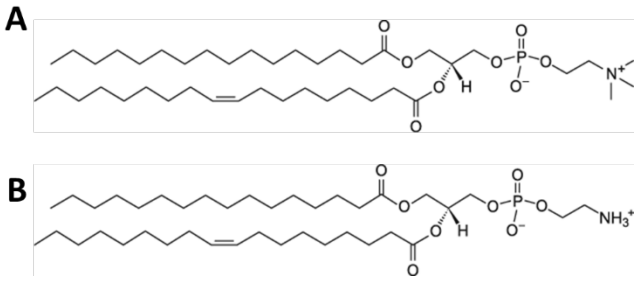

Fig. 18. Chemical structure of the lipids used in PLBs. (A) POPE and (B) POPC (Avanti Polar Lipids, https://avantilipids.com, August 2016).

To get the desired lipid mixture, the protocol was the following (Fig. 19):

1. 20 µl of POPE and 20 µl of POPC were mixed together.
2. The chloroform was evaporated under N_2 gas atmosphere to form a thin layer of lipids.
3. 20 µl n-decane was added to obtain a final concentration of lipids in solution of 20 mg/ml.
4. The solution was carefully vortexed to make sure that the lipids were well mixed.

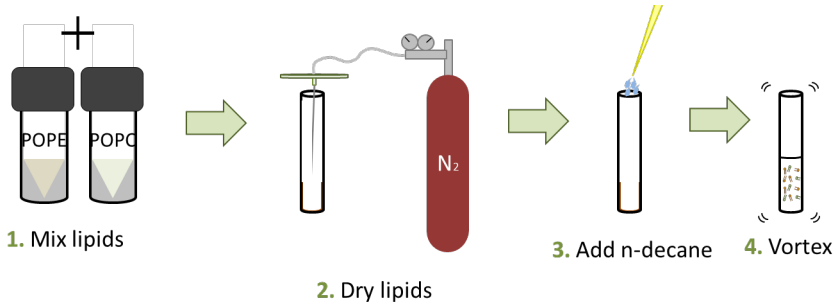

Fig. 19. Simplified description of the lipid mixture preparation protocol.

The bath solutions contained 150 mM KCl, 1 mM $CaCl_2$ and 10 mM of the appropriate buffer at each pH (MES for pH 5.5, HEPES for pH 7.5 and Tris for pH 9.5). $CaCl_2$ was added to the bath because it is thought to stabilize the pores formed by the toxin in the membrane. For selectivity experiments, the KCl concentration on the *cis* side of the membrane was raised to 450 mM.

2.2.1.3. Agar bridges

Disposable agar bridges are used in bilayer experiments for two reasons. Firstly, they are intended to reduce junction potentials at the level of the silver-silver chloride electrodes. Secondly, they are used to avoid the contamination of the electrodes. Thin wall glass capillary tubes (outside diameter 1.5 mm, inside diameter 1.17 mm, Warner Instruments, Hamden, CT, USA) were used to prepare the agar bridges using the following protocol (Fig. 20):

1. The glass capillaries were cut to around 5-cm long each.
2. They were bent in the heat of a flame.
3. They were filled with the conducting agar solution (2 M KCl, 1 mM EGTA and 2% agar).

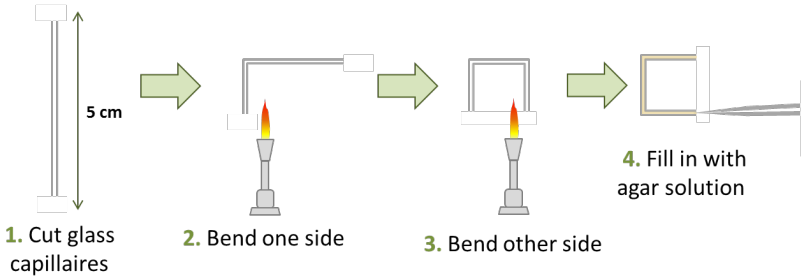

Fig. 20. Simplified schematic protocol used to make agar bridges.

2.2.1.4. Lipid pretreatment of the chamber

Before starting an experiment, 0.5 µl of the previously described lipid mixture was added to the aperture where the bilayer was going to be painted. The chamber was then dried under N_2 for 10 minutes to evaporate the n-decane solvent. The objective of the lipid pretreatment was to facilitate lipid bilayer attachment to the aperture of the chambers. This was later monitored by measuring the membrane capacitance, which should be between 150 and 200 pF.

2.2.1.5. Membrane preparation

The following protocol was used to prepare the PLBs (Fig. 21) and test the toxins (54):

1. The lipid mixture was painted on **the 250-µm aperture u**sing a custom shaped tip-occluded glass pipette.
2. Prior to adding the toxin to the bilayer, the stability of the membrane was assessed for 30 minutes. This was also used to make sure that there was no detectable channel activity due to contaminating agents.

3. The desired toxin concentration was added to the *cis* chamber.
4. Voltage steps of ±100 mV were sometimes applied to the bilayer to facilitate toxin insertion into the membrane.

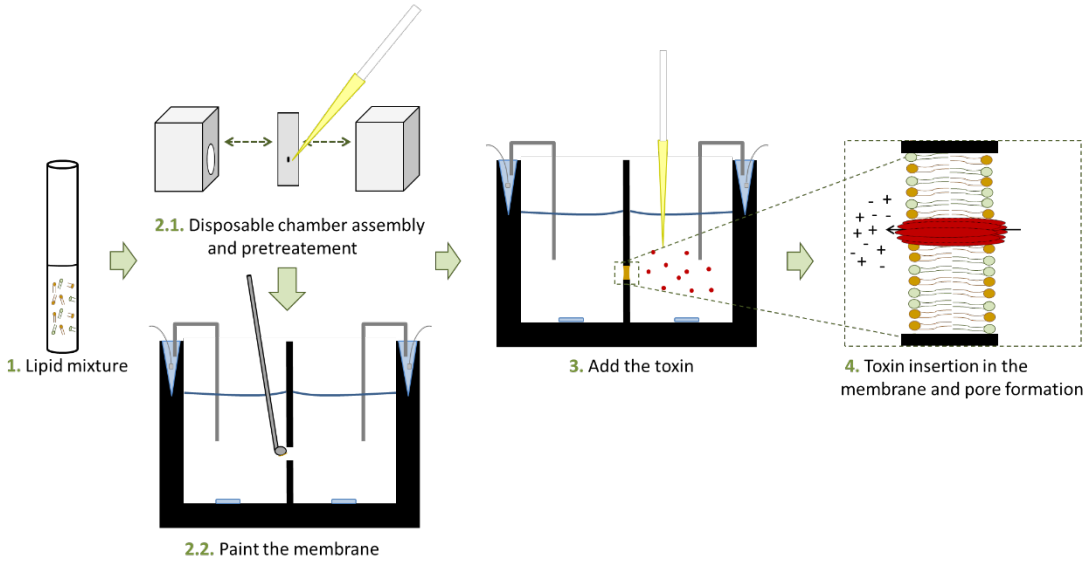

Fig. 21. Simplified representation of the protocol used for testing *Bt* toxins in PLBs.

2.2.2. Channel current recording

Once channel activity was observed, voltages were applied to the membrane in 20 mV steps from +80 mV to -80 mV and for variable durations to get enough information about the pore electrical activity during each holding voltage step.

2.3. Midgut brush border membrane reconstitution into PLBs

BBMs were purified from WCRW midguts and reconstituted into liposomes. Enriched liposomes were then fused mechanically to the bilayers.

2.3.1. Preparation of BBMs from WCRW dissected midguts

The apical BBM of WCRW midguts was isolated using the following protocol (150) (Fig. 9):

1. The larvae midguts were thoroughly cleaned and centrifuged at 5000 rpm for 5 minutes at 4°C and the supernatant was aspirated.

2. Nine times the weight (in g) of the midguts in volume (ml) of mannitol buffer (300 mM mannitol, 17 mM Tris, 5 mM EGTA, pH 7.5/ HCl) was added to the midguts. This solution was isosmotic to prevent lysis of the midgut cells.
3. The preparation was homogenized using a homogenizer.
4. Ten times the weight (in g) of the midguts in volume (ml) of $MgCl_2$ was added to the homogenate preparation to form aggregates of Mg^{2+} and membrane material.
5. The mixture was agitated during 15 minutes.
6. The mixture was centrifuged at 3500 rpm at 4°C for 10 minutes to separate the large aggregates from the small ones. The latter are the ones that contained the BBM material.
7. The mixture was centrifuged at 16000 rpm for 30 minutes at 4°C to precipitate the small aggregates.
8. The pellet of apical membrane was resuspended in mannitol buffer and step 2 to step 6 were repeated.
9. At the end, a pellet of BBM material was obtained. It was resuspended in HEPES buffer (10 mM HEPES/Tris pH= 7.5).

2.3.2. BBM-enriched liposome preparation

BBM liposomes were prepared with the following protocol (32) (Fig. 22):

1. L-alpha-phosphatydilcholine (PC) (Egg yolk, Avanti Polar Lipids) was used at a 9.1 mg/ml final concentration.
2. The lipids were dried under N_2 to form a thin layer and further dried in vacuum for 30 min.
3. One ml of liposome buffer (150 mM KCl, 1 mM EGTA, 10 mM Hepes, pH=7.4) was added.
4. The BBM preparation was added with a final lipid: protein ratio of 60: 1(w/w).
5. The mixture was vortexed for 5 minutes.
6. The liposomes were frozen with liquid nitrogen and thawed in a bath 5 times.
7. An extrusion instrument (Avanti Mini Extruder, Avanti Polar Lipids) was used to pass the lipids 21 times through a 0.2 μm membrane to obtain unilamellar enriched liposomes.

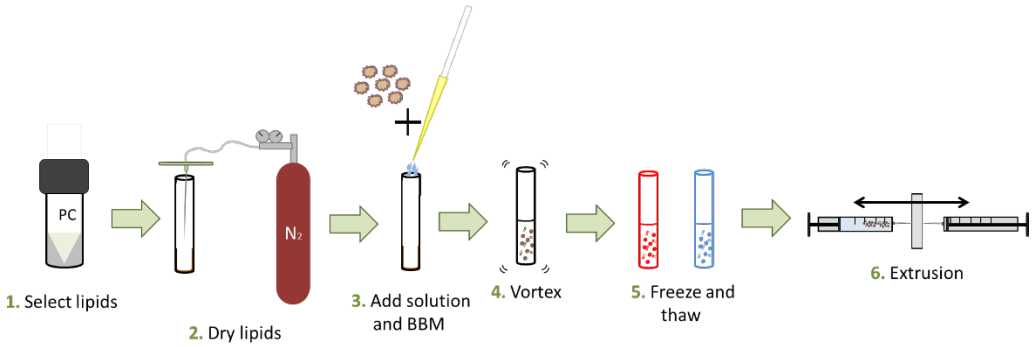

Fig. 22. Simplified schematic protocol of enriched liposome preparation

2.3.3. BBM fusion into PLBs

BBM fusion to the PLBs was done through a mechanical procedure, similar to the one used to paint the bilayer, by gently touching the *cis* side of the bilayer with the small round tip of a glass pipette that had been dipped before in the enriched liposome solution.

2.4. Analysis of pore formation in PLBs

Ionic currents were recorded using Clampex and analyzed using Clampfit of the pClamp version 10.5 software (Axon Instruments). Graphs were done in Excel (Microsoft Office 2016) and OriginPro8 (Wellesley Hills, MA, USA).

2.4.1. Current-voltage relationships (IV curves)

To construct IV curves, at least 25 current jumps were measured at each applied voltage, grouped with those of similar amplitude and averaged. Current-voltage graphs were then constructed and, when possible, data points were fitted with linear curves whose slopes are the conductances of the pores (Fig. 23).

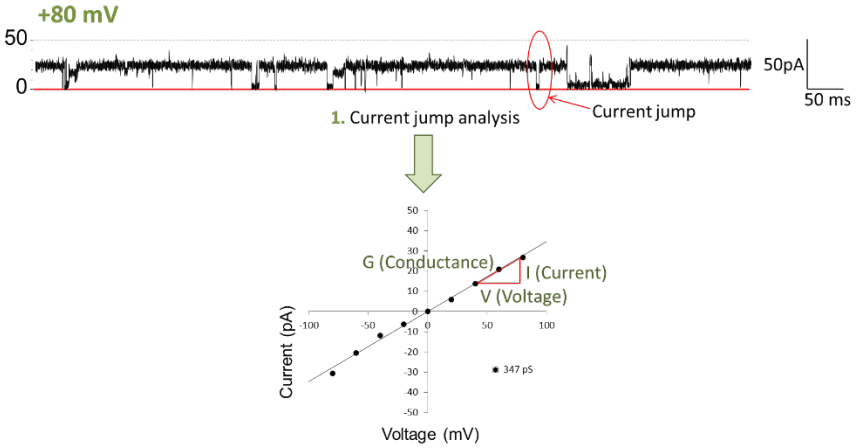

Fig. 23. Demonstration of the analysis of one type of pore conductance by doing an IV curve

2.4.2. Ionic selectivity

Reversal potentials in experiments conducted under asymmetrical ionic conditions (450 mM KCl *cis*:150 mM KCl *trans*) were measured on the corresponding current-voltage relationships. The shift to the positive or negative sides of the voltage axis provided an indication of anion- or cation-selectivity, respectively. The relative permeability of potassium ions vs chloride ions was evaluated using the Goldman-Hodgkin-Katz (151) equation from which P_{K^+} / P_{Cl^-} was derived:

$$V = \frac{RT}{F}\, x\, ln\left(\frac{P_{Na}[Na^+]_{trans} + P_K[K^+]_{trans} + P_{Cl}[Cl^-]_{cis}}{P_{Na}[Na^+]_{cis} + P_K[K^+]_{cis} + P_{Cl}[Cl^-]_{trans}}\right)$$

If no Na^+ is present:

$$\frac{VF}{RT} = ln\left(\frac{P_K[K^+]_{trans} + P_{Cl}[Cl^-]_{cis}}{P_K[K^+]_{cis} + P_{Cl}[Cl^-]_{trans}}\right)$$

$$e^{\frac{VF}{RT}} = \left(\frac{P_K[K^+]_{trans} + P_{Cl}[Cl^-]_{cis}}{P_K[K^+]_{cis} + P_{Cl}[Cl^-]_{trans}}\right)$$

$$e^{\frac{VF}{RT}}\, x\, (P_K[K^+]_{cis} + P_{Cl}[Cl^-]_{trans}) = P_K[K^+]_{trans} + P_{Cl}[Cl^-]_{cis}$$

$$P_K\, x\, (e^{\frac{VF}{RT}}\, x\, [K^+]_{cis} - [K^+]_{trans} = P_{Cl}\, x\, \left([Cl^-]_{cis} - e^{\frac{VF}{RT}}[Cl^-]_{trans}\right)$$

$$\frac{P_K}{P_{Cl}} = \frac{[Cl^-]_{cis} - e^{\frac{VF}{RT}}[Cl^-]_{trans}}{e^{\frac{VF}{RT}}\, x\, [K^+]_{cis} - [K^+]_{trans}}$$

In which V is the measured reversal potential (in V), $[K^+]_{cis}$ and $[K^+]_{trans}$ are the potassium ion concentrations on the *cis* and *trans* sides of the membrane, respectively, $[Na^+]_{cis}$ and $[Na^+]_{trans}$ are the sodium ion concentrations on the *cis* and *trans* sides of the membrane, respectively, $[Cl^-]_{cis}$ and $[Cl^-]_{trans}$ are the chloride ion concentrations on the *cis* and *trans* side of the membrane, respectively, R is the ideal gas constant (J/K x mol), T is the absolute temperature (K), which is 295°K in our experiments, and F is the Faraday constant (C/mol).

2.5. Data presentation

Data correspond to at least three experiments under each condition. The cumulative frequency distribution of pore conductances was done by grouping in a cumulative manner in 50-pS space bins all the conductances obtained in the experiments. The Mann-Whitney test for independent variables was used to evaluate the difference between the cumulative frequency distributions of the data ($p<0.05$).

CHAPTER 3. MANUSCRIPT

Submitted to the Journal of Biological Chemistry

Cry6Aa1, a *Bacillus thuringiensis* Nematocidal and Insecticidal Toxin, Forms Pores in Planar Lipid Bilayers at Extremely Low Concentrations and Without the Need of Proteolytic Processing

Eva Fortea[1], Vincent Lemieux[1,2], Léna Potvin[1], Vimbai Chikwana[3], Samantha Griffin[3], Timothy Hey[3], David McCaskill[3], Kenneth Narva[3], Sek Yee Tan[3], Xiaoping Xu[3], Vincent Vachon[1], and Jean-Louis Schwartz[1,4]

From the [1]Département de pharmacologie et physiologie and Groupe d'étude des protéines membranaires, Université de Montréal, Montreal, QC, Canada, the [2]Département de biologie, Université de Sherbrooke, Sherbrooke, QC, Canada, [3]Dow AgroSciences LLC, Indianapolis, IN, U.S.A., and the [4]Centre SÈVE de recherche en sciences du végétal, Université de Sherbrooke, Sherbrooke, QC, Canada

Running title: *Cry6Aa1 is a pore-forming* Bt *toxin*

To whom correspondence should be addressed: Prof. Jean-Louis Schwartz, Département de pharmacologie et physiologie, Université de Montréal, P.O. Box 6128, Centre-Ville Station, Montreal, QC, H3C 3J7, Canada, Telephone: (514) 343-6364; FAX: (514) 343-7146; E-mail: jean-louis.schwartz@umontreal.ca

Keywords: Bacillus, bacterial toxin, insect, membrane, permeability, pore-forming toxin, planar lipid bilayers, midgut brush border membrane

ABSTRACT

Cry6Aa1 is a *Bacillus thuringiensis* (*Bt*) toxin active against nematodes and corn rootworm insects. Its 3-D molecular structure, which has been recently elucidated, is unique among those known for other *Bt* toxins. Typical three-domain *Bt* toxins permeabilise receptor-free planar lipid bilayers (PLBs) by forming pores at doses in the 1-50 μg/ml range. Solubilisation and proteolytic activation are necessary steps for PLB permeabilisation. In contrast to other *Bt* toxins, Cry6Aa1 formed pores in receptor-free bilayers at doses as low as 200 pg/ml in a wide range of pH (5.5-9.5) and without the need of protease treatment. When Cry6Aa1 was pre-incubated with Western corn rootworm (WCRW) midgut juice or trypsin, 100 fg/ml of the toxin was sufficient to form pores in PLBs. The overall biophysical properties of the pores were similar for all three forms of the toxin (native, midgut juice- and trypsin-treated), with conductances ranging from 28 to 689 pS, except for their ionic selectivity which was slightly cationic for the native and midgut juice-treated Cry6Aa1, whereas dual selectivity (to cations or anions) was observed for the pores formed by the trypsin-treated toxin. Enrichment of PLBs with WCRW midgut brush border membrane material resulted in a 2000-fold reduction of the amount of native Cry6Aa1 required to form pores and affected the biophysical properties of both the native and trypsin-treated forms of the toxin. These results indicate that, although Cry6Aa1 forms pores, the molecular determinants of its mode of action are significantly different from those reported for other *Bt* toxins.

The Gram-positive bacterium *Bacillus thuringiensis* (*Bt*) forms crystal-like parasporal inclusions during sporulation (1,2), which often comprise insecticidal proteins (3). *Bt* insecticides have a long history of successful use (4,5) against pests, in agriculture (6) forestry (7), and disease vectors (8). Since 1996, various transgenic crops that express *Bt* toxins have been grown over a rapidly increasing area (9).

Known *Bt* toxins belong in majority to the Cry (crystal) family of proteins, whose most extensively studied members are insecticidal. Because of their importance and long use in pest management programs, the elucidation of their mode of action has been the object of considerable work (reviewed in (10-13)). In broad general terms, the *Bt* mode of action can be

described as follows: crystal proteins are first ingested as protoxins which are solubilised and proteolytically converted to smaller polypeptides in the insect midgut. These activated toxins then bind to specific receptors at the surface of midgut epithelial cells, allowing them to insert and form pores in the cell membrane (14,15). The presence of such pores interferes with cell physiology by abolishing transmembrane ionic gradients and may lead to colloid-osmotic lysis of the cells by allowing a massive influx of solutes from the midgut lumen (16), resulting in extensive damage to the midgut epithelium and death of the intoxicated larvae. However, many details of this scheme remain unresolved, as critically analysed in our recent review (17).

Alterations in any one of the steps mentioned above can allow the insect to become resistant to the toxin (18-22). A clear and detailed knowledge of a toxin's susceptibility to intestinal proteases, interaction with membrane receptors and pore-forming ability, and of the consequences of the resulting membrane permeabilisation on cellular physiology, including intracellular signalling and putative cell defence mechanisms (23), is therefore crucial for understanding and managing insect resistance development.

Bt-corn hybrids have been planted since 1996. They were initially designed to control lepidopteran larvae of corn borers, stalk borers, fall armyworms and other important pests. These corn varieties express one or more Cry toxins conferring them insect resistance traits, often stacked with herbicide-tolerance traits. The multiple toxin approach (pyramiding) of hybrids expressing different *Bt* toxins targeted to the same insects is useful for managing insect resistance (24). The introduction in corn of Vip3A, a toxin produced during the vegetative growing phase of *Bt* (25,26), has increased the spectrum of lepidopteran targets controlled by *Bt*-corn (24).

Several coleopteran insects are also major pests of corn worldwide. Damage from corn rootworms (the Western corn rootworm *Diabrotica virgifera virgifera* LeConte (WCRW) and the Northern corn rootworm *Diabrotica barbieri* Smith & Lawrence) accounts for over $1 billion in losses in North America annually (27). Single *Bt* toxin traits for corn rootworm protection were introduced in the US in 2003 (Cry3Bb *Bt*-corn), 2005 (binary Cry34Ab1/Cry35Ab1 *Bt*-corn) and 2007 (mCry3Aa *Bt*-corn). However, recent reports of resistance to Cry3 toxins have highlighted the urgent need to develop new strategies to delay resistance development, based on the use of toxins with different modes of action to be deployed

in trait pyramids (24,28,29). Furthermore, the high-dose/refuge strategy may not be as efficient as predicted for recent hybrid corns, due to a lower level of expression of the toxins in the plant and inappropriate refuge size (30). Finally, northward advancement of the limit of WCRW habitat as a result of climate change may result in more severe outbreaks in Northern United States and Canada (31,32).

Cry6Aa1 is a *Bt* nematocidal toxin (33-35) which is also highly active against corn rootworms (36-38). Its interaction at the cellular and molecular levels with target insects has received limited attention until now. Recently, the high-resolution, three-dimensional structures of this 475-amino acid protein have been elucidated for its native (39) and trypsinized (39,40) forms. The structure of this protein is completely different from those previously reported for three-domain *Bt* toxins (41-48), a *Bt* protoxin (49), β-sheet-rich, aerolysin-like, *Bt* toxins (50,51) and a *Bt* crystal protein for which no toxicity has yet been identified (52). On the other hand, the Cry6Aa structure is very similar to that of *Escherichia coli* hemolysin E (53) and other hemolysins produced by *Bacillus cereus* (54,55).

In this work, the molecular mode of action of Cry6Aa1, in its native and protease-treated forms, was investigated with the planar lipid bilayer electrophysiology technique that was successfully used to demonstrate pore formation by several other *Bt* toxins (56-60). The results show that the protein forms pores at very low doses and in a wide range of pH. Moreover, the native Cry6Aa1 does not need proteolytic processing to form pores. Finally, the pore properties are altered by the presence of WCRW midgut brush border material.

RESULTS

Biochemistry and Bioassays—Solubilisation is the initial step in the classical mode of action of Cry toxins. The solubilisation efficiency of Cry6Aa1 crystals was assessed between pH 3.0 and pH 10.0 (Fig. 1A). The protein was 100% soluble at pH 10.0. At pH 3.0, 7.0, 8.0 and 9.0, the toxin's crystal solubilisation efficiency was reduced, ranging between 15% and 25%. Solubilisation was the lowest between pH 4.0 and 6.0.

In agreement with previously published data (38), the native Cry6Aa1 produced in *Pseudomonas fluorescens* runs as a 55-kDa protein on SDS-PAGE (Fig. 1B) with a faint band corresponding to a 110-kDa protein, suggesting the presence of dimers. Treatment with WCRW

midgut juice produced a 45-kDa protein (Cry6Aa1 WCR). The trypsin-treated toxin (Cry6Aa1 TT) migrated as a major 45-kDa protein with a second, faint band corresponding to a slightly smaller polypeptide.

The native Cry6Aa1, Cry6Aa1 WCR and Cry6Aa1 TT were bioassayed on WCRW larvae at a single dose of 100 μg/cm^2. Complete (100%) growth inhibition was observed in response to the three toxins, compared with 81-95% for the binary toxin Cry34Ab1/Cry35Ab1. Mortality after 5 days in response to native Cry6Aa1 was 100%, but only 69-82% for Cry6Aa1 WCR and 81-82% for Cry6Aa1 TT.

Different Protease Treatments of the Toxin Affect its Biophysical Properties—Because Cry6Aa1 naturally exerts its effect in the insect midgut environment, PLB experiments were first performed with Cry6Aa1 WCR (Fig. 2A). The toxin was most likely to insert into the bilayer and display channel activity at positive voltages. It usually became silent at voltages more negative than -60 mV. The minimal dose for clear protein insertion and channel activity was 100 fg/ml, a dose at which the current jumps were well resolved and the success rate of pore formation was close to 100%. The pores usually stayed open for long periods of time, from several hundreds of milliseconds to seconds, with short closures of 250 ms or less. At least five distinct conductance levels could be identified in individual experiments (Fig. 2B). The current-voltage relationships were linear, indicating that the channels were essentially ohmic. In three similar experiments, the conductance was between 28 and 459 pS under symmetrical (150 mM KCl) conditions at pH 5.5, the physiological pH of the target insect. The pores were slightly cation-selective, as shown by the leftward shift of the current-voltage relationships obtained under 450 mM:150 mM KCl (*cis*:*trans*) conditions (Fig. 2C and 2D). The fact that, under these conditions, a positive current was detected in the absence of an applied voltage demonstrates that potassium ions diffuse through the pores faster than chloride ions. The relative permeability of potassium ions over chloride ions was close to 2.6 (Table 1). However, due to the complexity of the recordings with various current jump sizes within the same experiment, further biophysical analysis of channel activity, such as kinetic and opening probability studies, was extremely difficult to perform.

Cry6Aa1 was able to form pores in PLBs without any prior protease treatment (Fig. 3A, two upper traces). However, insertion was less efficient, as a minimum of 200 pg/ml of toxin

was required to observe channel activity, a dose 2000 times higher than that used for Cry6Aa1 WCR under the same experimental conditions. The conductance of the pores formed by native Cry6Aa1 ranged from 71 to 499 pS in three similar experiments under symmetrical conditions at pH 5.5 (IV curves not shown). The pores were slightly cationic at that pH and under asymmetrical conditions. The potassium to chloride ion permeability ratio was around 2.7 (Table 1).

On the other hand, Cry6Aa1 TT was able to form pores in PLBs at the same dose (100 fg/ml) as Cry6Aa1 WCR (Fig. 3A, two lower traces). The conductance of the pores ranged from 29 to 450 pS under symmetrical conditions at pH 5.5. Smaller amplitude current jumps (corresponding to lower values of conductance) were more often seen, suggesting that the Cry6Aa1 TT protein channels were preferentially staying in their lower conducting states or substates (not shown). Depending on the experiment, the ionic selectivity of Cry6Aa1 TT was either slightly cationic or slightly anionic, with potassium to chloride ion permeability ratios of 2.2 and 0.3, respectively (Table 1). Native Cry6Aa1 and Cry6Aa1 WCR remained active for hours. On the other hand, while Cry6Aa1 TT displayed well-resolved current jumps, it usually became silent after 5 min, suggesting a less stable partition of this protein into the membrane. In summary, protease treatment of the native Cry6Aa1 toxin affected the amount of protein needed for pore formation and the biophysical properties of the pores, but such treatment was not necessary for efficient pore formation by Cry6Aa1.

Effect of pH on the Properties of Cry6Aa1—To explore the possibility that the intestinal pH of target organisms may play a significant role in the specificity of Cry6Aa1, pore formation experiments were conducted at pH 5.5, 7.5 and 9.5 using the native form of Cry6Aa1. The toxin was able to form pores at all three pH values, although the current jumps were better resolved at pH 5.5 and 7.5 than at pH 9.5 (Fig. 3B). Table 1 shows the conductance range of the Cry6Aa1 pore at acidic, almost neutral and alkaline pHs. The cumulative frequency distributions of the toxin conductance (in 50 pS bins) were constructed for each pH (Fig. 4). The conductance distribution of Cry6Aa1 at pH 9.5 was significantly different from those at pH 5.5 and 7.5 (Mann-Whitney test at 5% significance level). The pores were slightly selective to cations at all three pH values. However, as shown in Table 1, the potassium to chloride ion permeability ratio was higher at alkaline pH (3.5 at pH 9.5, compared to 2.7 at pH 5.5 and 7.5), but the differences

were not statistically significant (Student's two samples t-test at 5% significance level). This indicates that the toxin had a very similar behaviour at pH 5.5 and 7.5 but, at pH 9.5, the environment was somewhat less favorable to insertion and stable channel activity. These results indicate that other factors play a role in the target specificity of Cry6Aa1 besides pH.

Effect of PLB Enrichment with WCRW Midgut Brush Border Membrane Material— Binding to receptors on the midgut brush border membrane is a critical step of the classical mode of action of *Bt* toxins (17). So far, no receptor of Cry6Aa toxins has been identified in WCRW larvae. To test the role of putative receptors or other docking molecules of Cry6Aa1 on the formation and properties of the toxin's pores, experiments were conducted at pH 5.5 using Cry6Aa1, either in its native form or treated with WCRW gut juice, in PLBs in which WCRW midgut brush border membrane fractions (BBMF) had been reconstituted.

Cry3Aa is a *Bt* toxin that is active against the WCRW and that binds to a yet unidentified receptor in this insect's midgut (38). It was used to ascertain that PLB enrichment with BBMF was achieved. Chymotrypsin-activated Cry3Aa triggered channel activity in enriched PLBs at doses 200 times lower than what was required to form pores in BBMF-free PLBs (1-5 μg/ml), a toxin dose reduction (data not shown), comparable to those observed in earlier PLB studies on the interaction of Cry1 toxins with *Manduca sexta* (Lepidoptera) (57) and *Lymantria dispar* (Lepidoptera) (59) midgut receptors.

The native Cry6Aa1 inserted itself in a very stable way in the enriched PLB at a minimal dose of 100 fg/ml, 2000-fold less than what was required in BBMF-free bilayers (Fig. 5A). Current jumps were well-resolved and several conductance levels could be measured in each experiment (Fig. 5B). Conductance ranged from 56 to 637 pS (Table 1), which included slightly larger values than those measured in the absence of midgut material. A more striking difference was observed at the level of pore selectivity. From slightly cationic in the absence of BBMF in PLBs, the pores became very slightly anionic in enriched bilayers, with the K^+/Cl^- permeability ratio shifting from 2.7 to 0.8 (Table 1).

The effect of WCRW midgut material on Cry6Aa1 WCR pores was different. Whereas the protein's insertion efficiency, i.e., the minimal dose required to form pores, remained equal to 100 fg/ml in both BBMF-rich and BBMF-free PLBs, apparent rectification of the currents was observed (Fig. 5C). As shown in Fig. 5D, the range of conductances measured at positive

holding voltages was larger than at negative ones in this particular experiment. However, the opposite situation was observed in other experiments, i.e., conductances at negative voltages being larger than those at positive voltages, suggesting that midgut juice-treated Cry6Aa1 inserted itself into PLBs in more than one way. In any case, the conductances at non-rectifying voltages ranged between 40 and 306 pS, while those at rectifying voltages were comprised between 15 and 95 pS (Table 1). Just like the native Cry6Aa1, Cry6Aa1 WCR pores were slightly anionic, with a potassium to chloride permeability ratio of 0.8 (Table 1).

To make sure that the Cry6Aa1 proteins were not further processed by intrinsic proteases in BBMF-enriched PLBs, control experiments in the presence of a protease inhibitor cocktail were performed that confirmed that pore formation and biophysical properties were similar to those described above (data not shown).

These results suggest that the midgut protease digestion step of Cry6Aa1 is not critical for pore formation in PLBs. However, it cannot be excluded that it may affect the toxin's molecular recognition process and in turn influence its pore formation ability.

DISCUSSION

This study clearly shows, for the first time, that Cry6Aa1, a *Bt* toxin that is active against nematodes and coleopteran pests, is a pore-forming toxin. Pore insertion and channel activity were demonstrated in phospholipid PLBs and in target insect midgut BBMF-enriched PLBs. Moreover, the native, unprocessed Cry6Aa1 protein displayed channel activity in both types of membranes, a finding which was never reported for other *Bt* protoxins. Furthermore, pore formation by Cry6Aa1, in its native or protease-processed forms, took place at unprecedented low protein concentrations, several orders of magnitude lower than those used for any other *Bt* toxin. Finally, it was established that the ability of Cry6Aa1 to form pores was affected by proteases, pH and midgut brush border membrane material, which are major components of the insect intestinal environment to which the toxin is exposed *in vivo*.

Our results on the pH dependence of the solubilisation of Cry6Aa1 indicated that pH 10 was the optimal pH at which the native toxin was solubilised. This very alkaline environment is quite different from that of the midgut of WCRW, the Cry6Aa1 susceptible insect, which was reported to be acidic (pH 5.75) (61). Likewise, the intestinal pH of nematodes, such as

Caenorhabditis elegans, which are also targeted by Cry6A toxins, has been found to range between 4.4 and 6.3 (62,63). It should be noted, however, that pH measurements are extremely difficult to conduct in tiny organisms like nematodes and coleoptera. Actually, the documented pH of WCRW was measured in homogenised midgut juice collected from larvae of this insect (62). There is also a pH gradient along the midgut of coleopteran larvae, as measured in *Tenebrio molitor* and *Morimus funereus* midguts in which the pH of the anterior midguts was around 5.5, whereas it was close to 8.5 in their posterior part (64,65). Therefore, it cannot be excluded that such gradients also exist in the WCRW midgut. On the other hand, the pH dependence of Cry6Aa1 solubility is comparable to that of Cry3A, another *Bt* toxin that targets coleopteran pests (66).

Bioassays of Cry6Aa1 on WCRW larvae showed that the dose of Cry6Aa1 needed to inhibit larval growth or kill the insects was similar to that reported for Cry3Aa1 and Cry34Ab1/Cry35Ab1 (38). It was therefore very surprising to find out that the toxin dose required for pore formation in PLBs was several orders of magnitude lower, even under experimental conditions designed to mimic the *in vivo* environment in the WCRW midguts (pH, proteolytic processing of the toxin and presence of apical membrane material). The origin of this huge dose difference remains to be investigated.

It is considered that the most biologically relevant form of the Cry6Aa1 proteins investigated in the present study is Cry6Aa1 WCR, the target insect midgut juice-treated Cry6Aa1. This protein formed pores in PLBs displaying very well resolved current jumps. The conductance of the pores was smaller than that reported for other toxins active against coleoptera. The binary toxin Cry34Ab1/Cry35Ab1, which is also active against WCRW, formed pores in PLBs, whose conductance ranged between 310 and 920 pS under the same experimental conditions as those used here (60). Likewise, the conductance of Cry3A pores formed in PLBs under identical experimental conditions was 505 pS (58). On the other hand, the conductance of Cry6Aa1 WCR is similar to that of lepidopteran toxins, such as Cry1Aa, tested in PLBs under identical experimental conditions, whose principal conductance was 450 pS (42), and larger than those of Cry1B and Cry1C, whose principal conductances were 350 pS and 90 pS, respectively (57).

As mentioned before, the largest difference with any other protease-treated *Bt* toxins tested so far was at the level of the dose used to observe channel activity. Usually, the dose needed for Cry toxins to efficiently partition into PLBs was in the order of µg/ml (see for example (56,60)). In the case of Cry6Aa1, a dose as low as 100 fg/ml was sufficient for pore formation. Such a dose is also smaller by 3-4 orders of magnitude than those used for the structurally similar bacterial toxins hemolysin E to form pores in lipid bilayers (67,68).

The sequence of steps involved in the classical mode of action of *Bt* toxins includes solubilisation and protease activation in the gut of target insects (17). However, it was demonstrated in the present study that Cry6Aa1, a *Bt* toxin whose 3-D structure at atomic resolution is entirely different from those of any other known *Bt* toxin (39,40), displayed channel activity in PLBs at extremely low dose, without protease processing and over a wide pH range, conditions under which pore formation by other *Bt* toxins was never reported before. The biophysical properties of the pores formed by Cry6Aa1 were not much affected by pH, unlike other *Bt* toxins that target coleopteran insects such as Cry3Aa, which precipitates and is not able to form pores at acidic pH (unpublished data of this laboratory) or Cry34Ab1/Cry35Ab1 which was not able to efficiently form pores at alkaline pH (60), as well as *Bt* toxins that are active against lepidopteran pests, like Cry1C, which has been shown to display different pore properties, such as ionic selectivity, depending on pH (56). Trypsin or WCRW midgut juice treatment provided proteins with identical molecular weights, even though trypsin is not a major protease in WCRW midgut juice (61). Furthermore, the products of such protease treatment, Cry6Aa1 TT and Cry6Aa1 WCR, formed pores at a similar dose and with similar conductances, but different ion selectivities. Cry6Aa1 WCR pores were slightly cationic, while those made by Cry6Aa1 TT displayed dual selectivity, sometimes to anions and at other times to cations, depending on the experiment. Such unusual behaviour was never observed with other *Bt* toxins. It may be indicative of two different membrane insertion modes of Cry6Aa1 TT. More work is needed to fully understand the structure-function relationships involved in the role of pH and protease processing on Cry6Aa1 pore formation and properties. The recent publication of the 3-D structures of the native and the trypsin-treated toxins should provide the necessary information at the molecular level to undertake structure-function studies, in particular in the

light of the discovery that these two structures are very similar to the α-helix rich molecules of other bacterial pore-forming toxins (39,40).

The molecular recognition step of the mode of action of *Bt* has been difficult to study for coleopteran active toxins due to the lack of information on the proteins that may constitute their putative receptors. In this study, target insect midgut BBMFs were successfully reconstituted in PLBs and it was shown that both the native Cry6Aa1 and the protease-treated Cry6Aa1 WCR toxins interacted with the apical membrane of the WCRW midgut, although in different ways. For pore formation in the presence of midgut membrane material, a 2000-fold reduction in the dose of the native Cry6A1 toxin was observed, down to the same dose as that of Cry6Aa1 WCR, whereas the Cry6Aa1 WCR dose remained the same with or without midgut material. Such effect of midgut BBMFs on the dose required for *Bt* pores has been reported for Cry1Aa (59) and Cry1Ac (57) for which a significant, but not as large as here, dose reduction was observed. Moreover, the conductance of the Cry6Aa1 WCR pores was also affected by the presence of WCRW midgut apical membrane fractions, showing some kind of current rectification. Such current rectifying effect and change in the biophysical characteristics of the pores was shown for Cry1Ac toxins when *M. sexta* midgut brush border aminopeptidase N, which acts as a receptor to a range of *Bt* toxins, was reconstituted in PLBs (57). Finally, the pore selectivity of both native Cry6Aa1 and Cry6Aa1 WCR changed from cationic to anionic in BBMF-enriched PLBs. This has never been observed before with other *Bt* toxins.

It is generally accepted that pH, specific proteases and receptors in the midgut of target insects are major determinants of *Bt* Cry toxin specificity. However, in this PLB study of Cry6Aa1 under various pH, proteolytic processing and BBMF exposure conditions, it was demonstrated that, although these factors affected pore formation and properties to some extent, the toxin was actually extremely efficient *in vitro* under any of the experimental conditions that were used. The doses required for pore formation in PLBs, as well as the specificity of the toxin to particular nematodes and coleopteran insects, suggest that Cry6Aa1 does not necessarily have the same mode of action as other Cry toxins.

EXPERIMENTAL PROCEDURES

Chemicals—The lipids used in the planar lipid bilayer experiments were 1-palmitoyl-2-oleoyl-*sn*-glycero-3-phosphocholine (POPC) and 1-palmitoyl-2-oleoyl-*sn*-glycero-3-phosphoethanolamine (POPE). Liposomes were prepared with L-α-phosphatidylcholine (PC) from egg yolk. All the lipids were purchased from Avanti Polar Lipids (Alabaster, AL, USA). Analytical grade salts, MES, HEPES, Tris, 2-(Cyclohexylamino)ethanesulfonic acid (CHES), 3-(Cyclohexylamino)-1-propanesulfonic acid (CAPS), EGTA and n-decane were purchased from Sigma **(**Oakville, Ontario, Canada**)**. Additionally, a protease inhibitor cocktail (P8340) containing inhibitors of each major class of proteases, N-p-tosyl-L-phenylalanine chloromethyl ketone (TPCK)-treated trypsin and N-p-tosyl-L-lysine chloromethyl ketone (TLCK)-treated α-chymotrypsin (both from bovine pancreas) were all purchased from Sigma.

Full Length Cry6Aa1 Expression and Purification—The Cry6Aa1 protein was expressed in *P. fluorescens* and the inclusion bodies were purified using the methods described previously (69). Approximately, 100 mg of Cry6Aa1 inclusion bodies were thawed at 4°C and centrifuged at 31,000 x *g* for 20 min at 4°C. The pellet was mixed with 20 ml of 0.1 M CAPS/KOH (pH 10) and incubated at room temperature with rocking to extract the target protein.

The solubilized Cry6Aa1 was purified at room temperature by ion-exchange chromatography on a 5 ml HiTrap Q HP column with an AKTA protein purifier (GE Healthcare Life Sciences, Pittsburgh, PA, USA). The toxin extracts were diluted to 20 mM CAPS/KOH, pH 10, and filtered by a vacuum driven filter with a 0.45-µm pore diameter low protein-binding membrane. The samples were injected at 3 ml/min on a column pre-equilibrated with buffer A (50 mM CAPS/KOH, pH 10). The column was washed with approximately 25 ml of buffer A, and the protein was eluted using a linear gradient of 0-100% buffer B (50 mM CAPS, pH 10 + 1 M NaCl) over 40 column volumes. The fractions containing the purified target protein were identified by SDS-PAGE analysis. Peak fractions containing the target protein were pooled and concentrated using a centrifugal filter device with a 30-kDa molecular weight cut off. Quantification of target bands was done by comparing densitometric values of the bands against bovine serum albumin standard samples run on the same gel to generate a standard curve using the ImageQuant software package (GE Healthcare Life Sciences).

Trypsin Processing of Cry6Aa1—Approximately 100 mg of Cry6Aa inclusion bodies were thawed at 4°C and centrifuged at 23,000 x *g* for 25 min at 4°C. The pellet was mixed with 10 ml of digestion buffer (0.1 M CAPS/KOH buffer, pH 10), and 6.6 mg of TPCK-treated trypsin from bovine pancreas was added to the sample to attain a Cry6Aa1:trypsin ratio of 15:1 (w/w). The reaction tube was incubated overnight at room temperature (~16 hours) with gentle rocking. After digestion, the mixture was centrifuged at 31,000 x *g* for 25 min at 4°C. The supernatant was saved for ion-exchange chromatography purification. The buffer of the purified toxin fractions was finally exchanged by dialysis against 4 liters of 20 mM CAPS/KOH, pH 10.

Midgut Juice Collection and Extraction—Approximately 150 third-instar WCRW larvae were obtained from Crop Characteristics (Farmington, MN, USA) and shipped with corn roots. Using a scalpel, both the anterior and posterior ends of the larvae were removed. The gut was pulled out using forceps and stored on ice in 0.15 M NaCl and 8.5% sucrose. The tissue was homogenized on ice using a glass tissue homogenizer and the insoluble material was removed by centrifugation in a microcentrifuge at 7,500 x *g* for 15 min at 4°C. The supernatants were quantified for total protein concentration using a Bradford assay (Fisher, Hampton, NH, USA) and then stored in small aliquots at -80°C until further use.

WCRW Midgut Juice Processing of Cry6Aa1—Full length Cry6Aa1 (10 mg) purified as described above was mixed with 1 mg total protein of WCRW gut juice in 10 ml of 0.2 M sodium citrate at pH 6.0 and 4 mM EDTA. After 3 hours of incubation at room temperature, aliquots were removed and analyzed by SDS-PAGE to ensure completion of the digestion. The reaction was stopped by the addition of a cocktail of protease inhibitors, and the mixture was dialyzed overnight against 20 mM CAPS/KOH, pH 10 before ion-exchange chromatography purification. Fractions containing target protein were pooled and concentrated using a Millipore 30-kDa molecular weight cut off membrane ultrafiltration device.

Cry3Aa Preparation—Cry3Aa toxin inclusion bodies were prepared as described previously using the *P. fluorescens* heterologous expression system (69). Inclusion bodies were solubilized in 20 ml of 0.1 M CAPS pH 10 at room temperature for 2 hours. The solubilized protein was centrifuged for 20 min at 31,000 x *g* at 4°C. The technique used for activation of the protoxin was modified from that described by Carroll et al. (70). The solubilized protoxin (10 mg in 2 ml) was mixed with 10 mg of TLCK-treated chymotrypsin in 9 ml of 25 mM Tris,

pH 8.5. The sample was incubated for 16 hours at 37°C. The chymotrypsin-treated Cry3A was purified by ion exchange chromatography as described above, except that the pH of buffers A and B was increased to 11. Fractions containing the target protein were identified by SDS-PAGE analysis, pooled, concentrated to approximately 2 ml with Amicon spin concentrators (30-kDa molecular weight cut off) and further purified by chromatography on a Superdex 75 column (approximately 180 ml bed volume) at 1 ml/min.

Solubilisation Experiments—The solutions used to evaluate the solubility of native Cry6Aa1 contained 150 mM KCl and 50 mM of either sodium citrate (pH 3, 4 and 5), MES/KOH (pH 6), HEPES/KOH (pH 7), Tris/HCl (pH 8), CHES/KOH (pH 9) or CAPS/KOH (pH 10). The inclusion bodies were incubated for 2h at room temperature. The suspension was then centrifuged at 100,000 x *g* for 1 h and the protein content of the supernatant was estimated with the Bradford assay.

Bioassays—The toxicity of the purified native, midgut juice- and trypsin-treated Cry6Aa1 proteins was assayed at 100 μg/cm^2 by diet surface contamination as described previously (38). Sixteen insects were used for each condition.

Planar Lipid Bilayers—Membranes were formed with a mixture of POPE:POPC 1:1 (w/w) at a final concentration of 20 mg/ml in n-decane. Pasteur pipets that were previously pulled and sealed on a Bunsen burner were used to paint a bilayer across a 250-μm aperture in a Delrin membrane separating two 1 ml chambers (*cis* and *trans*). Disposable chamber-membrane systems were used to prevent contamination from one experiment to the next. The aperture was pretreated with 0.5 μl of the lipid mixture dissolved in n-decane. The lipids were dried under N_2 for 10 minutes before use.

Experiments were conducted in a solution composed of 150 mM KCl, 1 mM $CaCl_2$ and 10 mM of either MES/KOH (pH 5.5), HEPES/KOH (pH 7.5) or Tris/HCl (pH 9.5). For asymmetrical conditions experiments, the KCl concentration was raised to 450 mM, on the *cis* side of the membrane, using a stock solution of 3 M KCl, 1 mM $CaCl_2$ and 10 mM of either MES/KOH (pH 5.5), HEPES/KOH (pH 7.5) or Tris/HCl (pH 9.5).

The lipid bilayer quality was assessed by measuring the membrane capacitance, whose value was optimally around 180 pF. Before injection of the proteins, the membrane current was monitored for 30 min with holding voltages ranging from -150 to +150 mV to make sure that

there was no contaminating pore-forming material in the bilayer system. Magnetic stirrers were used in both *cis* and *trans* compartments. All experiments were performed at room temperature. The proteins to be tested were added to the *cis* to reach final concentrations that ranged from 100 fg/ml to 1 µg/ml.

The electrical connections between the experimental chambers and the recording instrumentation were made with Ag/AgCl electrodes and agar salt bridges (2 M KCl, 1 mM EGTA and 2% agar). Currents were recorded with an Axopatch-1D patch-clamp amplifier (Axon Instruments, Molecular Devices, Sunnyvale, CA, USA), filtered at 10 kHz, digitized at a 50 kHz sampling frequency (Digidata 1440, Molecular Devices). They were processed and analyzed using pClamp 10.5 software (Axon Instruments).

Holding voltages were applied to the membrane from +80 mV to -80 mV in 20 mV steps and for variable durations. For each applied voltage, the amplitudes of the current jumps were measured, grouped and averaged. Current-voltage (IV) plots were then constructed and the data points were fitted with linear curves whose slopes provided the conductances of the pores. Reversal potentials were obtained from IV relationships of experiments conducted under asymmetrical ionic conditions. Potassium over chloride permeability ratios were calculated from the reversal potential, which is given by the horizontal axis-intercept, with the Goldman-Hodgkin-Katz equation (71).

Brush Border Membrane Fragment Fusion in PLBs— Previously isolated WCRW larvae midguts were used to prepare brush border membrane fragments (BBMFs) as described elsewhere (72). The BBMFs were aliquoted, stored at -80°C in 10 mM HEPES/KOH, pH 7.5, and used within the next five months. Compared with the initial crude homogenate, the BBMF were enriched 8.4-fold, as indicated by aminopeptidase N activity (73). BBMF-enriched liposomes were prepared as described elsewhere (74) with some modifications. Egg yolk PC was used as the base lipid. It was dried under N_2 and hydrated in 150 mM KCl, 1 mM EGTA and 10 mM HEPES/KOH (pH 7.5) at a final BBMF proteins:lipid ratio of 1:60 (w/w). The BBMF enriched-liposomes were mechanically fused to the PLBs (59) from the *cis* side using a Pasteur pipette with a very small round tip. The membrane current was monitored for 30 minutes before toxin addition. No contaminating or BBMF intrinsic channel activity could be observed during these control periods.

Data Presentation—All experiments were performed at least three times. The cumulative frequency distribution of pore conductances was obtained by grouping the conductances in 50 pS-bins and the Mann-Whitney test for independent variables was used to evaluate the significance at $p<0.05$ of the difference between the data obtained under each experimental condition.

Acknowledgment: We thank Ted Letherer for supporting *Diabrotica virgifera virgifera* bioassays.

Conflict of interest: EF, VL, LP, VV and JLS declare that they have no conflicts of interest with the contents of this article. SG, VC, DM, KN are employed by Dow AgroSciences, LLC. TH and XX are former employees of that company.

Author contributions: VC, TH, DM, KN, VV and JLS conceived experiments; VC and XX prepared the experimental materials and SG performed protein analysis; SYT conducted WCRW bioassay experiments; EF conducted the solubilisation and PLB experiments, with the help of VL and LP, and wrote the first draft of the manuscript; the subsequent versions were discussed and written by VC, KN, VV and JLS.

REFERENCES

1. Bulla, L. A., Bechtel, D. B., Kramer, K. J., Shethna, Y. I., Aronson, A. I., and Fitz-James, P. C. (1980) Ultrastructure, physiology, and biochemistry of *Bacillus thuringiensis*. *Crit. Rev. Microbiol.* **8**, 147-204
2. Aronson, A. I. (2002) Sporulation and δ-endotoxin synthesis by *Bacillus thuringiensis*. *Cell. Mol. Life Sci.* **59**, 417-425
3. van Frankenhuyzen, K. (2009) Insecticidal activity of *Bacillus thuringiensis* crystal proteins. *J. Invertebr. Pathol.* **101**, 1-16
4. Federici, B. A. (2005) Insecticidal bacteria: an overwhelming success for invertebrate pathology. *J. Invertebr. Pathol.* **89**, 30-38

5. Bravo, A., Likitvivatanavong, S., Gill, S. S., and Soberón, M. (2011) *Bacillus thuringiensis*: a story of a successful bioinsecticide. *Insect Biochem. Mol. Biol.* **41**, 423-431
6. Sanchis, V., and Bourguet, D. (2008) *Bacillus thuringiensis*: applications in agriculture and insect resistance management. A review. *Agron. Sustain. Dev.* **28**, 11-20
7. van Frankenhuyzen, K. (2000) Application of *Bacillus thuringiensis* in forestry. In *Entomopathogenic Bacteria: from Laboratory to Field Application* (Charles, J. F., Delécluse, A., and Nielsen-Leroux, C. eds.), Kluwer Associate Publishing, Norwell, MA, USA. pp 371-376
8. Becker, N. (2000) Bacterial control of vector-mosquitoes and blackflies. In *Entomopathogenic Bacteria: from Laboratory to Field Application* (Charles, J. F., Delécluse, A., and Nielsen-Leroux, C. eds.), Kluwer Associate Publishing, Norwell, MA, USA. pp 383-396
9. James, C. (2015) 20th Anniversary (1996 to 2015) of the Global Commercialization of Biotech Crops and Biotech Crop Highlights in 2015. ISAAA Brief No. 51, ISAAA, Ithaca, NY, URL: http://www.isaaa.org/resources/publications/briefs/51/executivesummary/default.asp
10. Rajamohan, F., Lee, M. K., and Dean, D. H. (1998) *Bacillus thuringiensis* insecticidal proteins: molecular mode of action. *Prog. Nucleic Acid Res. Mol. Biol.* **60**, 1-27
11. Schnepf, E., Crickmore, N., Van Rie, J., Lereclus, D., Baum, J., Feitelson, J., Zeigler, D. R., and Dean, D. H. (1998) *Bacillus thuringiensis* and its pesticidal crystal proteins. *Microbiol. Mol. Biol. Rev.* **62**, 775-806
12. Aronson, A. I., and Shai, Y. (2001) Why *Bacillus thuringiensis* insecticidal toxins are so effective: unique features of their mode of action. *FEMS Microbiol. Lett.* **195**, 1-8
13. Bravo, A., Gill, S. S., and Soberón, M. (2007) Mode of action of *Bacillus thuringiensis* Cry and Cyt toxins and their potential for insect control. *Toxicon* **49**, 423-435
14. Carroll, J., and Ellar, D. J. (1993) An analysis of *Bacillus thuringiensis* δ-endotoxin action on insect midgut membrane permeability using a light-scattering assay. *Eur. J. Biochem.* **214**, 771-778

15. Kirouac, M., Vachon, V., Rivest, S., Schwartz, J. L., and Laprade, R. (2003) Analysis of the properties of *Bacillus thuringiensis* insecticidal toxins using a potential-sensitive fluorescent probe. *J. Membr. Biol.* **196**, 51-59

16. Knowles, B. H., and Ellar, D. J. (1987) Colloid-osmotic lysis is a general feature of the mechanism of action of *Bacillus thuringiensis* δ-endotoxins with different insect specificity. *Biochim. Biophys. Acta* **924**, 509-518

17. Vachon, V., Laprade, R., and Schwartz, J. L. (2012) Current models of the mode of action of *Bacillus thuringiensis* insecticidal crystal proteins: a critical review. *J. Invertebr. Pathol.* **111**, 1-12

18. McGaughey, W. H., and Oppert, B. (1998) Mechanism of insect resistance to *Bacillus thuringiensis* toxins. *Israel J. Entomol.* **32**, 1-14

19. Frutos, R., Rang, C., and Royer, F. (1999) Managing insect resistance to plants producing *Bacillus thuringiensis* toxins. *Crit. Rev. Biotechnol.* **19**, 227-276

20. Ferré, J., and Van Rie, J. (2002) Biochemistry and genetics of insect resistance to *Bacillus thuringiensis*. *Annu. Rev. Entomol.* **47**, 501-533

21. Pigott, C. R., and Ellar, D. J. (2007) Role of receptors in *Bacillus thuringiensis* crystal toxin activity. *Microbiol. Mol. Biol. Rev.* **71**, 255-281

22. Pardo-López, L., Soberón, M., and Bravo, A. (2013) *Bacillus thuringiensis* insecticidal three-domain Cry toxins: mode of action, insect resistance and consequences for crop protection. *FEMS Microbiol. Rev.* **37**, 3-22

23. Kao, C. Y., Los, F. C. O., Huffman, D. L., Wachi, S., Kloft, N., Husmann, M., Karabrahimi, V., Schwartz, J. L., Bellier, A., Ha, C., Sagong, Y., Fan, H., Ghosh, P., Hsieh, M., Hsu, C. S., Chen, L., and Aroian, R. V. (2011) Global functional analyses of cellular responses to pore-forming toxins. *PLoS Pathog.* **7**, doi:10.1371/journal.ppat.1001314

24. Head, G. P., and Greenplate, J. (2012) The design and implementation of insect resistance management programs for Bt crops. *GM Crops Food* **3**, 144-153

25. Estruch, J. J., Warren, G. W., Mullins, M. A., Nye, G. J., Craig, J. A., and Koziel, M. G. (1996) Vip3A, a novel *Bacillus thuringiensis* vegetative insecticidal protein with a wide

spectrum of activities against lepidopteran insects. *Proc. Natl. Acad. Sci. USA* **93**, 5389-5394

26. Milne, R., Liu, Y. H., Gauthier, D., and van Frankenhuyzen, K. (2008) Purification of Vip3Aa from *Bacillus thuringiensis* HD-1 and its contribution to toxicity of HD-1 to spruce budworm (*Choristoneura fumiferana*) and gypsy moth (*Lymantria dispar*) (Lepidoptera). *J. Invertebr. Pathol.* **99**, 166-172
27. Ma, B. L., Meloche, F., and Wei, L. (2009) Agronomic assessment of Bt trait and seed or soil-applied insecticides on the control of corn rootworm and yield. *Field Crops Res.* **111**, 189-196
28. Hibbard, B. E., Clark, T. L., Ellersieck, M. R., Meihls, L. N., El Khishen, A. A., Kaster, V., Steiner, H. Y., and Kurtz, R. (2010) Mortality of Western corn rootworm larvae on MIR604 transgenic maize roots: field survivorship has no significant impact on survivorship of F1 progeny on MIR604. *J. Econ. Entomol.* **103**, 2187-2196
29. Gassmann, A. J., Petzold-Maxwell, J. L., Keweshan, R. S., and Dunbar, M. W. (2011) Field-evolved resistance to Bt maize by Western corn rootworm. *PLoS One* **6**, doi:10.1371/journal.pone.0022629
30. Tabashnik, B. E., and Gould, F. (2012) Delaying corn rootworm resistance to Bt corn. *J. Econ. Entomol.* **105**, 767-776
31. Aragón, P., Baselga, A., and Lobo, J. M. (2010) Global estimation of invasion risk zones for the Western corn rootworm *Diabrotica virgifera virgifera*: integrating distribution models and physiological thresholds to assess climatic favourability. *J. Appl. Ecol.* **47**, 1026-1035
32. Aragón, P., and Lobo, J. M. (2012) Predicted effect of climate change on the invasibility and distribution of the Western corn rootworm. *Agric. For. Entomol.* **14**, 13-18
33. Narva, K. E., Schwab, G. E., Galasan, T., and Payne, J. M. (1993) Gene encoding a novel nematode-active toxin cloned from a *Bacillus thuringiensis* isolate. United States Patent 5,236,843
34. Wei, J. Z., Hale, K., Carta, L., Platzer, E., Wong, C., Fang, S. C., and Aroian, R. V. (2003) *Bacillus thuringiensis* crystal proteins that target nematodes. *Proc. Natl. Acad. Sci. USA* **100**, 2760-2765

35. Luo, H., Xiong, J., Zhou, Q. N., Xia, L. Q., and Yu, Z. Q. (2013) The effects of *Bacillus thuringiensis* Cry6A on the survival, growth, reproduction, locomotion, and behavioral response of *Caenorhabditis elegans*. *Appl. Microbiol. Biotech.* **97**, 10135-10142

36. Narva, K. E., Schwab, G. E., and Bradfisch, G. A. (1993) Novel *Bacillus thuringiensis* gene encoding coleopteran-active toxin. United States Patent 5,186,934

37. Bradfisch, G. A., Muller-Cohn, J., Narva, K. E., Fu, J. M., and Thompson, M. (1999) *Bacillus thuringiensis* isolates, toxins, and genes for controlling certain coleopteran pests. United States Patent 5,973,231

38. Li, H., Olson, M., Lin, G., Hey, T., Tan, S. Y., and Narva, K. E. (2013) *Bacillus thuringiensis* Cry34Ab1/Cry35Ab1 interactions with Western corn rootworm midgut membrane binding sites. *PLoS One* **8**, doi:10.1371/journal.pone.0053079

39. Dementiev, A., Board, J., Sitaram, A., Hey, T., Kelker, M. S., Xu, X., Hu, Y., Vidal-Quist, C., Chikwana, V., Griffin, S., McCaskill, D., Wang, N. X., Hung, S.-C., Chan, M. K., Lee, M. M., Hughes, J., Wegener, A., Aroian, R. V., Narva, K. E., and Berry, C. (2016) The pesticidal Cry6Aa toxin from *Bacillus thuringiensis* is structurally similar to HlyE-family alpha pore-forming toxins. *BMC Biology* **14**, 71

40. Huang, J., Guan, Z., Wan, L., Zou, T., and Sun, M. (2016) Crystal structure of Cry6Aa: a novel nematicidal ClyA-type α-pore-forming toxin from *Bacillus thuringiensis*. *Biochem. Biophys. Res. Commun.* **478**, 307-313

41. Li, J., Carroll, J., and Ellar, D. J. (1991) Crystal structure of insecticidal δ-endotoxin from *Bacillus thuringiensis* at 2.5 Å resolution. *Nature* **353**, 815-821

42. Grochulski, P., Masson, L., Borisova, S., Pusztai-Carey, M., Schwartz, J. L., Brousseau, R., and Cygler, M. (1995) *Bacillus thuringiensis* CrylA(a) insecticidal toxin: crystal structure and channel formation. *J. Mol. Biol.* **254**, 447-464

43. Galitsky, N., Cody, V., Wojtczak, A., Ghosh, D., Luft, J. R., Pangborn, W., and English, L. (2001) Structure of the insecticidal bacterial δ-endotoxin Cry3Bb1 of *Bacillus thuringiensis*. *Acta Crystallogr. Sect. D - Biol. Crystallogr.* **57**, 1101-1109

44. Morse, R. J., Yamamoto, T., and Stroud, R. M. (2001) Structure of Cry2Aa suggests an unexpected receptor binding epitope. *Structure* **9**, 409-417

45. Boonserm, P., Davis, P., Ellar, D. J., and Li, J. (2005) Crystal structure of the mosquito-larvicidal toxin Cry4Ba and its biological implications. *J. Mol. Biol.* **348**, 363-382

46. Boonserm, P., Mo, M., Angsuthanasombat, C., and Lescar, J. (2006) Structure of the functional form of the mosquito larvicidal Cry4Aa toxin from *Bacillus thuringiensis* at a 2.8-Angstrom resolution. *J. Bacteriol.* **188**, 3391-3401

47. Guo, S. Y., Ye, S., Liu, Y. F., Wei, L., Xue, J., Wu, H. F., Song, F. P., Zhang, J., Wu, X. A., Huang, D. F., and Rao, Z. H. (2009) Crystal structure of *Bacillus thuringiensis* Cry8Ea1: an insecticidal toxin toxic to underground pests, the larvae of *Holotrichia parallela*. *J. Struct. Biol.* **168**, 259-266

48. Hui, F., Scheib, U., Hu, Y., Sommer, R. J., Aroian, R. V., and Ghosh, P. (2012) Structure and glycolipid binding properties of the nematicidal protein Cry5B. *Biochemistry* **51**, 9911-9921

49. Evdokimov, A. G., Moshiri, F., Sturman, E. J., Rydel, T. J., Zheng, M. Y., Seale, J. W., and Franklin, S. (2014) Structure of the full-length insecticidal protein Cry1Ac reveals intriguing details of toxin packaging into *in vivo* formed crystals. *Protein Sci.* **23**, 1491-1497

50. Akiba, T., Abe, Y., Kitada, S., Kusaka, Y., Ito, A., Ichimatsu, T., Katayama, H., Akao, T., Higuchi, K., Mizuki, E., Ohba, M., Kanai, R., and Harata, K. (2009) Crystal structure of the parasporin-2 *Bacillus thuringiensis* toxin that recognizes cancer cells. *J. Mol. Biol.* **386**, 121-133

51. Xu, C. C., Chinte, U., Chen, L. R., Yao, Q. Q., Meng, Y., Zhou, D., Bi, L. J., Rose, J., Adang, M. J., Wang, B. C., Yu, Z. N., and Sun, M. (2015) Crystal structure of Cry51Aa1: a potential novel insecticidal aerolysin-type β-pore-forming toxin from *Bacillus thuringiensis*. *Biochem. Biophys. Res. Commun.* **462**, 184-189

52. Akiba, T., Higuchi, K., Mizuki, E., Ekino, K., Shin, T., Ohba, M., Kanai, R., and Harata, K. (2006) Nontoxic crystal protein from *Bacillus thuringiensis* demonstrates a remarkable structural similarity to pore-forming toxins. *Proteins* **63**, 243-248

53. Wallace, A. J., Stillman, T. J., Atkins, A., Jamieson, S. J., Bullough, P. A., Green, J., and Artymiuk, P. J. (2000) *E. coli* hemolysin E (HlyE, ClyA, SheA): X-ray crystal

structure of the toxin and observation of membrane pores by electron microscopy. *Cell* **100**, 265-276

54. Fagerlund, A., Lindback, T., Storset, A. K., Granum, P. E., and Hardy, S. P. (2008) *Bacillus cereus* Nhe is a pore-forming toxin with structural and functional properties similar to the ClyA (HIyE, SheA) family of haemolysins, able to induce osmotic lysis in epithelia. *Microbiology* **154**, 693-704
55. Madegowda, M., Eswaramoorthy, S., Burley, S. K., and Swaminathan, S. (2008) X-ray crystal structure of the B component of Hemolysin BL from *Bacillus cereus*. *Proteins* **71**, 534-540
56. Schwartz, J. L., Garneau, L., Savaria, D., Masson, L., Brousseau, R., and Rousseau, E. (1993) Lepidopteran-specific crystal toxins from *Bacillus thuringiensis* form cation- and anion-selective channels in planar lipid bilayers. *J. Membr. Biol.* **132**, 53-62
57. Schwartz, J. L., Lu, Y. J., Söhnlein, P., Brousseau, R., Laprade, R., Masson, L., and Adang, M. J. (1997) Ion channels formed in planar lipid bilayers by *Bacillus thuringiensis* toxins in the presence of *Manduca sexta* midgut receptors. *FEBS Lett.* **412**, 270-276
58. Schwartz, J. L., and Laprade, R. (2000) Membrane permeabilisation by *Bacillus thuringiensis* toxins: protein insertion and pore formation. In *Entomopathogenic Bacteria: from Laboratory to Field Application* (Charles, J. F., Delécluse, A., and Nielsen-Leroux, C. eds.), Kluwer Associate Publishing, Norwell, MA, USA. pp 199-218
59. Peyronnet, O., Vachon, V., Schwartz, J. L., and Laprade, R. (2001) Ion channels induced in planar lipid bilayers by the *Bacillus thuringiensis* toxin Cry1Aa in the presence of gypsy moth (*Lymantria dispar*) brush border membrane. *J. Membr. Biol.* **184**, 45-54
60. Masson, L., Schwab, G., Mazza, A., Brousseau, R., Potvin, L., and Schwartz, J. L. (2004) A novel *Bacillus thuringiensis* (PS149B1) containing a Cry34Ab1/Cry35Ab1 binary toxin specific for the Western corn rootworm *Diabrotica virgifera virgifera* LeConte forms ion channels in lipid membranes. *Biochemistry* **43**, 12349-12357
61. Kaiser-Alexnat, R. (2009) Protease activities in the midgut of Western corn rootworm (*Diabrotica virgifera virgifera* LeConte). *J. Invertebr. Pathol.* **100**, 169-174

62. Allman, E., Johnson, D., and Nehrke, K. (2009) Loss of the apical V-ATPase a-subunit VHA-6 prevents acidification of the intestinal lumen during a rhythmic behavior in *C. elegans*. *Am. J. Physiol. Cell Physiol.* **297**, C1071-C1081

63. Chauhan, V. M., Orsi, G., Brown, A., Pritchard, D. I., and Aylott, J. W. (2013) Mapping the pharyngeal and intestinal pH of *Caenorhabditis elegans* and real-time luminal pH oscillations using extended dynamic range pH-sensitive nanosensors. *ACS Nano* **7**, 5577-5587

64. Vinokurov, K. S., Elpidina, E. N., Oppert, B., Prabhakar, S., Zhuzhikov, D. P., Dunaevsky, Y. E., and Belozersky, M. A. (2006) Diversity of digestive proteinases in *Tenebrio molitor* (Coleoptera: Tenebrionidae) larvae. *Comp. Biochem. Physiol. B Biochem. Mol. Biol.* **145**, 126-137

65. Lončar, N., Božić, N., Nenadović, V., Ivanović, J., and Vujčić, Z. (2009) Characterization of trypsin-like enzymes from the midgut of *Morimus funereus* (Coleoptera: Cerambycidae) larvae. *Arch. Biol. Sci. Belgrade* **61**, 713-718

66. Koller, C. N., Bauer, L. S., and Hollingworth, R. M. (1992) Characterization of the pH-mediated solubility of *Bacillus thuringiensis* var. *san diego* native δ-endotoxin crystals. *Biochem. Biophys. Res. Commun.* **184**, 692-699

67. Ludwig, A., Bauer, S., Benz, R., Bergmann, B., and Goebel, W. (1999) Analysis of the SlyA-controlled expression, subcellular localization and pore-forming activity of a 34 kDa haemolysin (ClyA) from *Escherichia coli* K-12. *Mol. Microbiol.* **31**, 557-567

68. Oscarsson, J., Mizunoe, Y., Li, L., Lai, X.-H., Wieslander, Å., and Uhlin, B. E. (1999) Molecular analysis of the cytolytic protein ClyA (SheA) from *Escherichia coli*. *Mol. Microbiol.* **32**, 1226-1238

69. Tan, S. Y., Rangasamy, M., Wang, H. C., Velez, A. M., Hasler, J., McCaskill, D., Xu, T., Chen, H., Jurzenski, J., Kelker, M., Xu, X. P., Narva, K., and Siegfried, B. D. (2016) RNAi induced knockdown of a cadherin-like protein (EF531715) does not affect toxicity of Cry34/35Ab1 or Cry3Aa to *Diabrotica virgifera virgifera* larvae (Coleoptera: Chrysomelidae). *Insect Biochem. Mol. Biol.* **75**, 117-124

70. Carroll, J., Convents, D., Van Damme, J., Boets, A., Van Rie, J., and Ellar, D. J. (1997) Intramolecular proteolytic cleavage of *Bacillus thuringiensis* Cry3A δ-endotoxin may facilitate its coleopteran toxicity. *J. Invertebr. Pathol.* **70**, 41-49

71. Hille, B. (2001) Selective permeability: independence. In *Ion Channels of Excitable Membranes*, 3rd Ed., Sinauer Associates, Inc., Sunderland, MA, USA. pp 441-470

72. Wolfersberger, M., Lüthy, P., Maurer, A., Parenti, P., Sacchi, V. F., Giordana, B., and Hanozet, G. M. (1987) Preparation and partial characterization of amino acid transporting brush border membrane vesicles from the larval midgut of the cabbage butterfly (*Pieris brassicae*). *Comp. Biochem. Physiol. A Physiol.* **86**, 301-308

73. George, S. G., and Kenny, A. J. (1973) Studies on the enzymology of purified preparations of brush border from rabbit kidney. *Biochem. J.* **134**, 43-57

74. MacDonald, R. C., MacDonald, R. I., Menco, B. P. M., Takeshita, K., Subbarao, N. K., and Hu, L.-r. (1991) Small-volume extrusion apparatus for preparation of large, unilamellar vesicles. *Biochim. Biophys. Acta* **1061**, 297-303

FOOTNOTES

This work was supported by the Natural Sciences and Engineering Research Council of Canada (NSERC) and by Dow AgroSciences Canada Inc. (Collaborative Research and Development grant CRDPJ 44052-12), a Université de Montréal graduate student scholarship to EF and an NSERC undergraduate student research award to VL.

The abbreviations used are: *Bt*, *Bacillus thuringiensis*; PLB, planar lipid bilayer; WCRW, Western corn rootworm; Cry6Aa1 WCR, WCRW midgut juice-treated Cry6Aa1; Cry6Aa1 TT, trypsin-treated Cry6Aa1; BBMF, brush border membrane fraction, POPC, 1-palmitoyl-2-oleoyl-*sn*-glycero-3-phosphocholine; POPE, 1-palmitoyl-2-oleoyl-*sn*-glycero-3-phosphoethanolamine; PC, L-α-phosphatidylcholine; CHES, 2-(Cyclohexylamino)ethanesulfonic acid; CAPS, 3-(Cyclohexylamino)-1-propanesulfonic acid; TPCK, N-p-tosyl-L-phenylalanine chloromethyl ketone; TLCK, N-p-tosyl-L-lysine chloromethyl ketone.

TABLE 1
Biophysical properties of the native Cry6Aa1 toxin, Cry6Aa1 TT and Cry6Aa1 WCR

	Conductance range [a]		K^+/Cl^- permeability ratio (± SEM) [a]	Minimal protein dose
Native Cry6Aa1, pH 5.5	71 – 499 pS		2.68 ± 0.18	200 pg/ml
Native Cry6Aa1, pH 7.5	31 – 330 pS		2.73 ± 0.50	1 ng/ml [b]
Native Cry6Aa1, pH 9.5	47 – 689 pS		3.46 ± 0.33	1 ng/ml [b]
Cry6Aa1 WCR, pH 5.5	28 – 459 pS		2.56 ± 0.19	100 fg/ml
Cry6Aa1 TT, pH 5.5	29 – 450 pS		2.19 ± 0.12 0.32 ± 0.01	100 fg/ml
Native Cry6Aa1 + BBMF, pH 5.5	56 – 637 pS		0.82 ± 0.02	100 fg/ml
	At non rectifying voltages	At rectifying voltages		
Cry6Aa1 WCR + BBMF, pH 5.5	40 – 306 pS	15 – 95 pS	0.77 ± 0.05	100 fg/ml

[a] n = 3 or more
[b] Not tested below this dose

FIGURE LEGENDS

FIGURE 1. Biochemistry of Cry6Aa1. *A,* solubilisation of native Cry6Aa1 inclusion bodies. Results are means ± SEM for three separate experiments. *B*, SDS-PAGE of purified Cry6Aa1. The samples were boiled for five minutes before being loaded onto a 12% acrylamide gel (2 µg of protein per well). Lane 1: molecular weight markers. Lane 2: Native Cry6Aa1. Lane 3: Cry6Aa1 WCR. Lane 4: Cry6Aa1 TT.

FIGURE 2. Cry6Aa1 WCR forms pores in planar lipid bilayers. *A*, representative single channel current traces of Cry6Aa1 WCR at various holding voltages. 100 fg/ml of protein was added in the *cis* side compartment of the PLB setup and channel activity was recorded after a few minutes under symmetrical (150 mM KCl) conditions at pH 5.5. The traces were filtered at 1 kHz. *B*, typical current-voltage relationship graph (IV curves) constructed from data of one Cry6Aa1 WCR experiment under symmetrical conditions. The conductances ranged from 28 to 459 pS. *C*, representative single channel current traces of Cry6Aa1 WCR at ±60 mV and 0 mV under asymmetrical (450 mM:150 mM KCl *cis*:*trans*) conditions at pH 5.5. *D*, IV curves of one single type of channel observed in each of three experiments conducted under asymmetrical (450 mM:150 mM KCl *cis*:*trans*) conditions. The reversal potential was -11.39 mV ± 0.8 (n = 3). In *A* and *C*, the letters **c** and the dotted lines show the closed state of all channels.

FIGURE 3. Both native Cry6Aa1 and Cry6Aa1 TT form pores in PLBs. *A*, representative traces of channel currents recorded under symmetrical (150 mM KCl) conditions at pH 5.5 at ±40 mV for the native Cry6Aa1 toxin (two upper traces) and at ±60mV for Cry6Aa1 TT (two lower traces). Traces were filtered at 1 kHz. *B,* representative current traces of Cry6Aa1 at pH 5.5, 7.5 and 9.5. The holding voltage was -60 mV. The trace at pH 5.5 was unfiltered. The traces at pH 7.5 and 9.5 were filtered at 1 kHz. The letters **c** and the dotted lines indicate the closed state of all channels.

FIGURE 4. Cumulative frequency distributions of Cry6Aa1 conductances at pH 5.5, 7.5 and 9.5. Conductance values were obtained from IV curves derived from at least 3 experiments under symmetrical conditions and at each pH. They were grouped in 50-pS bins and their

cumulative frequency of occurrence was plotted vs conductance. Data were fitted with 5th order polynomials. Legend symbols with different superscripts indicate a significant difference between the corresponding frequency curves (Mann-Whitney test at 5% significance level).

FIGURE 5. Cry6Aa1 and Cry6Aa1 WCR form pores in PLBs enriched with WCRW midgut BBMFs. *A,* representative current traces of the native Cry6Aa1 at ±60 mV in BBMF-rich PLBs under symmetrical (150 mM KCl) conditions at pH 5.5. *B*, typical IV curves constructed from recordings obtained in one typical experiment. *C*, representative current traces of Cry6Aa1 WCR at ±40mV in BBMF-rich PLBs under symmetrical (150 mM KCl) conditions at pH 5.5. The current records were filtered at 100 Hz. *D*, IV curves derived from a typical Cry6Aa1 WCR experiment conducted under the same conditions as in *C*. Note that the current scales in *C* and *D* are not the same. In *A* and *C*, the letters **c** and the dotted lines show the closed state of all channels.

FIGURE 1

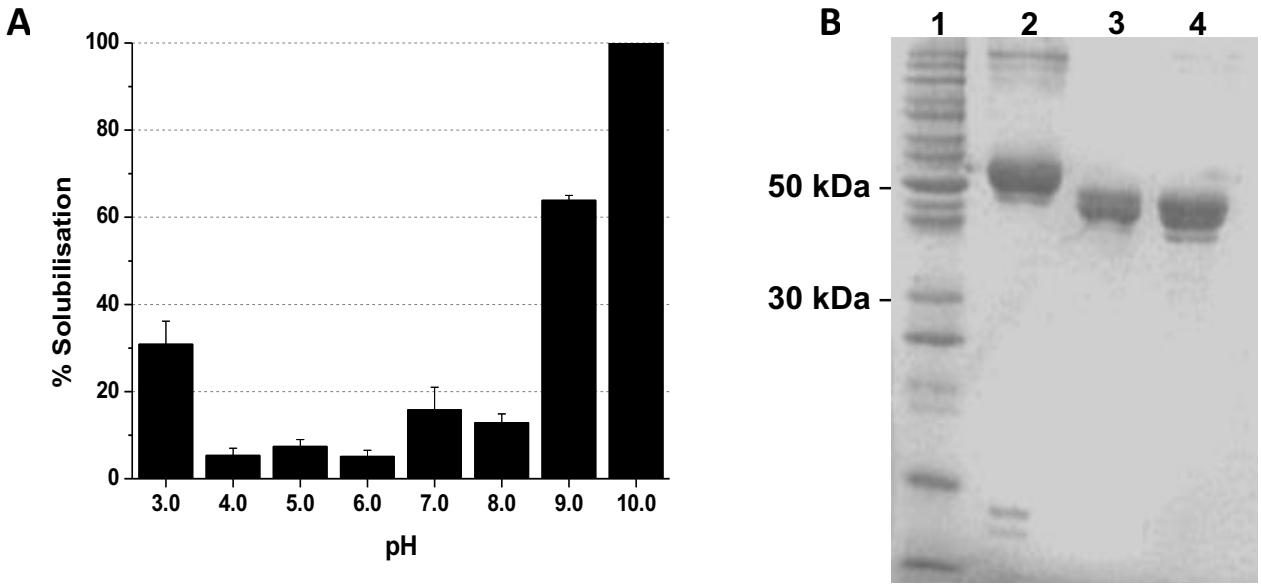
A
100
80
60
40
20
0
% Solubilisation
3.0
4.0
5.0
6.0
7.0
8.0
9.0
10.0
pH
B
1
2
3
4
50 kDa
30 kDa

FIGURE 2

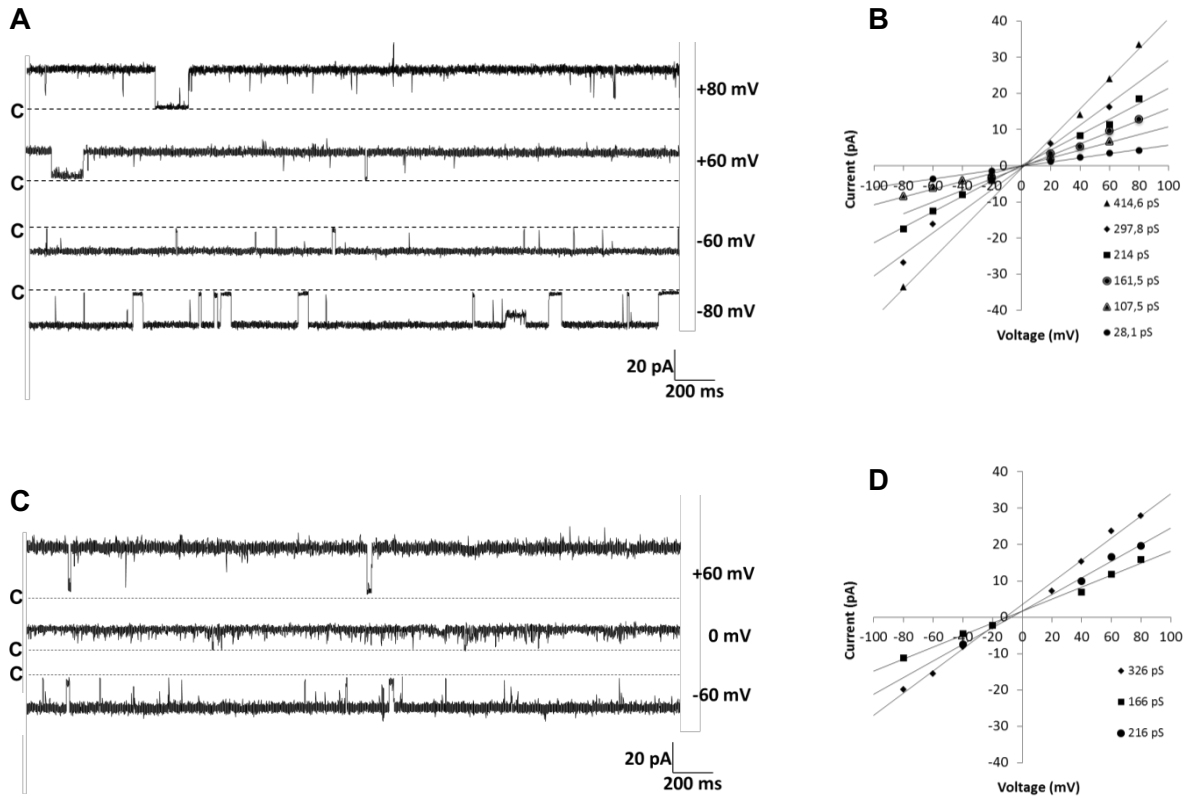
A
C
C
C
C
+80 mV
+60 mV
-60 mV
-80 mV
20 pA
200 ms
B
Current (pA)
Voltage (mV)
414,6 pS
297,8 pS
214 pS
161,5 pS
107,5 pS
28,1 pS
C
C
C
C
+60 mV
0 mV
-60 mV
20 pA
200 ms
D
Current (pA)
Voltage (mV)
326 pS
166 pS
216 pS

FIGURE 3

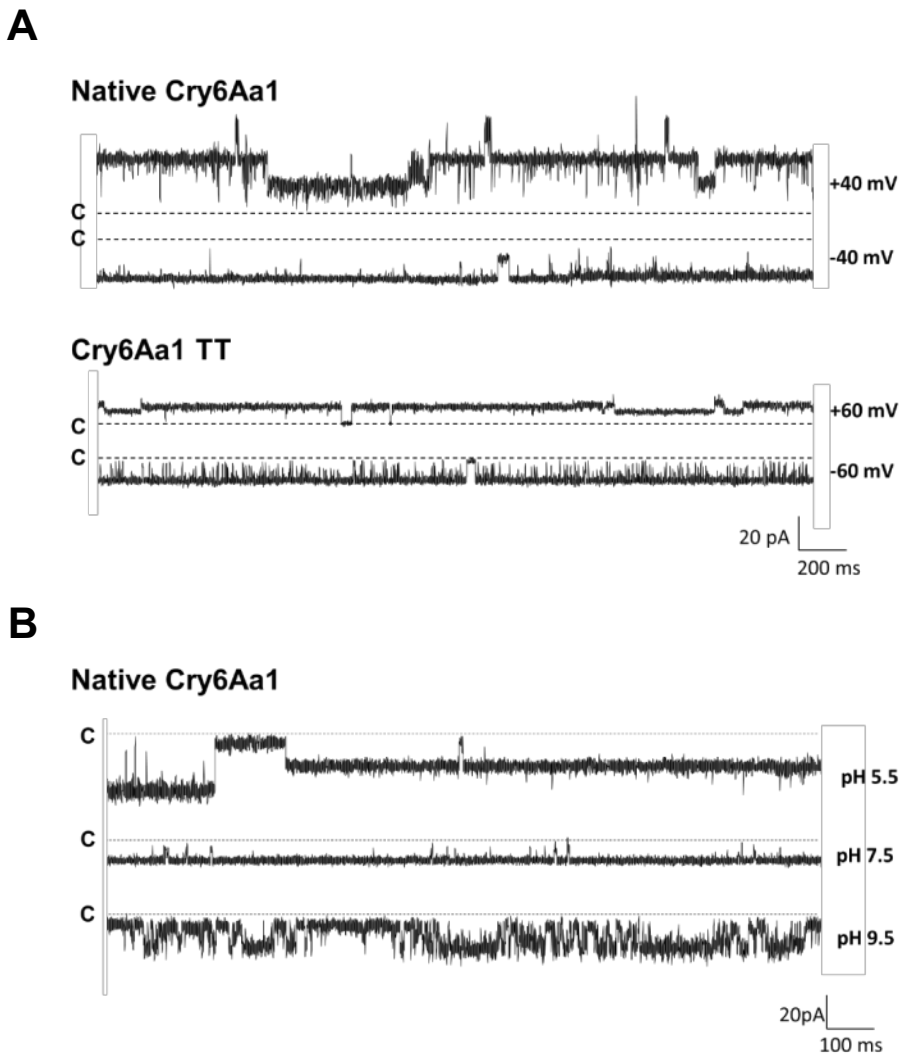
A
Native Cry6Aa1
C
C
+40 mV
-40 mV
Cry6Aa1 TT
C
C
+60 mV
-60 mV
20 pA
200 ms
B
Native Cry6Aa1
C
C
C
pH 5.5
pH 7.5
pH 9.5
20pA
100 ms

FIGURE 4

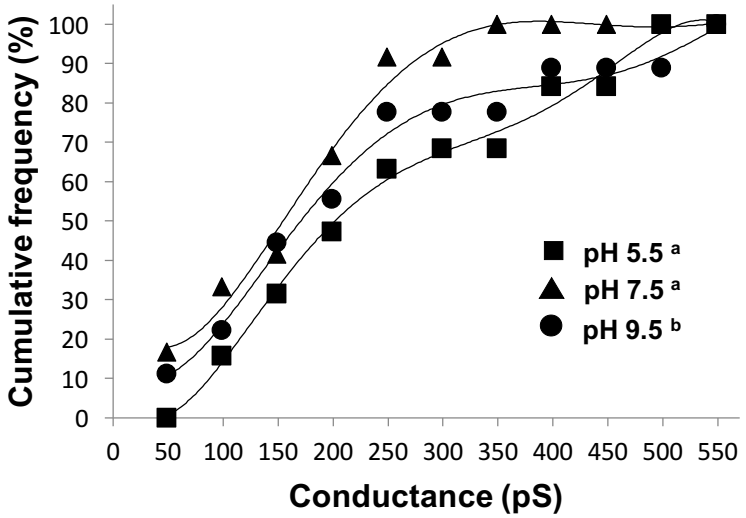
Cumulative frequency (%)
100
90
80
70
60
50
40
30
20
10
0
0
50
100
150
200
250
300
350
400
450
500
550
Conductance (pS)
pH 5.5 a
pH 7.5 a
pH 9.5 b

FIGURE 5

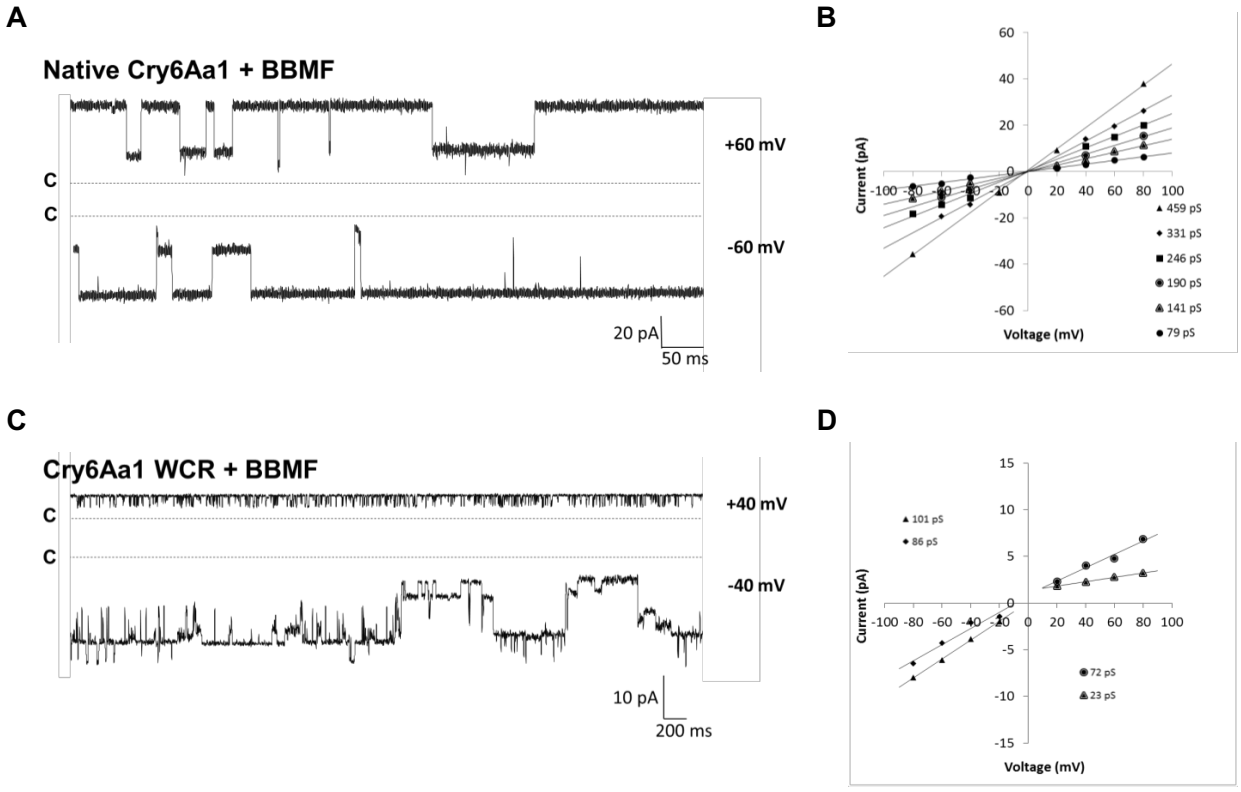
A
Native Cry6Aa1 + BBMF
C
C
+60 mV
-60 mV
20 pA
50 ms
B
Current (pA)
Voltage (mV)
459 pS
331 pS
246 pS
190 pS
141 pS
79 pS
C
Cry6Aa1 WCR + BBMF
C
C
+40 mV
-40 mV
10 pA
200 ms
D
Current (pA)
Voltage (mV)
101 pS
86 pS
72 pS
23 pS

CHAPTER 4. ADDITIONAL RESULTS AND DISCUSSION

4.1. Similarity between Cry6Aa1 and ClyA: primary and secondary structures

The amino acid sequence of Cry6Aa1 only shares 10% similarity with ClyA. However, Cry6Aa1 is composed of 10 α-helices and 4 β-sheets (Fig. 24) (136,137) and shows a very similar secondary structure to ClyA, which is composed by 6 α-helices and two β-sheets (Fig. 25). To relate the structures, a sequence alignment of Cry6A1a and ClyA was run, not only to confirm the sequence similarity but also to see to which helices did the conserved amino acids belong. The ultimate goal was to be able to relate all the available information on ClyA to Cry6Aa1.

Fig. 24. Relation of Cry6Aa1 TT secondary structure to its amino acid sequence (136).

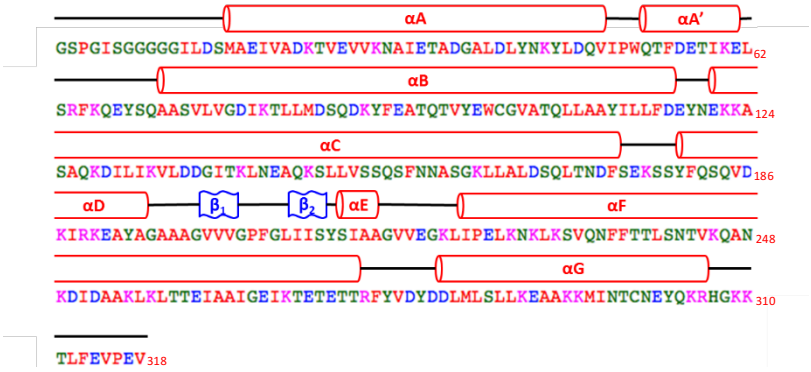

Fig. 25. Relation of ClyA secondary structure to its amino acid sequence (141).

Looking more closely at the secondary structure of Cry6Aa1, particularly at helices that share sequences with those of ClyA (Fig. 26), it can be seen that α1 and the two first β-sheets of Cry6Aa1 are highly similar to αA from ClyA. Helix α4 and the first half of α5 of Cry6Aa1 include a conserved sequence also found in αB of ClyA. This is also true for the C-terminal part of α5 of Cry6Aa1 and αC of ClyA. The β-tongue regions from ClyA and Cry6Aa1, despite their low sequence similarity, possess amino acids that show similar properties, such that the β-tongue is hydrophobic in both proteins. Helix α7 and the N-terminal half of α8 of Cry6Aa1 show high sequence similarity to αF of ClyA. Finally, the sequence of α9 of Cry6Aa1 is highly similar to αG of ClyA. On the other hand, α10 of Cry6Aa1, has no amino acid similarity with any region of ClyA.

Fig. 26. Sequence alignment of Cry6Aa and ClyA using ClustalW. The small hydrophobic amino acids including aromatic amino acid Tyr are shown in red. The acidic amino acids are shown in blue. The basic amino acids are shown in magenta and the hydroxyl, sulfhydryl, amines and Gly amino acids are shown in green. Fully conserved residues are indicated by asterisks, conservation between groups of amino acids that have strongly similar properties is shown by colons and conservation between groups of amino acids with weakly similar properties is shown by periods.

Taken into account the information on the structure-function relationship of ClyA (see section 1.5.3.1.3.) and comparing it to Cry6Aa, all of the key features of ClyA, including the role of αA and the β-tongue in ClyA membrane interaction, are found in Cry6Aa1. However, contrary to Cry6Aa1, there is no disulphide bridge in ClyA but αG of the latter protein plays an important role in its function. Therefore, the role of the C-terminal part of Cry6Aa1 was investigated to get a better understanding of the protein's pore formation ability. To do so, the native Cry6Aa1 toxin was treated with various insect midgut proteases and the resulting products were tested in PLBs.

4.2. Testing structure-function relationships in Cry6Aa1

Cry6Aa1 was treated either with WCRW midgut juice or with trypsin. A variant (Cry6Aa1 mod), in which a short 7AA linker was engineered to confer additional flexibility to the toxin, was also tested. Figure 15 (Section 2.1.1.) shows the secondary structures of these proteins together with that of ClyA.

N-terminal sequencing of Cry6Aa1 treated with WCRW midgut juice showed that two different forms of the toxin were obtained (Cry6Aa1 WCR1 and Cry6Aa1 WCR2). The most interesting difference between the two is that Cry6Aa1 WCR2 is completely missing the first α helix (α1), while Cry6Aa1 WCR1 is only missing the first 7 amino acids. On the other hand, trypsin treatment of Cry6Aa1 (Cry6Aa1 TT) resulted in the loss of the first 11 amino acids and the region between Gln 391 and Arg 443, although the two segments remain bound together by a disulphide bridge between Cys88 and Cys451(136). The role of this bridge was tested in PLBs by adding MET, a reducing agent to separate the two segments of the toxin (Cry6Aa1 TT MET). Finally, in Cry6Aa1 mod, the region that is cleaved off by trypsin between Gln 391 and Arg443 was replaced by a 7 amino acid linker that attaches α10 to the rest of the protein, without the presence of a disulphide bridge, as Cys451 is no more part of the variant. All mutants and forms of the toxin where prepared at Dow AgroSciences.

4.3. Biophysical properties of the pores formed in PLBs

It has been demonstrated earlier in this work that Cry6Aa1 is a PFT and that treatment with midgut juice did not dramatically affect the biophysical properties of Cry6Aa1 WCR, only

increasing the pore formation efficiency under our experimental conditions. In the case of treatment with trypsin, two different selectivities were observed for Cry6Aa1 TT depending on the experiment, but its pore formation efficiency remained the same as that of the midgut juice-treated toxin Cry6Aa1 WCR.

However, two different forms of Cry6Aa1 were obtained after treatment with midgut juice, WCR1 and WCR2. Although Cry6Aa1 WCR1 was shown to be the most efficient pore-forming form of Cry6Aa1, pore formation was not detected at all with Cry6Aa1 WCR2 under our experimental conditions. To better understand the structural origin of this difference between Cry6Aa1 WCR1 and WCR2, both forms of Cry6Aa1 were subjected to mass spectrometry at Dow AgroSciences. Unfortunately, it proved to be very difficult to obtain the exact sequence of amino acids between Gln 391 and Arg 443 in these forms of the toxin, which makes it difficult to fully understand the structure-function relationship of the C-terminal part of the toxin.

In PLB experiments with Cry6Aa1 TT and Cry6Aa1 TT MET, the pore activity lifespan in the membrane was reduced compared to that of all the other forms of Cry6Aa1, from hours to a few minutes. Cry6Aa1 TT MET retained its pore formation ability and its biophysical properties remained similar to those of Cry6Aa1 TT (Table III), except for one major difference: Cry6Aa1 TT MET became slightly anion-selective ($P_{K^+}/P_{Cl^-} = 0.80 \pm 0.07$). This appears to be related to α10 being freed from the N-terminal fragment of the toxin.

The other major difference between Cry6Aa1TT (treated or not with MET) and the other toxins studied here is related to their spectrum of conductance amplitudes. This was analyzed by comparing the cumulative frequency distributions of the pore conductances that were determined for each of the toxins and variants. Figure 28 shows that Cry6Aa1 TT and Cry6Aa1 TT MET conductances clearly tended to become smaller, even though the overall conductance range was very similar for all the toxins (Fig. 27) (Table III).

Finally, the biophysical signature of the pores formed by Cry6Aa1 mod was also affected (Table III). Cry6Aa1 mod displayed dual selectivity, which did not match with that of the toxin treated with trypsin. Furthermore, the dose needed for pore formation was 250-fold higher than that of the native Cry6Aa1 and it took longer for Cry6Aa1 mod to insert into the PLBs.

Table III. Biophysical properties of the different forms of Cry6Aa1.

	Conductance	P_{K^+/Cl^-} [a,b]	Dose [c]	Observations
Native Cry6Aa1	71 – 499 pS[d]	2.68 (± 0.18) [d]	200 pg/ml[d]	Unitary current jumps are not well resolved
Cry6Aa1 WCR1	28 – 459 pS[d]	2.56 (± 0.19) [d]	100 fg/ml[d]	Most stable channels in PLBs
Cry6Aa1 TT	29 – 450 pS[d]	2.19 (± 0.12) [d] 0.32 (± 0.01) [d]	100 fg/ml[d]	Shorter channel activity lifespan
Cry6Aa1 TT MET	32 – 481 pS	0.80 (± 0.07)	100 fg/ml	Shorter channel activity lifespan
Cry6Aa1 mod	27 – 538 pS	1.57 (± 0.04) 0.40 (± 0.01)	50 ng/ml	Takes longer to partition into PLBs

[a] $P_{K+/Cl-}$: relative permeability of potassium ions over chloride ions. [b] SEM are given in parentheses. [c] Minimal dose for which channel activity is observed. [d] Data already shown (see Chapter 3).

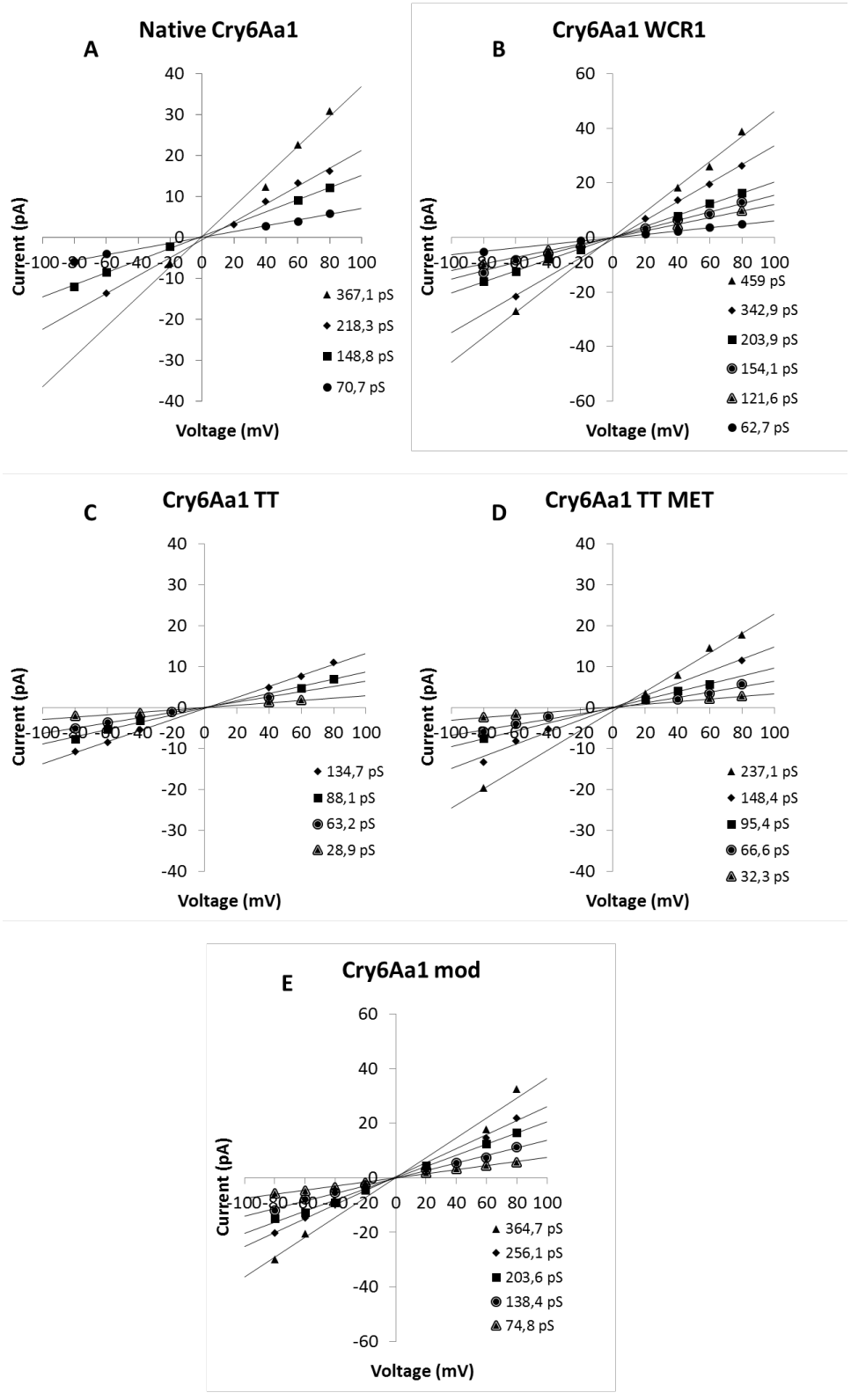

Fig. 27. Representative IV curves for one experiment for each form of Cry6Aa1. (A) Native Cry6Aa1, (B) Cry6Aa1 WCR1, (C) Cry6Aa1 TT, (D) Cry6Aa1 TT MET (E) Cry6Aa1 mod

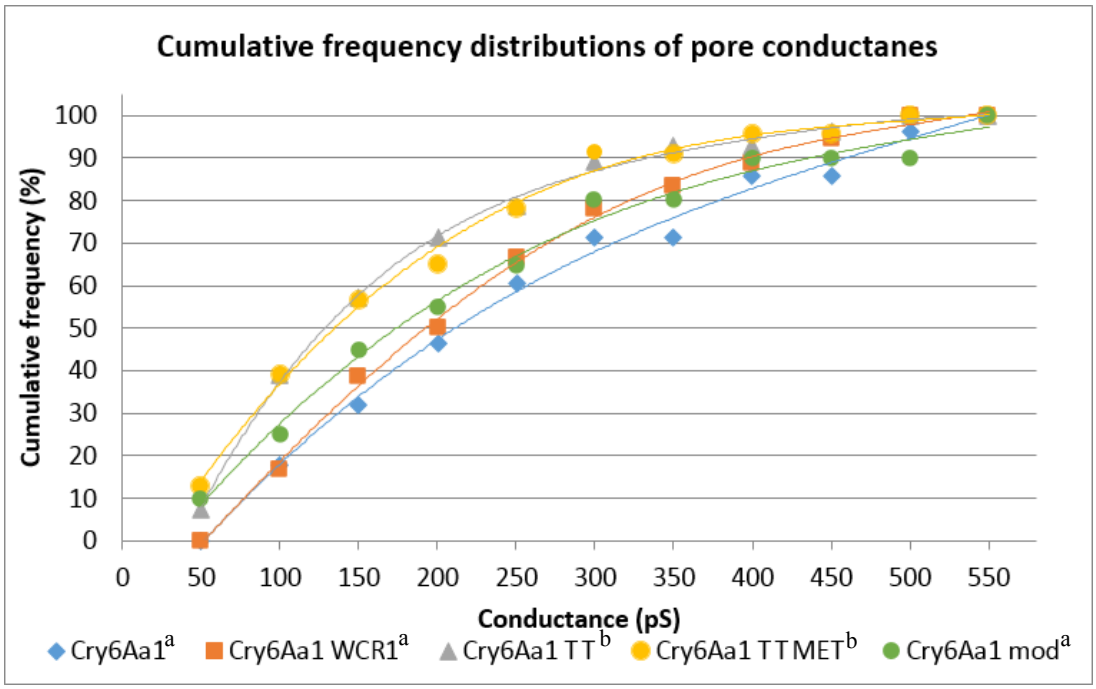

Fig. 28. Cumulative frequency distribution of pore conductances for the different forms of Cry6Aa1. The Man-Whitney test was used to quantify the difference in the cumulative frequency distribution (non-parametric, independent samples, $p<0.05$). The conductance distributions of toxins with different protease superscripts are significantly different. Thus, the cumulative frequency distributions of pore conductances of Cry6Aa1, Cry6Aa1 WCR1 and Cry6Aa1 mod are significantly different from those of Cry6Aa1 TT and Cry6Aa1 TT MET.

4.4. Structure-function relationships

4.4.1. The head subdomain: interaction with the membrane

The first helix αA of ClyA, which is located in the head subdomain of the toxin (see Fig. 29) has been shown to interact with biological membranes and is necessary for conservation of the biophysical characteristics of the pore formed by the toxin (144), which suggests that it is directly involved in the channel structure. This was further demonstrated by the elucidation of the 3-D structure of the pore of ClyA at atomic resolution (139).

It is suggested that α1 of Cry6Aa1 interacts with the membrane. This is hinted by the shorter lifespan of the channel activity of Cry6Aa1 TT and Cry6Aa1 TT MET in PLBs, which are missing the first 10 amino acids of the native toxin. Further support to the role of α1 is provided by the inability of Cry6Aa1 WCR2, which is missing the whole α1, to form pores.

Finally, our experiments suggest that α1 is involved in the pore structure, because the conductances of Cry6Aa1 TT tend to be smaller. This is in agreement with the fact that the loss of at least four and up to nine amino acids in the N-terminal part of ClyA (from Ala6 up to Ala20) reduces the lifespan of the ClyA pore activity in PLBs (144). Interestingly Glu11 is the first amino acid from ClyA that is part of the transmembrane domain of the protein (139), which may explain why the protease treatment of Cry6Aa1 that removes the first few amino acids does not have an important impact unless half of α1 is cleaved off, as it happens in Cry6Aa1 TT.

Like ClyA, Cry6Aa1 has a strongly hydrophobic β-tongue region (See Fig. 33). This region is thus predicted to play an important role in toxin-membrane interaction, just like it does in ClyA (144). However, it should be noted that although mutations in this part of ClyA do not prevent pore formation, they do decrease the pore-formation efficiency and abolish the hemolytic ability of the toxin (144,145). It has been demonstrated that a mutant of Cry6Aa1 that reduces the hydrophobicity of the β-tongue does not kill nematodes (136), but this does not imply that the protein is not able to form pores in PLBs. To further study the role of the β-tongue in Cry6Aa1 pore formation, mutants should be created with alterations in this regions or disulphide bridge introduced to lock it to other parts of the toxin. Such variants of Cry6Aa1 are currently being produced by Dow AgroSciences.

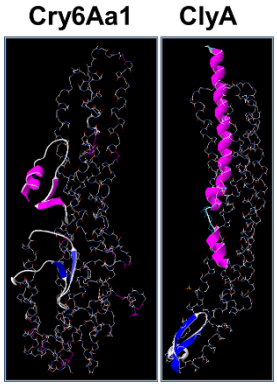

Fig. 29. β tongues (blue) and α1 and αA (magenta) of Cry6Aa1 and ClyA, respectively

4.4.2. The tail subdomain: selectivity and pore-formation efficiency

In ClyA the tail subdomain is formed by αG (See Fig. 30). By comparing the primary sequences and the 3-D structures of Cry6Aa1 and ClyA, it was found that α9 of Cry6Aa1 has the highest similarity to αG. However, α10 of Cry6Aa1 has no similar equivalent region in ClyA. In Cry6Aa1 TT, this last helix is only bound to the rest of the protein by a single disulphide bridge that is reduced in Cry6Aa1 TT MET. Both proteins form pores at doses 2000 times less than the dose required for pore formation by the native Cry6Aa1. However, when α10 is permanently linked to the rest of the toxin, as it is the case in the Cry6Aa1 mod variant, a significantly larger dose, 250 times larger than that used for the native form of the toxin, is necessary for the variant to form pores. It appears therefore that the way by which α10 is bound to the protein affects the pore formation efficiency of the latter.

Furthermore, α10 is also affecting the selectivity of the pores-formed by Cry6Aa1, as demonstrated by the dual selectivity observed with Cry6Aa1 TT and Cry6Aa1 mod. Depending on the experiment, these two proteins are either cation- or anion-selective. In both proteins, α10 is present, which might indicate that they insert differently or get differently re-associated into the membrane in the presence of α10, compared to the full length Cry6Aa1 toxin. We hypothesize that this dual selectivity is related to either specific residues in α10 or the interaction of α10 with another region of the toxin involved in its selectivity. In ClyA, the C-terminal part of αA is the most negatively charged region and is located in the narrowest part of the pore (139). It may be possible, therefore, that α10 interacts with α1 in Cry6Aa1, the helix that corresponds to αA in ClyA. This hypothesis is further supported by the fact that Cry6Aa1 TT

MET, which is lacking α10, displays selectivity to anions only. Interestingly, in the presence of WCRW BBM, the selectivity of Cry6Aa1 TT MET is the same as that of Cry6Aa1 and Cry6Aa1 WCR1 (see Chapter 3), suggesting that the proteins lacking α10 form pores in PLBs that adopt a configuration that resembles that of the toxin in the presence of the docking molecules present in the target insect midgut.

More work is necessary to better understand the role of α10 in Cry6Aa1. Firstly, experiments should be done in the absence of α10, since the disulphide bridge reduction does not necessarily imply that α10 is fully detached from the rest of Cry6Aa1, as other types of bonds may still exist. Such experiments would confirm the loss of α10 has a positive effect on the insertion of the toxin. Secondly, because the selectivity of Cry6Aa1 WCR1 is very similar to that of the native Cry6Aa1, it would be important to determine the exact primary structure of the former and how α10 is bound to the rest of the protein. Finally, considering that the absence of the C-terminal half or of the whole αG diminishes the hemolytic activity of ClyA, whereas membrane activity in PLBs and the biophysical characteristics of the pores are preserved (144), it is suggested to test how the loss of α9 in Cry6Aa1 may affect pore formation and insecticidal activity of the toxin. So far, it was shown that a Cry6Aa1 segment extending to Asn389, and thus including α9, was required to keep nematocidal activity (133), which is similar to what happens in ClyA. Therefore, it is hypothesized that the loss of the whole or the C-terminal half of α9 in Cry6Aa1 should not affect the biophysical properties of the pore and may only increase the dose needed to insert the toxin into PLBs.

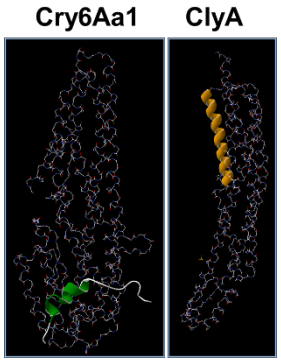

Fig. 30. α10 (green) and αG (brown) of Cry6Aa1 TT and ClyA, respectively.

4.4.3. Role of the disulphide bridges

There is a debate regarding the need of a disulphide bridge for pore formation by ClyA. It was initially reported that oxidized ClyA had no hemolytic activity (146), but this was later challenged (145,147), implying that the movement of αG away from the core of the protein was not necessary for pore formation. In Cry6Aa1, which has also a disulphide bridge (Fig. 31), it is α10, and not α9, which is the helix that best corresponds to αG. It was shown in the present study that the disulphide bridge in between α4 and α10 is not necessary for efficient pore-formation. Therefore, results indicate that α9 may have a similar function to that of αG in ClyA in terms of pore formation. Bioassays confirmed that a reduced Cry6Aa1 is toxic to *Diabrotica*. However, it cannot be excluded that, like in ClyA (145), a disulphide bridge in Cry6Aa1 may be important for protein export from the bacterial cell.

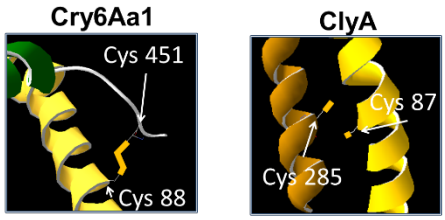

Fig. 31. Disulphide bridge in Cry6Aa1 TT and corresponding location in ClyA.

All in all, ClyA looks like a good model to generally understand the structure-function of Cry6Aa1. However, we are still far from fully understand the conformational changes that occur in Cry6Aa1 when it inserts into the membrane.

CHAPTER 5. DISCUSSION, FUTURE RESEARCH AND CONCLUSION

It has been shown before that *Bt* proteins are PFTs, using different techniques such as PLBs, light scattering assays and fluorescent assays (47,49,52,54,55). Cry6Aa1 is a *Bt* toxin. It has a very different structure from that of any other *Bt* toxin studied before, but it is structurally very similar to proteins of the family of α-PFTs (136,137). At the beginning of this study, we hypothesised that Cry6Aa1 was a PFT. To demonstrate this, we did experiments in PLBs and we showed that indeed Cry6Aa1 was able to form pores in PLBs.

In this study we have shown that the native Cry6Aa1 was able to form pores in PLBs at a wide range of pH, even though its solubilisation is strongly pH-dependent. This is the first time that a toxin produced by *Bt* was able to form pores without a previous treatment with proteases. Nevertheless, treatment with different proteases did have an effect on pore formation by Cry6Aa1. Activation with midgut juice of the target insect, the WCR1, did not affect the biophysical properties of the pores but reduced the dose needed 2000-fold. Treatment with trypsin, which is not a main protease in the target insects' midgut (17), had a similar effect on the required dose. Furthermore, this latter treatment changed the biophysical properties of the pores, affecting both conductance and selectivity. Moreover, it was shown that the presence of WCRW midgut apical membrane material affected Cry6Aa1 pore formation and properties. This effect was different for the native Cry6Aa1 and Cry6Aa1 WCR1. A 200-fold dose reduction was observed for the native Cry6Aa1, whereas there was no dose reduction for Cry6Aa1 WCR1, but its conductance was affected by being smaller at one polarity than the other during the same experiment. However, the selectivity of both proteins changed the same way, from slightly cationic to slightly anionic.

Cry6Aa1 3-D structure is very similar to that of ClyA (137,141). To get a better understanding of how Cry6Aa1 inserts into membranes and forms pores, ClyA was used as a model. It was shown that the disulphide bridge that is naturally found in Cry6Aa1 is not necessary for pore formation of the toxin. It was also established that when the disulphide bridge was reduced, the pore selectivity changed in a very similar manner to what happened when the toxin was reconstituted in BBMF-enriched PLBs. Furthermore, it was demonstrated that α1 is

necessary for pore formation and that it is possibly this helix that inserts into the membrane. Finally, we have also shown that α10 is directly related to the selectivity of the toxin.

Since *Bt* toxins are used as biopesticides, there is a strong debate on their possible effects on mammalian cells (152). So far, Cry6Aa1 has been shown to be highly specific, affecting only a few species of nematodes and coleopteran insects (see section 1.5.1.) and that it is not able to kill HeLa cells, a human cell line derived from cervical cancer (*unpublished data from this laboratory*). However, the fact that the toxin does not require activation and that it works at such low doses in PLBs makes it difficult to understand the origin of its specificity to particular invertebrates. In fact the doses needed for Cry6Aa1 pore formation in PLBs are extremely low in comparison to those of other PFTs. *Bt* PFTs form pores in PLBs at 1-5 µg/ml (32,51,54). On the other hand, in PLBs, the CyaA hemolysin secreted by *Bordetella pertussis* forms pores at 1 µg/ml (153), RtxA secreted by *Kingella kingae* forms pores at 1 mg/ml (154), C2IIa secreted by *Clostridium botulinum* forms pores at 260 ng/ml (155) and it takes at least 50 ng/ml for ClyA to form pores (142).

The present study has provided a better understanding of the mode of action of Cry6Aa1, particularly at the level of pore formation *in vitro*. However, the mechanism by which Cry6Aa1 kills WCRW larvae remains elusive. Cry6Aa1 kills target insects at doses at the same order of magnitude than those for other *Bt* toxins, as shown by the bioassays of this study, doses that are far higher than those used in PLB experiments. As previously discussed in Chapter 3, we propose two hypotheses to explain the low dose but high specificity of the toxin: (1) there is an extra step in the *in vivo* mode of action before pore formation that affects negatively the protein preventing it from forming pores; (2) pore formation is not the decisive step that kills the target insects and there is another step that is responsible for such high specificity of the toxin.

At this point, the process by which a Cry6Aa1 monomer forms pores is still poorly understood. To learn more about it we propose to engineer cysteine mutants such that possible conformational changes in the β-tongue of Cry6Aa1, α9 and α1 will be prevented. Ideally, the the structure of the Cry6Aa1 pore should be elucidated by using crystallography or cryoelectron microscopy, two techniques which have proven to be very useful for the study of other PFT structures before (139,156).

To better understand the specificity of Cry6Aa1, it should be studied at a closer physiological level. Future experiments should address how pore formation occurs at the cellular level using for example the patch-clamp technique on dissociated cells of WCRW midguts. Since *Bt* toxins have been shown to trigger intracellular calcium release in cells (55), it would also be interesting to find out if Cry6Aa1 has an effect at the intracellular level.

Furthermore, Cry6Aa1 has also been shown to have nematocidal activity (135). It has been shown that resistant nematodes to Cry5B are still killed by Cry6Aa (134). It would therefore be interesting to study the modulation of Cry6Aa1 pore formation in PLBs enriched with BBM of target nematodes such as *C. elegans* and to compare the results to the available information obtained in this study.

All in all, we conclude that Cry6Aa1 is a PFT in PLBs enriched or not with biological material from the target insect organ. Our results suggest that the pore formation step is different of that of other *Bt* toxins. Therefore, it makes a good candidate for the production of an efficient biopesticide, in particular for the design of new transgenic plants expressing Cry6Aa1 together with other *Bt* toxins in order to delay the onset of corn rootworm resistance to *Bt*.

CHAPTER 6. BIBLIOGRAPHY

1. Martin, P. A., and Travers, R. S. (1989) Worldwide abundance and distribution of *Bacillus thuringiensis* isolates. *Appl. Environ. Microbiol.* **55**, 2437-2442
2. Schnepf, E., Crickmore, N., Van Rie, J., Lereclus, D., Baum, J., Feitelson, J., Zeigler, D. R., and Dean, D. H. (1998) *Bacillus thuringiensis* and its pesticidal crystal proteins. *Microbiol. Mol. Biol. Rev.* **62**, 775-806
3. van Frankenhuyzen, K. (2009) Insecticidal activity of *Bacillus thuringiensis* crystal proteins. *J. Invertebr. Patho.l* **101**, 1-16
4. van Frankenhuyzen, K. (2013) Cross-order and cross-phylum activity of *Bacillus thuringiensis* pesticidal proteins. *J. Invertebr. Pathol.* **114**, 76-85
5. Palma, L., Munoz, D., Berry, C., Murillo, J., and Caballero, P. (2014) *Bacillus thuringiensis* toxins: an overview of their biocidal activity. *Toxins* **6**, 3296-3325
6. Kronstad, J. W., and Whiteley, H. R. (1984) Inverted repeat sequences flank a *Bacillus thuringiensis* crystal protein gene. *J. Bacteriol.* **160**, 95-102
7. Hofte, H., and Whiteley, H. R. (1989) Insecticidal crystal proteins of *Bacillus thuringiensis*. *Microbiol. Rev.* **53**, 242-255
8. Crickmore, N., Zeigler, D. R., Feitelson, J., Schnepf, E., Van Rie, J., Lereclus, D., Baum, J., and Dean, D. H. (1998) Revision of the nomenclature for the *Bacillus thuringiensis* pesticidal crystal proteins. *Microbiol. Mol. Biol. Rev.* **62**, 807-813
9. Yudina, T. G., Brioukhanov, A. L., Zalunin, I. A., Revina, L. P., Shestakov, A. I., Voyushina, N. E., Chestukhina, G. G., and Netrusov, A. I. (2007) Antimicrobial activity of different proteins and their fragments from *Bacillus thuringiensis* parasporal crystals against clostridia and archaea. *Anaerobe* **13**, 6-13
10. Nielsen-LeRoux, C., Gaudriault, S., Ramarao, N., Lereclus, D., and Givaudan, A. (2012) How the insect pathogen bacteria *Bacillus thuringiensis* and *Xenorhabdus/Photorhabdus* occupy their hosts. *Curr. Opin. Microbiol.* **15**, 220-231
11. Vachon, V., Laprade, R., and Schwartz, J. L. (2012) Current models of the mode of action of *Bacillus thuringiensis* insecticidal crystal proteins: a critical review. *J. Invertebr. Pathol.* **111**, 1-12
12. MacIntosh, S. C., McPherson, S. L., Perlak, F. J., Marrone, P. G., and Fuchs, R. L. (1990) Purification and characterization of *Bacillus thuringiensis* var. *tenebrionis* insecticidal proteins produced in *E. coli*. *Biochem. Biophys. Res. Commun.* **170**, 665-672
13. Bietlot, H. P., Vishnubhatla, I., Carey, P. R., Pozsgay, M., and Kaplan, H. (1990) Characterization of the cysteine residues and disulphide linkages in the protein crystal of *Bacillus thuringiensis*. *Biochem. J.* **267**, 309-315
14. Aronson, A. I., Han, E. S., McGaughey, W., and Johnson, D. (1991) The solubility of inclusion proteins from *Bacillus thuringiensis* is dependent upon protoxin composition and is a factor in toxicity to insects. *Appl. Environ. Microbiol.* **57**, 981-986
15. Du, C., Martin, P. A., and Nickerson, K. W. (1994) Comparison of disulfide contents and solubility at alkaline pH of insecticidal and noninsecticidal *Bacillus thuringiensis* protein crystals. *Appl. Environ. Microbiol.* **60**, 3847-3853
16. Koller, C. N., Bauer, L. S., and Hollingworth, R. M. (1992) Characterization of the pH-mediated solubility of *Bacillus thuringiensis* var. *san diego* native δ-endotoxin crystals. *Biochem. Biophys. Res. Commun.* **184**, 692-699

17. Kaiser-Alexnat, R. (2009) Protease activities in the midgut of Western corn rootworm (*Diabrotica virgifera virgifera* LeConte). *J. Invertebr. Pathol.* **100**, 169-174
18. Haider, M. Z., Knowles, B. H., and Ellar, D. J. (1986) Specificity of *Bacillus thuringiensis* var. *colmeri* insecticidal δ-endotoxin is determined by differential proteolytic processing of the protoxin by larval gut proteases. *Eur. J. Biochem.* **156**, 531-540
19. Carroll, J., Convents, D., Van Damme, J., Boets, A., Van Rie, J., and Ellar, D. J. (1997) Intramolecular proteolytic cleavage of *Bacillus thuringiensis* Cry3A δ-endotoxin may facilitate its coleopteran toxicity. *J. Invertebr. Pathol.* **70**, 41-49
20. Rukmini, V., Reddy, C. Y., and Venkateswerlu, G. (2000) *Bacillus thuringiensis* crystal δ-endotoxin: role of proteases in the conversion of protoxin to toxin. *Biochimie* **82**, 109-116
21. Lambert, B., Höfte, H., Annys, K., Jansens, S., Soetaert, P., and Peferoen, M. (1992) Novel *Bacillus thuringiensis* insecticidal crystal protein with a silent activity against coleopteran larvae. *Appl. Environ. Microbiol.* **58**, 2536-2542
22. Oppert, B., Kramer, K. J., Johnson, D. E., MacIntosh, S. C., and McGaughey, W. H. (1994) Altered protoxin activation by midgut enzymes from a *Bacillus thuringiensis* resistant strain of *Plodia interpunctella*. *Biochem. Biophys. Res. Commun.* **198**, 940-947
23. Smedley, D. P., Armstrong, G., and Ellar, D. J. (1997) Channel activity caused by a *Bacillus thuringiensis* δ-endotoxin preparation depends on the method of activation. *Mol. Membr. Biol.* **14**, 13-18
24. Richards, A. G., and Richards, P. A. (1977) The peritrophic membrane of insects. *Ann. Rev. Entomol.* **22**, 219-240
25. Rees, J. S., Jarrett, P., and Ellar, D. J. (2009) Peritrophic membrane contribution to *Bt* Cry δ-endotoxin susceptibility in Lepidoptera and the effect of Calcofluor. *J. Invertebr. Pathol.* **100**, 139-146
26. Feng, D., Chen, Z., Wang, Z., Zhang, C., He, K., and Guo, S. (2015) Domain III of *Bacillus thuringiensis* Cry1Ie toxin plays an important role in binding to peritrophic membrane of Asian corn borer. *PLoS One* **10**, doi: 10.1371/journal.pone.0136430
27. Hofmann, C., Lüthy, P., Hütter, R., and Pliska, V. (1988) Binding of the delta endotoxin from *Bacillus thuringiensis* to brush-border membrane vesicles of the cabbage butterfly (*Pieris brassicae*). *Eur. J. Biochem.* **173**, 85-91
28. Liang, Y. Z., Patel, S. S., and Dean, D. H. (1995) Irreversible binding kinetics of *Bacillus thuringiensis* CryIA δ-endotoxins to gypsy moth brush border membrane vesicles is directly correlated to toxicity. *J. Biol. Chem.* **270**, 24719-24724
29. Pigott, C. R., and Ellar, D. J. (2007) Role of receptors in *Bacillus thuringiensis* crystal toxin activity. *Microbiol. Mol. Biol. Rev.* **71**, 255-281
30. Knight, P. J. K., Crickmore, N., and Ellar, D. J. (1994) The receptor for *Bacillus thuringiensis* CrylA(c) delta-endotoxin in the brush border membrane of the lepidopteran *Manduca sexta* is aminopeptidase N. *Mol. Microbiol.* **11**, 429-436
31. Sangadala, S., Walters, F. S., English, L. H., and Adang, M. J. (1994) A mixture of *Manduca sexta* aminopeptidase and phosphatase enhances *Bacillus thuringiensis* insecticidal CryIA(c) toxin binding and $^{86}Rb^{+}$-K^{+} efflux in vitro. *J. Biol. Chem.* **269**, 10088-10092
32. Schwartz, J. L., Lu, Y. J., Sohnlein, P., Brousseau, R., Laprade, R., Masson, L., and Adang, M. J. (1997) Ion channels formed in planar lipid bilayers by *Bacillus thuringiensis* toxins in the presence of *Manduca sexta* midgut receptors. *FEBS Lett*. **412**, 270-276
33. Gill, M., and Ellar, D. (2002) Transgenic *Drosophila* reveals a functional *in vivo* receptor for the *Bacillus thuringiensis* toxin Cry1Ac1. *Insect. Mol. Biol.* **11**, 619-625

34. Vadlamudi, R. K., Ji, T. H., and Bulla, L. A., Jr. (1993) A specific binding protein from *Manduca sexta* for the insecticidal toxin of *Bacillus thuringiensis* subsp. *berliner*. *J. Bio.l Chem.* **268**, 12334-12340
35. Keeton, T. P., and Bulla, L. A., Jr. (1997) Ligand specificity and affinity of BT-R1, the *Bacillus thuringiensis* Cry1A toxin receptor from *Manduca sexta*, expressed in mammalian and insect cell cultures. *Appl. Environ. Microbiol.* **63**, 3419-3425
36. Tsuda, Y., Nakatani, F., Hashimoto, K., Ikawa, S., Matsuura, C., Fukada, T., Sugimoto, K., and Himeno, M. (2003) Cytotoxic activity of *Bacillus thuringiensis* Cry proteins on mammalian cells transfected with cadherin-like Cry receptor gene of *Bombyx mori* (silkworm). *Biochem. J.* **369**, 697-703
37. Hua, G., Zhang, R., Abdullah, M. A. F., and Adang, M. J. (2008) *Anopheles gambiae* cadherin AgCad1 binds the Cry4Ba toxin of *Bacillus thuringiensis israelensis* and a fragment of AgCad1 synergizes toxicity. *Biochemistry* **47**, 5101-5110
38. Fernández, L. E., Aimanova, K. G., Gill, S. S., Bravo, A., and Soberón, M. (2006) A GPI-anchored alkaline phosphatase is a functional midgut receptor of Cry11Aa toxin in *Aedes aegypti* larvae. *Biochem. J.* **394**, 77-84
39. Lee, S. B., Aimanova, K. G., and Gill, S. S. (2014) Alkaline phosphatases and aminopeptidases are altered in a Cry11Aa resistant strain of *Aedes aegypti*. *Insect. Biochem. Mol. Biol.* **54**, 112-121
40. Dennis, R. D., Wiegandt, H., Haustein, D., Knowles, B. H., and Ellar, D. J. (1986) Thin layer chromatography overlay technique in the analysis of the binding of the solubilized protoxin of *Bacillus thuringiensis* var. *kurstaki* to an insect glycosphingolipid of known structure. *Biomed. Chromatogr.* **1**, 31-37
41. Garczynski, S. F., and Adang, M. J. (2000) Investigations of *Bacillus thuringiensis* Cry1 toxins receptor structure and function. in *Entomophathogenic bacteria: from laboratory to field application* (Charles, J. F., Delécluse, A., and Nielsen-Leroux, C. eds.), Kluwer Academic, Norwell, MA, USA. pp 181-197
42. Griffitts, J. S., Haslam, S. M., Yang, T. L., Garczynski, S. F., Mulloy, B., Morris, H., Cremer, P. S., Dell, A., Adang, M. J., and Aroian, R. V. (2005) Glycolipids as receptors for *Bacillus thuringiensis* crystal toxin. *Science* **307**, 922-925
43. Gahan, L. J., Pauchet, Y., Vogel, H., and Heckel, D. G. (2010) An ABC transporter mutation is correlated with insect resistance to *Bacillus thuringiensis* Cry1Ac toxin. *PLoS Genet.* **6**, doi: 10.1371/journal.pgen.1001248
44. Tanaka, S., Miyamoto, K., Noda, H., Jurat-Fuentes, J. L., Yoshizawa, Y., Endo, H., and Sato, R. (2013) The ATP-binding cassette transporter subfamily C member 2 in *Bombyx mori* larvae is a functional receptor for Cry toxins from *Bacillus thuringiensis*. *FEBS J.* **280**, 1782-1794
45. Slatin, S. L., Abrams, C. K., and English, L. (1990) δ-Endotoxins form cation-selective channels in planar lipid bilayers. *Biochem. Biophys. Res. Commun.* **169**, 765-772
46. Knowles, B. H., Blatt, M. R., Tester, M., Horsnell, J. M., Carroll, J., Menestrina, G., and Ellar, D. J. (1989) A cytolytic δ-endotoxin from *Bacillus thuringiensis* var. *israelensis* forms cation-selective channels in planar lipid bilayers. *FEBS Lett.* **244**, 259-262
47. Schwartz, J. L., and Laprade, R. (2000) Membrane permeabilisation by *Bacillus thuringiensis* toxins: protein insertion and pore formation. in *Entomopathogenic Bacteria: from Laboratory to Field Application* (Charles, J. F., Delécluse, A., and Nielsen-Leroux, C. eds.), Kluwer Academic, Norwell, MA, USA. pp 199-217
48. Grochulski, P., Masson, L., Borisova, S., Pusztai-Carey, M., Schwartz, J. L., Brousseau, R., and Cygler, M. (1995) *Bacillus thuringiensis* CryIA(a) insecticidal toxin: crystal structure and channel formation. *J. Mol. Biol.* **254**, 447-464

49. Kirouac, M., Vachon, V., Rivest, S., Schwartz, J. L., and Laprade, R. (2003) Analysis of the properties of *Bacillus thuringiensis* insecticidal toxins using a potential-sensitive fluorescent probe. *J. Membr. Biol.* **196**, 51-59
50. Schwartz, J. L., Garneau, L., Savaria, D., Masson, L., Brousseau, R., and Rousseau, E. (1993) Lepidopteran-specific crystal toxins from *Bacillus thuringiensis* form cation- and anion-selective channels in planar lipid bilayers. *J. Membr. Biol.* **132**, 53-62
51. Masson, L., Schwab, G., Mazza, A., Brousseau, R., Potvin, L., and Schwartz, J. L. (2004) A novel *Bacillus thuringiensis* (PS149B1) containing a Cry34Ab1/Cry35Ab1 binary toxin specific for the Western corn rootworm *Diabrotica virgifera virgifera* LeConte forms ion channels in lipid membranes. *Biochemistry* **43**, 12349-12357
52. Carroll, J., and Ellar, D. J. (1993) An analysis of *Bacillus thuringiensis* δ-endotoxin action on insect midgut membrane permeability using a light-scattering assay. *Eur. J. Biochem.* **214**, 771-778
53. Martin, F. G., and Wolfersberger, M. G. (1995) *Bacillus thuringiensis* delta-endotoxin and larval *Manduca sexta* midgut brush-border membrane vesicles act synergistically to cause very large increases in the conductance of planar lipid bilayers. *J. Exp. Biol.* **198**, 91-96
54. Peyronnet, O., Vachon, V., Schwartz, J. L., and Laprade, R. (2001) Ion channels induced in planar lipid bilayers by the *Bacillus thuringiensis* toxin Cry1Aa in the presence of gypsy moth (*Lymantria dispar*) brush border membrane. *J. Membr. Biol.* **184**, 45-54
55. Schwartz, J. L., Garneau, L., Masson, L., and Brousseau, R. (1991) Early response of cultured lepidopteran cells to exposure to δ-endotoxin from *Bacillus thuringiensis*: involvement of calcium and anionic channels. *Biochim. Biophys. Acta* **1065**, 250-260
56. Carroll, J., and Ellar, D. J. (1997) Analysis of the large aqueous pores produced by a *Bacillus thuringiensis* protein insecticide in *Manduca sexta* midgut-brush-border-membrane vesicles. *Eur. J. Biochem.* **245**, 797-804
57. Peyronnet, O., Nieman, B., Généreux, F., Vachon, V., Laprade, R., and Schwartz, J. L. (2002) Estimation of the radius of the pores formed by the *Bacillus thuringiensis* Cry1C δ-endotoxin in planar lipid bilayers. *Biochim. Biophys. Acta* **1567**, 113-122
58. Wieczorek, H. (1992) The insect V-ATPase, a plasma membrane proton pump energizing secondary active transport: molecular analysis of electrogenic potassium transport in the tobacco hornworm midgut. *J. Exp. Biol.* **172**, 335-343
59. Wieczorek, H., Putzenlechner, M., Zeiske, W., and Klein, U. (1991) A vacuolar-type proton pump energizes K+/H+ antiport in an animal plasma membrane. *J. Biol. Chem.* **266**, 15340-15347
60. Wieczorek, H., Weerth, S., Schindlbeck, M., and Klein, U. (1989) A vacuolar-type proton pump in a vesicle fraction enriched with potassium transporting plasma membranes from tobacco hornworm midgut. *J. Biol. Chem.* **264**, 11143-11148
61. Peyronnet, O., Vachon, V., Brousseau, R., Baines, D., Schwartz, J. L., and Laprade, R. (1997) Effect of *Bacillus thuringiensis* toxins in the membrane potential of lepidopteran insect midgut cells. *Appl. Environ. Microbiol.* **63**, 1679-1684
62. Kao, C. Y., Los, F. C. O., Huffman, D. L., Wachi, S., Kloft, N., Husmann, M., Karabrahimi, V., Schwartz, J. L., Bellier, A., Ha, C., Sagong, Y., Fan, H., Ghosh, P., Hsieh, M., Hsu, C. S., Chen, L., and Aroian, R. V. (2011) Global functional analyses of cellular responses to pore-forming toxins. *PLoS Pathog.* **7**, doi: 10.1371/journal.ppat.1001314
63. Gómez, I., Sánchez, J., Miranda, R., Bravo, A., and Soberón, M. (2002) Cadherin-like receptor binding facilitates proteolytic cleavage of helix α-1 in domain I and oligomer pre-pore formation of *Bacillus thuringiensis* Cry1Ab toxin. *FEBS Lett.* **513**, 242-246

64. Gómez, I., Sánchez, J., Muñoz-Garay, C., Matus, V., Gill, S. S., Soberón, M., and Bravo, A. (2014) *Bacillus thuringiensis* Cry1A toxins are versatile proteins with multiple modes of action: two distinct pre-pores are involved in toxicity. *Biochem. J.* **459**, 383-396
65. Zhang, X., Candas, M., Griko, N. B., Rose-Young, L., and Bulla, L. A. (2005) Cytotoxicity of *Bacillus thuringiensis* Cry1Ab toxin depends on specific binding of the toxin to the cadherin receptor BT-R1 expressed in insect cells. *Cell Death Differ.* **12**, 1407-1416
66. Zhang, X., Candas, M., Griko, N. B., Taussig, R., and Bulla, L. A. (2006) A mechanism of cell death involving an adenylyl cyclase/PKA signaling pathway is induced by the Cry1Ab toxin of *Bacillus thuringiensis*. *Proc. Natl. Acad. Sci. USA* **103**, 9897-9902
67. Palma, L., and Berry, C. (2016) Understanding the structure and function of *Bacillus thuringiensis* toxins. *Toxicon* **109**, 1-3
68. Li, J. D., Carroll, J., and Ellar, D. J. (1991) Crystal structure of insecticidal δ-endotoxin from *Bacillus thuringiensis* at 2.5 Å resolution. *Nature* **353**, 815-821
69. de Maagd, R. A., Bravo, A., and Crickmore, N. (2001) How *Bacillus thuringiensis* has evolved specific toxins to colonize the insect world. *Trends Genet* **17**, 193-199
70. Morse, R. J., Yamamoto, T., and Stroud, R. M. (2001) Structure of Cry2Aa suggests an unexpected receptor binding epitope. *Structure* **9**, 409-417
71. Widner, W. R., and Whiteley, H. R. (1990) Location of the dipteran specificity region in a lepidopteran-dipteran crystal protein from *Bacillus thuringiensis*. *J. Bacteriol.* **172**, 2826-2832
72. Xu, C., Wang, B. C., Yu, Z., and Sun, M. (2014) Structural insights into *Bacillus thuringiensis* Cry, Cyt and parasporin toxins. *Toxins* **6**, 2732-2770
73. Li, J., Derbyshire, D. J., Promdonkoy, B., and Ellar, D. J. (2001) Structural implications for the transformation of the *Bacillus thuringiensis* delta-endotoxins from water-soluble to membrane-inserted forms. *Biochem. Soc. Trans.* **29**, 571-577
74. Evdokimov, A. G., Moshiri, F., Sturman, E. J., Rydel, T. J., Zheng, M., Seale, J. W., and Franklin, S. (2014) Structure of the full-length insecticidal protein Cry1Ac reveals intriguing details of toxin packaging into *in vivo* formed crystals. *Protein Sci.* **23**, 1491-1497
75. Galitsky, N., Cody, V., Wojtczak, A., Ghosh, D., Luft, J. R., Pangborn, W., and English, L. (2001) Structure of the insecticidal bacterial delta-endotoxin Cry3Bb1 of *Bacillus thuringiensis*. *Acta. Crystallogr. Sect. D-Biol. Crystallogr.* **57**, 1101-1109
76. Boonserm, P., Mo, M., Angsuthanasombat, C., and Lescar, J. (2006) Structure of the functional form of the mosquito larvicidal Cry4Aa toxin from *Bacillus thuringiensis* at a 2.8-Angstrom resolution. *J. Bacteriol.* **188**, 3391-3401
77. Boonserm, P., Davis, P., Ellar, D. J., and Li, J. (2005) Crystal structure of the mosquito-larvicidal toxin Cry4Ba and its biological implications. *J. Mol. Biol.* **348**, 363-382
78. Guo, S. Y., Ye, S., Liu, Y. F., Wei, L., Xue, J., Wu, H. F., Song, F. P., Zhang, J., Wu, X. A., Huang, D. F., and Rao, Z. (2009) Crystal structure of *Bacillus thuringiensis* Cry8Ea1: an insecticidal toxin toxic to underground pests, the larvae of *Holotrichia parallela*. *J. Struct. Biol.* **168**, 259-266
79. Hui, F., Scheib, U., Hu, Y., Sommer, R. J., Aroian, R. V., and Ghosh, P. (2012) Structure and glycolipid binding properties of the nematicidal protein Cry5B. *Biochemistry* **51**, 9911-9921
80. Walters, F. S., Slatin, S. L., Kulesza, C. A., and English, L. H. (1993) Ion channel activity of N-terminal fragments from CryIA(c) delta-endotoxin. *Biochem. Biophys. Res. Commun.* **196**, 921-926

81. Gazit, E., Bach, D., Kerr, I. D., Sansom, M. S. P., Chejanovsky, N., and Shai, Y. (1994) The alpha-5 segment of *Bacillus thuringiensis* delta-endotoxin: in vitro activity, ion channel formation and molecular modelling. *Biochem. J.* **304,** 895-902
82. Von Tersch, M. A., Slatin, S. L., Kulesza, C. A., and English, L. H. (1994) Membrane-permeabilizing activities of *Bacillus thuringiensis* coleopteran-active toxin CryIIIB2 and CryIIIB2 domain I peptide. *Appl. Environ. Microbiol.* **60**, 3711-3717
83. Puntheeranurak, T., Uawithya, P., Potvin, L., Angsuthanasombat, C., and Schwartz, J. L. (2004) Ion channels formed in planar lipid bilayers by the dipteran-specific Cry4B *Bacillus thuringiensis* toxin and its α1-α5 fragment. *Mol. Membr. Biol.* **21**, 67-74
84. Knowles, B. H., Francis, P. H., and Ellar, D. J. (1986) Structurally related *Bacillus thuringiensis* δ-endotoxins display major differences in insecticidal activity *in vivo* and *in vitro*. *J. Cell Sci.* **84**, 221-236
85. Girard, F., Vachon, V., Lebel, G., Prefontaine, G., Schwartz, J. L., Masson, L., and Laprade, R. (2009) Chemical modification of *Bacillus thuringiensis* Cry1Aa toxin single-cysteine mutants reveals the importance of domain I structural elements in the mechanism of pore formation. *Biochim. Biophys. Acta* **1788**, 575-580
86. Lebel, G., Vachon, V., Prefontaine, G., Girard, F., Masson, L., Juteau, M., Bah, A., Larouche, G., Vincent, C., Laprade, R., and Schwartz, J. L. (2009) Mutations in domain I interhelical loops affect the rate of pore formation by the *Bacillus thuringiensis* Cry1Aa toxin in insect midgut brush border membrane vesicles. *Appl Environ Microbiol* **75**, 3842-3850
87. Masson, L., Tabashnik, B. E., Liu, Y. B., Brousseau, R., and Schwartz, J. L. (1999) Helix 4 of the *Bacillus thuringiensis* Cry1Aa toxin lines the lumen of the ion channel. *J. Biol. Chem.* **274**, 31996-32000
88. Vachon, V., Préfontaine, G., Rang, C., Coux, F., Juteau, M., Schwartz, J. L., Brousseau, R., Frutos, R., Laprade, R., and Masson, L. (2004) Helix 4 mutants of the *Bacillus thuringiensis* insecticidal toxin Cry1Aa display altered pore-forming abilities. *Appl. Environ. Microbiol.* **70**, 6123-6130
89. Girard, F., Vachon, V., Préfontaine, G., Marceau, L., Schwartz, J. L., Masson, L., and Laprade, R. (2009) Helix α4 of the *Bacillus thuringiensis* Cry1Aa toxin plays a critical role in the postbinding steps of pore formation. *App.l Environ. Microbiol.* **75**, 359-365
90. Vachon, V., Préfontaine, G., Coux, F., Rang, C., Marceau, L., Masson, L., Brousseau, R., Frutos, R., Schwartz, J. L., and Laprade, R. (2002) Role of helix 3 in pore formation by the *Bacillus thuringiensis* insecticidal toxin Cry1Aa. *Biochemistry* **41**, 6178-6184
91. Coux, F., Vachon, V., Rang, C., Moozar, K., Masson, L., Royer, M., Bes, M., Rivest, S., Brousseau, R., Schwartz, J. L., Laprade, R., and Frutos, R. (2001) Role of interdomain salt bridges in the pore-forming ability of the *Bacillus thuringiensis* toxins Cry1Aa and Cry1Ac. *J. Biol. Chem.* **276**, 35546-35551
92. Rajamohan, F., Lee, M. K., and Dean, D. H. (1998) Bacillus thuringiensis insecticidal proteins: molecular mode of action. *Prog. Nucleic Acid Res. Mol. Biol.* **60**, 1-27
93. Ge, A. Z., Rivers, D., Milne, R., and Dean, D. H. (1991) Functional domains of *Bacillus thuringiensis* insecticidal crystal proteins. Refinement of *Heliothis virescens* and *Trichoplusia ni* specificity domains on CryIA(c). *J. Biol. Chem.* **266**, 17954-17958
94. Schwartz, J. L., Potvin, L., Chen, X. J., Brousseau, R., Laprade, R., and Dean, D. H. (1997) Single-site mutations in the conserved alternating arginine region affect ionic channels formed by CryIAa, a *Bacillus thuringiensis* toxin. *Appl. Environ. Microbiol.* **63**, 3978-3984
95. Kelker, M. S., Berry, C., Evans, S. L., Pai, R., McCaskill, D. G., Wang, N. X., Russell, J. C., Baker, M. D., Yang, C., Pflugrath, J. W., Wade, M., Wess, T. J., and Narva, K. E. (2014) Structural and

biophysical characterization of *Bacillus thuringiensis* insecticidal proteins Cry34Ab1 and Cry35Ab1. *PLoS One* **9**, doi: 10.1371/journal.pone.0112555

96. Akiba, T., Abe, Y., Kitada, S., Kusaka, Y., Ito, A., Ichimatsu, T., Katayama, H., Akao, T., Higuchi, K., Mizuki, E., Ohba, M., Kanai, R., and Harata, K. (2004) Crystallization of parasporin-2, a *Bacillus thuringiensis* crystal protein with selective cytocidal activity against human cells. *Acta. Crystallogr. Sectl D-Biol. Crystallogr.* **60**, 2355-2357
97. Ito, A., Sasaguri, Y., Kitada, S., Kusaka, Y., Kuwano, K., Masutomi, K., Mizuki, E., Akao, T., and Ohba, M. (2004) A *Bacillus thuringiensis* crystal protein with selective cytocidal action to human cells. *J. Biol. Chem.* **279**, 21282-21286
98. Parker, M. W., Buckley, J. T., Postma, J. P. M., Tucker, A. D., Leonard, K., Pattus, F., and Tsernoglou, D. (1994) Structure of the *Aeromonas* toxin proaerolysin in its water-soluble and membrane-channel states. *Nature* **367**, 292-295
99. Akiba, T., Abe, Y., Kitada, S., Kusaka, Y., Ito, A., Ichimatsu, T., Katayama, H., Akao, T., Higuchi, K., Mizuki, E., Ohba, M., Kanai, R., and Harata, K. (2009) Crystal structure of the parasporin-2 *Bacillus thuringiensis* toxin that recognizes cancer cells. *J. Mol. Biol.* **386**, 121-133
100. Xu, C. C., Chinte, U., Chen, L. R., Yao, Q. Q., Meng, Y., Zhou, D., Bi, L. J., Rose, J., Adang, M. J., Wang, B. C., Yu, Z. N., and Sun, M. (2015) Crystal structure of Cry51Aa1: A potential novel insecticidal aerolysin-type β-pore-forming toxin from *Bacillus thuringiensis*. *Biochem. Biophys. Res. Commun.* **462**, 184-189
101. Thomas, W. E., and Ellar, D. J. (1983) Mechanism of action of *Bacillus thuringiensis* var *israelensis* insecticidal δ-endotoxin. *FEBS Lett.* **154**, 362-368
102. Butko, P. (2003) Cytolytic toxin Cyt1A and its mechanism of membrane damage: data and hypotheses. *Appl. Environ. Microbiol.* **69**, 2415-2422
103. Goldberg, L. J., and Margalit, J. (1977) A bacterial spore demonstrating rapid larvicidal activity against *Anopheles sergentii*, *Uranotaenia unguiculata*, *Culex univittatus*, *Aedes aegypti* and *Culex pipiens*. *Mosquito News* **37**, 355-358
104. Gill, S. S., Singh, G. J., and Hornung, J. M. (1987) Cell membrane interaction of *Bacillus thuringiensis* subsp. *israelensis* cytolytic toxins. *Infect. Immun.* **55**, 1300-1308
105. Thomas, W. E., and Ellar, D. J. (1983) *Bacillus thuringiensis* var *israelensis* crystal δ-endotoxin: effects on insect and mammalian cells *in vitro* and *in vivo*. *J. Cell Sci.* **60**, 181-197
106. Li, J., Koni, P. A., and Ellar, D. J. (1996) Structure of the mosquitocidal delta-endotoxin CytB from *Bacillus thuringiensis* sp. *kyushuensis* and implications for membrane pore formation. *J. Mol. Biol.* **257**, 129-152
107. Cohen, S., Dym, O., Albeck, S., Ben-Dov, E., Cahan, R., Firer, M., and Zaritsky, A. (2008) High-resolution crystal structure of activated Cyt2Ba monomer from *Bacillus thuringiensis* subsp. *israelensis*. *J. Mol. Biol.* **380**, 820-827
108. Cohen, S., Albeck, S., Ben-Dov, E., Cahan, R., Firer, M., Zaritsky, A., and Dym, O. (2011) Cyt1Aa toxin: crystal structure reveals implications for its membrane-perforating function. *J. Mol. Biol.* **413**, 804-814
109. Lin, S. C., Lo, Y. C., Lin, J. Y., and Liaw, Y. C. (2004) Crystal structures and electron micrographs of fungal volvatoxin A2. *J. Mol. Biol.* **343**, 477-491
110. Chakroun, M., Banyuls, N., Bel, Y., Escriche, B., and Ferré, J. (2016) Bacterial vegetative insecticidal Proteins (Vip) from entomopathogenic bacteria. *Microbiol. Mol. Biol. Rev.* **80**, 329-350
111. Leuber, M., Orlik, F., Schiffler, B., Sickmann, A., and Benz, R. (2006) Vegetative insecticidal protein (Vip1Ac) of *Bacillus thuringiensis* HD201: evidence for oligomer and channel formation. *Biochemistry* **45**, 283-288

112. Jucovic, M., Walters, F. S., Warren, G. W., Palekar, N. V., and Chen, J. S. (2008) From enzyme to zymogen: engineering Vip2, an ADP-ribosyltransferase from *Bacillus cereus*, for conditional toxicity. *Protein. Eng. Des. Sel.* **21**, 631-638
113. Han, S., Craig, J. A., Putnam, C. D., Carozzi, N. B., and Tainer, J. A. (1999) Evolution and mechanism from structures of an ADP-ribosylating toxin and NAD complex. *Nat. Struct. Biol.* **6**, 932-936
114. Lee, M. K., Walters, F. S., Hart, H., Palekar, N., and Chen, J. S. (2003) The mode of action of the *Bacillus thuringiensis* vegetative insecticidal protein Vip3A differs from that of Cry1Ab δ-endotoxin. *Appl. Environ. Microbiol.* **69**, 4648-4657
115. Donovan, W. P., Engleman, J. T., Donovan, J. C., Baum, J. A., Bunkers, G. J., Chi, D. J., Clinton, W. P., English, L., Heck, G. R., Ilagan, O. M., Krasomil-Osterfeld, K. C., Pitkin, J. W., Roberts, J. K., and Walters, M. R. (2006) Discovery and characterization of Sip1A: a novel secreted protein from *Bacillus thuringiensis* with activity against coleopteran larvae. *Appl. Microbiol. Biotechnol.* **72**, 713-719
116. Tinsley, N. A., Estes, R. E., and Gray, M. E. (2013) Validation of a nested error component model to estimate damage caused by corn rootworm larvae. *J. Appl. Entomol.* **137**, 161-169
117. Krysan , J. L., and Miller, T. A. (1986) *Methods for the study of pest Diabrotica*, Springer-Verlag, New-York, USA. doi: 10.1007/978-1-4612-4868
118. Krysan , J. L., and Smith, R. F. (1987) Systematics of the *virgifera* species group of *Diabrotica* (Coleoptera: Chrysomelidae: Galerucinae). *Etomography* **5**, 375-484
119. Marquardt, P. T., and Krupke, C. H. (2009) Dispersal and mating behavior of *Diabrotica virgifera virgifera* (Coleoptera: *Chrysomelidae*) in Bt cornfields. *Environ. Entomol.* **38**, 176-182
120. Tabashnik, B. E., and Gould, F. (2012) Delaying corn rootworm resistance to Bt corn. *J. Econ. Entomol.* **105**, 767-776
121. Siegfried, B. D., Waterfield, N., and ffrench-Constant, R. H. (2005) Expressed sequence tags from *Diabrotica virgifera virgifera* midgut identify a coleopteran cadherin and a diversity of cathepsins. *Insect Mol. Biol.* **14**, 137-143
122. Sayed, A., Nekl, E. R., Siqueira, H. A. A., Wang, H. C., ffrench-Constant, R. H., Bagley, M., and Siegfried, B. D. (2007) A novel cadherin-like gene from Western corn rootworm, *Diabrotica virgifera virgifera* (Coleoptera: Chrysomelidae), larval midgut tissue. *Insect Mol. Biol.* **16**, 591-600
123. Li, H., Olson, M., Lin, G., Hey, T., Tan, S. Y., and Narva, K. E. (2013) *Bacillus thuringiensis* Cry34Ab1/Cry35Ab1 interactions with Western corn rootworm midgut membrane binding sites. *PLoS One* **8**, doi: 10.1317/journal.pone.0053079
124. Byrne, D. 2003/766/EC: Commission Decision of 24 October 2003 on emergency measures to prevent the spread within the Community of Diabrotica virgifera Le Conte (notified under document number C(2003) 3880)
125. Gassmann, A. J., Petzold-Maxwell, J. L., Keweshan, R. S., and Dunbar, M. W. (2012) Western corn rootworm and Bt maize: challenges of pest resistance in the field. *GM Crops Food* **3**, 235-244
126. Cabanillas, H. E., Wright, R. J., and Vyas, R. V. , 2005, Cereal, fibre, oilseed and medicinal crop applications, Grewal, P. S., Ehlers, R. U., Shapiro-Ilan, D. I. eds. *Nematodes as biocontrol agents*, CABI publishing, Ohio, p. 265 - 280
127. Gassmann, A. J., and Weber, P., *Iowa evaluation of insecticides and plant-incorporated protectants*. Ames (Iowa): Department of enthomology (Iowa State University), 2012 April, 54p. Report no.: 289-11

128. Gassmann, A. J., Petzold-Maxwell, J. L., Keweshan, R. S., and Dunbar, M. W. (2011) Field-evolved resistance to Bt maize by Western corn rootworm. *PLoS One* **6**, doi: 10.1371/journal.pone.0022629
129. Rupar, M. J., Donovan, W. P., Groat, R. G., Slaney, A. C., Mattison, J. W., Johnson, T. B., Charles, J. F., Dumanoir, V. C., and de Barjac, H. (1991) Two novel strains of *Bacillus thuringiensis* toxic to coleopterans. *Appl. Environ. Microbiol.* **57**, 3337-3344
130. Walters, F. S., Stacy, C. M., Lee, M. K., Palekar, N., and Chen, J. S. (2008) An engineered chymotrypsin/cathepsin G site in domain I renders *Bacillus thuringiensis* Cry3A active against Western corn rootworm larvae. *Appl. Environ. Microbiol.* **74**, 367-374
131. Thompson, M., Knuth, M., and Cardineau, G., inventors; Mycogen corporation, assignee. *Bacillus thuringiensis* toxins with improved activity. United States patent US5874288 A. Jul 1997
132. Sharma, A., Kumar, S., and Bhatnagar, R. K. (2011) *Bacillus thuringiensis* protein Cry6B (BGSC ID 4D8) is toxic to larvae of *Hypera postica*. *Curr. Microbiol.* **62**, 597-605
133. Wei, J. Z., Hale, K., Carta, L., Platzer, E., Wong, C., Fang, S. C., and Aroian, R. V. (2003) *Bacillus thuringiensis* crystal proteins that target nematodes. *Proc. Natl. Acad. Sci. U S A* **100**, 2760-2765
134. Luo, H., Xiong, J., Zhou, Q. N., Xia, L. Q., and Yu, Z. Q. (2013) The effects of *Bacillus thuringiensis* Cry6A on the survival, growth, reproduction, locomotion, and behavioral response of *Caenorhabditis elegans*. *Appl. Microbiol. Biotechnol.* **97**, 10135-10142
135. Yu, Z., Luo, H., Xiong, J., Zhou, Q., Xia, L., Sun, M., Li, L., and Yu, Z. (2014) *Bacillus thuringiensis* Cry6A exhibits nematicidal activity to *Caenorhabditis elegans bre* mutants and synergistic activity with Cry5B to *C. elegans*. *Lett. Appl. Microbiol.* **58**, 511-519
136. Dementiev, A., Board, J., Sitaram, A., Hey, T., Kelker, M. S., Xu, X., Hu, Y., Vidal-Quist, C., Chikwana, V., Griffin, S., McCaskill, D., Wang, N. X., Hung, S., Chan, M. K., Lee, M. M., Hughes, J., Wegener, A., Aroian, R. V., Narva, K. E., and Berry, C. (2016) The pesticidal Cry6Aa toxin from *Bacillus thuringiensis* is structurally similar to HlyE-family α pore-forming toxins *BMC Biology* **14**, 71
137. Huang, J., Guan, Z., Wan, L., Zou, T., and Sun, M. (2016) Crystal structure of Cry6Aa: a novel nematicidal ClyA-type α-pore-forming toxin from *Bacillus thuringiensis*. *Biochem. Biophys. Res. Commun.* **478**, 307-313
138. Oscarsson, J., Mizunoe, Y., Li, L., Lai, X. H., Wieslander, A., and Uhlin, B. E. (1999) Molecular analysis of the cytolytic protein ClyA (SheA) from *Escherichia coli*. *Mol. Microbiol.* **32**, 1226-1238
139. Mueller, M., Grauschopf, U., Maier, T., Glockshuber, R., and Ban, N. (2009) The structure of a cytolytic α-helical toxin pore reveals its assembly mechanism. *Nature* **459**, 726-730
140. Ludwig, A., Tengel, C., Bauer, S., Bubert, A., Benz, R., Mollenkopf, H. J., and Goebel, W. (1995) SlyA, a regulatory protein from *Salmonella typhimurium*, induces a haemolytic and pore-forming protein in *Escherichia coli*. *Mol. Gen. Genet.* **249**, 474-486
141. Wallace, A. J., Stillman, T. J., Atkins, A., Jamieson, S. J., Bullough, P. A., Green, J., and Artymiuk, P. J. (2000) *E. coli* hemolysin E (HlyE, ClyA, SheA): X-ray crystal structure of the toxin and observation of membrane pores by electron microscopy. *Cell* **100**, 265-276
142. Ludwig, A., Bauer, S., Benz, R., Bergmann, B., and Goebel, W. (1999) Analysis of the SlyA-controlled expression, subcellular localization and pore-forming activity of a 34 kDa haemolysin (ClyA) from *Escherichia coli* K-12. *Mol. Microbiol.* **31**, 557-567
143. Soskine, M., Biesemans, A., Moeyaert, B., Cheley, S., Bayley, H., and Maglia, G. (2012) An engineered ClyA nanopore detects folded target proteins by selective external association and pore entry. *Nano Lett.* **12**, 4895-4900

144. Ludwig, A., Volkerink, G., von Rhein, C., Bauer, S., Maier, E., Bergmann, B., Goebel, W., and Benz, R. (2010) Mutations affecting export and activity of cytolysin A from *Escherichia coli*. *J. Bacteriol.* **192**, 4001-4011
145. Wai, S. N., Westermark, M., Oscarsson, J., Jass, J., Maier, E., Benz, R., and Uhlin, B. E. (2003) Characterization of dominantly negative mutant ClyA cytotoxin proteins in *Escherichia coli*. *J. Bacteriol.* **185**, 5491-5499
146. Atkins, A., Wyborn, N. R., Wallace, A. J., Stillman, T. J., Black, L. K., Fielding, A. B., Hisakado, M., Artymiuk, P. J., and Green, J. (2000) Structure-function relationships of a novel bacterial toxin, hemolysin E - The role of α_G. *J. Biol. Chem.* **275**, 41150-41155
147. Eifler, N., Vetsch, M., Gregorini, M., Ringler, P., Chami, M., Philippsen, A., Fritz, A., Muller, S. A., Glockshuber, R., Engel, A., and Grauschopf, U. (2006) Cytotoxin ClyA from *Escherichia coli* assembles to a 13-meric pore independent of its redox-state. *EMBO J.* **25**, 2652-2661
148. Madegowda, M., Eswaramoorthy, S., Burley, S. K., and Swaminathan, S. (2008) X-ray crystal structure of the B component of Hemolysin BL from *Bacillus cereus*. *Proteins* **71**, 534-540
149. Fagerlund, A., Lindback, T., Storset, A. K., Granum, P. E., and Hardy, S. P. (2008) *Bacillus cereus* Nhe is a pore-forming toxin with structural and functional properties similar to the ClyA (HlyE, SheA) family of haemolysins, able to induce osmotic lysis in epithelia. *Microbiology* **154**, 693-704
150. Wolfersberger, M. G., Lüthy, P., Maurer, A., Parenti, P., Sacchi, V. F., Giordana, B., and Hanozet, G. M. (1987) Preparation and partial characterization of amino acid transporting brush border membrane vesicles from the larval midgut of the cabbage butterfly (*Pieris brassicae*). *Comp. Biochem. Physiol.* **86**, 301–308
151. Hodgkin, A. L., and Katz, B. (1949) The effect of sodium ions on the electrical activity of giant axon of the squid. *J. Physiol.* **108**, 37-77
152. Rubio-Infante, N., and Moreno-Fierros, L. (2016) An overview of the safety and biological effects of *Bacillus thuringiensis* Cry toxins in mammals. *J. Appl. Toxicol.* **36**, 630-648
153. Kurehong, C., Kanchanawarin, C., Powthongchin, B., Katzenmeier, G., and Angsuthanasombat, C. (2015) Membrane-pore forming characteristics of the *Bordetella pertussis* CyaA-hemolysin Domain. *Toxins*, **7**, 1486-1496
154. Barcena-Uribarri, I., Benz, R., Winterhalter, M., Zakharian, E., and Balashova, N. (2015) Pore forming activity of the potent RTX-toxin produced by pediatric pathogen *Kingella kingae*: characterization and comparison to other RTX-family members. *Biochim. Biophys. Acta.* **1848**, 1536-1544
155. Forstner, P., Bayer, F., Kalu, N., Felsen, S., Fortsch, C., Aloufi, A., Ng, D. Y., Weil, T., Nestorovich, E. M., and Barth, H. (2014) Cationic PAMAM dendrimers as pore-blocking binary toxin inhibitors. *Biomacromolecules* **15**, 2461-2474
156. Jiang, J., Pentelute, B. L., Collier, R. J., and Zhou, Z. H. (2015) Atomic structure of anthrax protective antigen pore elucidates toxin translocation. *Nature* **521**, 545-549